A THOUSAND BELLS:
ACOUSTICAL IMPLEMENTATION OF BELL SPECTRA USING THE FINITE ELEMENT METHOD AND ITS COMPOSITIONAL REALIZATION

BY

DONGRYUL LEE

DISSERTATION

Submitted in partial fulfilment of the requirements
for the degree of Doctor of Musical Arts in Music
with a concentration in Music Composition
in the Graduate College of the
University of Illinois at Urbana-Champaign, 2020

Urbana, Illinois

Doctoral Committee:

Professor Heinrich Taube, Chair and Director of Research
Professor Carlos Armando Duarte
Professor Stephen Taylor
Associate Professor Reynold Tharp
Professor Sever Tipei

ABSTRACT

This dissertation focuses primarily on the analysis of acoustical models of bell sounds and the modelling of virtual bell shapes and their spectra using the Finite Element Method (FEM) technique.

The first chapter provides a brief introduction of pre and post-spectral music that is inspired by or employs bell sounds from which it derives its central materials.

The second chapter introduces bell acoustics and the creation of new spectral profiles of optimal bell tone colors based upon just tuning ratios. In this chapter, I discuss how the concepts of consonance and Just Noticeable Difference in psychoacoustics are applied to use the 96 tone equal temperament tuning system for bell harmonic profiles.

The third chapter includes the theoretical basis of the FEM and its application to the isoparametric 2-D quadrilateral elements, which are the fundamental theories of how bell harmonies are mathematically calculated. This includes the central concepts of the FEM, such as the Principle of Virtual Work/Displacement, master to global coordinate transformation, FE shape functions, usages of Jacobian matrices, numerical integration of the stiffness matrix and the equivalent nodal force vector for the element by using the Gauss-Lagrange quadrature.

In the fourth chapter, I create bell model geometry by using 2D bell nominal curve and adjustable design variables. Physical parameters, such as the Poisson ratio, Young's modulus, and material properties are also adopted from previous bell design research. Based upon the aforementioned prototypes, I create 24 different 3-D bell geometries, and analyze the spectra of these virtual bells. These bell models are analyzed, optimized and tuned to create tone colors that are defined in Chapter 2. After a validating process of the bell model, the general backgrounds of

optimization theory are also introduced and analyzed for the purpose of creating 3-D virtual bells.

For a general background of campanology, I use André Lehr's *Campanology textbook* to provide the brief history, types, mechanism, casting, forms and parts, and tones of different bells. For acoustical and computational realizations of virtual bells, the analysis focuses on the research of Albertus Johannes Gerardus Schoofs and his follower PJM Roozen-Kroon on the FEM bell optimization, upon which the first prototype of the major-third bell was designed and cast.

ACKNOWLEDGEMENTS

Since the beginning of my musical journey, there have been a variety of generous, open-minded, and truly accomplished artists-teachers to whom I want to express my deepest gratitude. I would like to thank to my advisor Professor Taube, from whom I learned and with whom I have worked for over six years of study at the University of Illinois. He has been a significant influence on me both in the personal and musical dimensions. His broad and deep knowledge in music and science, especially in algorithmic composition, and his concrete reasoning on all musical phenomena, guided me to revisit and cultivate those interests that I had put aside during my undergraduate studies at Eastman.

My relationship with Professor Taylor is not only limited to that of teacher and student. He performed a number of my works as a conductor with sincere commitment, which is an uncommon experience in the current new music field. Without his performances and counsel, I would not have learned a fraction of what I know now about contemporary performance practice. He has also been a mentor that I frequently consult with, and therefore I want to thank him for his long time support and friendship. I want to thank Professor Reynold Tharp who guided me to successfully develop in terms of the classical compositional disciplines, in ways that were both rigorous and inspirational, as well as innovative. I have learned much from his brilliant orchestration, and still frequently study his scores. He was also a guide for me in getting much from those proper teachers of music history, including Debussy and Britten. I am very grateful to my committee members. Professor Tipei has been always very supportive of my research, and also enlightened me with a variety of knowledge about the music and philosophy of Xenakis, which has a deep connection with my musical approaches. Without the response from Professor Armando Duarte, while I was looking for help from professors in other academic fields, this

research would have been frustrated. His generous but keen knowledge of the Finite Element Method really enabled me to explore this entirely foreign subject to me. Special thanks to my dear friend and editor, Eric Zurbin. Not only have we shared and discussed about a span of topics from electronic music to just tuning, he has been someone that I always wanted to talk with and laugh together. Without his precise and elegant editing, this dissertation would have been in very different shape. I want to thank Professor Errede, who has been always very supportive to me and my research, with his deep love of music, since my attendance in his Acoustical Physics of Music course in 2015.

It should be mentioned that I truly appreciate my former teachers. I want to give thanks to Professor Hasegawa who opened the door to spectral and microtonal music for me when I was an undergraduate student at Eastman. Professor Sanchez-Gutierrez was my mentor during my undergraduate studies, and I sincerely appreciate his support which continues even until now, and his insights of seeing the potential artist in me; he and other faculty members generously accepted me as a 30 years old freshman student back in 2008 who knew very little of new music and of composition from any period.

My parents have believed in me and have been supporting me with a tremendous amount of sacrifice and love during this extremely arduous period. It would have been absolutely impossible that I could have been my current self without them, so I want to express my innermost and deepest gratitude and love to them. Finally, I would like to thank my wife Hyelin and my dearest daughter Jera. While finalizing this dissertation during my residency at the Atlantic Center for the Arts in Florida in February 2020, and without their presence, I realized how much I depend upon their existence. They have been a warm home and my earth, in and

upon which I could stand, breathe, and dream, with true love. Thanks to the miraculous coincidence that we could be a family.

TABLE OF CONTENTS

PREFACE

In 2012 I spent an entire summer studying single and multivariable calculus, and differential equations by following online lectures provided by MIT OpenCourseWare. Before beginning these studies, I perused Xenakis' *Formalized Music* and Murail's *Model and Artifices*, and embarked on the study of acoustics. While these, my compositional heroes, established their musical systems (such as Xenakis' outside time structure) by adopting theories in an eclectic manner from science, mathematics, and philosophy, I was particularly interested in how actual sounds are created: the genesis of sounds. This was probably my provisional goal after years of undergraduate studies in new music while listening to a massive amount of dissonances from Schoenberg to Lachenmann. I was desperately searching for order in music, to answer *The Unanswered Question*, to find my own *Technique de mon langage musical*. During my studies in acoustics, I realized that all of my questions were pointing in one direction, where I always encountered those terms unfamiliar to me at the time: eigenvalues and eigenfrequencies. I could sense that these terms contained the secrets of sounds that I had been reaching for. After taking on-line courses and viewing lectures, I always tried to find the reasons for why specific objects or musical instruments had particular characteristic features in their sounds and timbres, and wanted to employ those mechanisms to create my own melo-harmonic vocabulary. From acoustics, I learned that the most important factor that enables an instrument to create its own idiosyncratic harmonic spectrum is determined by what are called vibrational modes. These are determined by their natural frequencies–another name for the eigenfrequencies of the instrument. More complex sounds can be created by more complex vibrations, and these vibrations are determined by the degree of freedom of displacement of the body-vibrating system. Benade

explains this as "several repetition rates in the motion,"[1] which implies that a vibrating body with two or more degrees of freedom has multiple modes of vibration, and the different modes will generally have different frequencies.[2]

In general, a vibrating system is governed by the linear 2nd order ordinary differential equation:

$$\ddot{y} + b\dot{y} + ky = 0^{3}$$

This can be understood if we consider a simple mass-spring system with simple damping force (a damped harmonic oscillator).

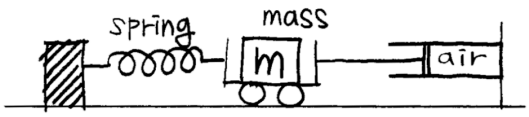

Figure 1. A damped harmonic oscillator

This system has a general solution of $y = e^{-pt}(c_1 \cos \omega_0 t + c_2 \sin \omega_0 t)$, which can be rewritten as $e^{-pt} A \cos(\omega_1 t - \phi)$ [4]. This means this system is vibrating with the frequency of ω_1.

When the vibrating system has more than one degree of freedom, we have multiple variables based on displacement directions. This differential equation with more than one variable is usually solved with the following matrix form:

$$\begin{bmatrix} x \\ y \end{bmatrix}' = \begin{bmatrix} a & b \\ c & d \end{bmatrix} \begin{bmatrix} x \\ y \end{bmatrix}$$

having a trial solution as:

---

[1] Arthur H. Benade, *Fundamentals of Musical Acoustics*, 2nd ed. (New York: Dover Publications, Inc., 1990)

[2] Thomas D. Rossing and F. Richard Moore et al, *The Science of Sound*, 3rd ed. (San Francisco: Addison Wesley, 2002)

[3] Most numerical solving processes of differential equations demonstrated here are from the MIT open courseware (OCW) online lecture "Differential Equations" at [https://ocw.mit.edu/courses/mathematics/18-03-differential-equations-spring-2010] taught by Arthur Mattuck in the Spring of 2003 (accessed July, 2012).

[4] Please read Appendix A – Simple Harmonic Motion for more details.

$$\begin{bmatrix} a_1 \\ a_2 \end{bmatrix} e^{\lambda t} = \begin{bmatrix} x \\ y \end{bmatrix}$$

The roots of this characteristic matrix equation λ_1, λ_2 are called the eigenvalues of the given matrix. This shows that this system is vibrating with two natural frequencies λ_1, λ_2, and this was the answer that I had long been searching for.[5] After finding this answer, I began to think about ways to employ eigenmatrices and eigenvalues for creating previously unimaginable harmonies (eigenfrequencies) in my music. For example, there is a thesis written by V.E. Howlea and Lloyd N. Trefethen, examining the eigenvalues of various ideal instruments such as guitar, flute, etc., and their decay rates.[6] Soon my research topic was focused on the area of Modal Synthesis, but this topic was more concentrated on the field of signal processing and synthesis than harmony, which I determined was not relevant to the kinds of compositional aims presented here.

Finally, I discovered the area of Finite Element Method while reading articles about bell acoustics[7], and conceived a theoretical model of creating virtual instruments and generating eigenfrequencies from them by using the FEM. By approaching sounds and harmonies in this way, one can create a number of amorphous instruments of various timbres and harmonies based on concrete acoustical models, control the results appropriately for artistic purposes, and create a linear harmonic progression by means of a gradual shift and morphology of the geometric profiles of 3-D virtual instruments and their structural analysis. The physical modeling of virtual instruments and the creation of their realistic sound/spectral-results can be applied in various

[5] Please read Appendix B for a solving process of a general first order linear system's Ordinary Differential Equation.

[6] V.E. Howlea and Lloyd N. Trefethen, "Eigenvalues and musical instruments" Journal of Computational and Applied Mathematics 135 (2001): 23–40.

[7] There were numerous articles about this, e.g., Thomas D. Rossing, "The Acoustics of Bell: Studying the vibrations of large and small bells helps us understand the sounds of one of the world's oldest musical instruments," American Scientist, vol. 72, no. 5 (September-October 1984): 440-447, and R. Perrin and T. Charnley, "Normal Modes of the Modern English Church Bell," Journal of Sound and Vibration, vol. 90, no. 1 (8 September 1983): 29-49.

compositional purposes both in the acoustic and electro-acoustic domain. By approaching harmonies in this way, I can inherit not only the philosophy and model-based compositional techniques of late 20th century spectralist composers, but also the purist approaches of American experimentalist composers such as Harry Partch and Ben Johnston, by using the idea of integer ratio-based harmonies of high prime numbers (harmonies in just tuning ratios) for the sound color or timbre of the bell tuning. In other words, the first five lowest partials of bells will be based on just tuning ratios, and the spectral components of created virtual bells can be incorporated in compositional practice as harmonic models. I believe that this multi-disciplinary research of synthesizing engineering physics with music will help to create idiosyncratic harmonic contexts based on physical modelling without the kind of limitations imposed by physical objects in the natural world, and enable the exploration of completely new harmonic dimensions. This yet unknown non-consonance/dissonance spectral domain presents the possibility of revealing new, iridescent timbral spectra of a potentially infinite number of amorphous instruments. From a compositional perspective, my aim is to adopt these newly generated harmonic parameters and demonstrate their realization in musical compositions with acoustical, notational, and practical expressions.

While conducting this research, I realized that there are a large number of relatively lesser-known research areas that could become strong impeti for discovering unknown musical possibilities, and I hope there will be active participation of artists and scholars in this interdisciplinary research in the future. Two books, *Studies in Musical Acoustics and Psychoacoustics*[8] and *Nonlinearities and Synchronization in Musical Acoustics and Music*

[8] Albrecht Schneider, eds., *Studies in Musical Acoustics and Psychoacoustics* (Hamburg:Springer, 2017.)

Psychology[9], published from the systematic musicology department at Universität Hamburg, encompass various topics of musical science / scientific music, and can suggest a good theoretical overview of this burgeoning field.

[9] Rolf Bader, *Nonlinearities and Synchronization in Musical Acoustics and Music Psychology* (Hamburg: Springer, 2013.)

CHAPTER 1: INTRODUCTION

1.1 BELL HARMONIES IN MUSIC HISTORY

Bell sounds have been a perennial inspiration to composers for centuries because of their idiosyncratic harmonic character as well as their religious connotations. From Mozart's magic bells in *Die Zauberflöte* to Harvey's synthesis of bell sounds using a digital computer, composers have ceaselessly tried to integrate the harmonies of bells in their compositions. Mahler used bells in most of his Symphonies (2, 3, 6, 7, 8, 9), and Debussy finalized his only opera with the bell sounds at the moment of Melisande's death. Compositions that feature bell images include Mussorgsky's *Boris Godunov*, Berlioz's *Symphonie fantastique*, Rachmaninoff's *The Bells,* Debussy's *Cloches à travers les feuilles,* Schoenberg's *Op. 19 no. 6* (inspired by Mahler's funeral bell sounds[10]), Messiaen's *Vingt Regards (II. Regard de l'etoile)*, and Toshiro Mayuzumi's *Nirvana Symphony,* to enlist a few examples. Since the acoustical discoveries by the first generation of Parisian spectral composers in the late 1970s, composers continued to expand and develop this different dimension of harmonic thinking, and tried to add new harmonic vocabularies on top of formulae-driven or overtones/ ratio based harmonies. Compositions from the second half of the 20th century in this category, e.g. Murail's *Gondwana*, Harvey's *Mortuos Plango, Vivos Voco*, Anderson's *Book of Hours*, and Chowning's *Stria* continued to explore the sound of bells based on a more scientific analysis or simulations of the sound (e.g., FM synthesis, bell acoustics, and acousmatic realizations and transformations of bell sounds.) The charming sonority of bell sounds kept attracting the ears of a younger generation of composers in the 21st century. The most recent compositions by young living composers at the time of this writing include Leah Reid's *Ring, Resonate, Resound*, Nina C. Young's *Kolokol*, and

[10] Eric McKee, "On the Death of Mahler: Schoenberg's Op. 19, No. 6.," *Theory and Practice* 30 (2005): 121.

Clara Iannotta's *Clangs*. It can be noted that most of these works combine acoustic and electronic sounds, realizing imaginary bell soundscapes by using extended techniques with high pitched instruments (*Musique concrète Instrumentale*), or by using live bell recordings and/or additive synthesis techniques.

1.2 BELL HARMONY IN SPECTRALIST COMPOSITIONS AND THEIR APPLICATIONS

Toshirō Mayuzumi (1929–1997)

The first composer in music history who applied bell sounds in music in a way that is directly connected to the technical and aesthetic approaches of late 20th century spectralism would be the Japanese composer, Toshirō Mayuzumi (黛 敏郎 Mayuzumi Toshirō, 1929 – 1997). It is remarkable that the approach used by Mayuzumi as early as the 1950s is very close to that of the Parisian spectralists later in the century. In his *Nirvana Symphony*, Mayuzumi created the bell harmony based on the early spectral analysis of a real Japanese bell sound:

> The *Nirvana Symphony* and the *Mandala Symphony* are based on the same overtone frequency data of bell sounds quoted from the paper called "Experimental Acoustics (Jikken-Onkyō-Gaku)" (1948), written by Japanese physicist Keiji Yamashita.[11]

[11] Yuriko Takakura (高倉優理子), "A Comparison of the Compositional Process between the Nirvana Symphony and the Mandala Symphony: An Analysis of the "Campanology Documents"," accessed March 5, 2020, https://www.musicology-japan.org/publish/v63/Takakura_en.pdf, trans. by unknown author, "黛敏郎《涅槃交響曲》と《曼荼羅交響曲》の成立過程比較ー「Campanology 資料」の分析を中心にー," *ONGAKUGAKU: Journal of the Musicological Society of Japan*, 63, no. 2 (2018), 61-77, https://doi.org/10.20591/ongakugaku.63.2_61.

Peter Burt explains how Mayazumi "anticipates the 'spectral music' later to be associated particularly with French composers such as Grisey and Murail"[12] in the 1970s. In one of his essays, the Japanese composer, Tōru Takemitsu (1930–1996), recalls Mayuzumi's explaination of his "campanology effect":

> Toshiro Mayuzumi wrote an article about his profound attachment to the Buddhist temple gong. … What was important was the way the sound of the gong, described by Mayuzumi as a "campanology effect," captured space and time beyond everyday life, shaping and moving according to the will of the composer.[13]

Mayuzumi used the frozen "bell chord" in the first movement of his *Nirvana Symphony* (1958), which is titled 'Campanology.' In this movement, he created and experimented with the bell sounds with a live orchestra, both presaging, and in an even more rigorous way, than György Ligeti's process in his monumental instrumental work, *Atmosphères* (that applied techniques learned from the Cologne electronic studio). Ligeti's applications of spectral concepts from electronic music to his acoustic works can be confirmed in his interview:

> My idea was that a sufficient number of overtones without the fundamental would, as a result of their combined acoustic effect, sound the fundamental. I wanted to select and record on tape overtones between 1,000 Hz and 6,000 Hz, use only these and expected the composite sounds to emerge automatically. […] When I tried to do all that in the studio, it turned out to be a quite illusory idea, unfeasible. It dawned on me that the sound I wanted could be realized much more easily with an orchestra. The first title I gave *Pièce électronique* no. 3 was *Atmosphères*.[14]

Yoshihiko Shimizu, in his paper: 'The Creative Quest into Temple Bell Sonorities: Works of *Musique Concrète* by Toshirō Mayuzumi,' introduces Mayuzumi as the pioneer of

---

[12] Peter Burt, *Overtones of Progress, Undertones of Reaction: Toshiro Mayuzumi and the Nirvana Symphony*, accessed Dec 20, 2019, https://web.archive.org/web/20060903144412/http://www.research.umbc.edu/~emrich/Burt.html

[13] Tōru Takemitsu, *Confronting Silence: Selected Writings*, trans. and ed., Yoshiko Kakudo and Glenn Glasow. Berkeley (California: Fallen Leaf Press, 1995), 22-23.

[14] György Ligeti, *Ligeti in Conversation*, ed. Péter Várnai et al., (London: Eulenburg Books, 1983), 37–39. Ligeti didn't use the actual spectral analysis here, but used the shape of overall distribution of spectrum in the large orchestra.

Japan's electroacoustic music tradition, and who "actively pursued the acoustic analysis of the sound of Buddhist temple bells, as well as the experimental synthesis of electronic sounds similar to the sound of temple bells. … created works of musique concrète using the sound of temple bells as raw material."[15] The *Nirvana Symphony* was composed during the period when he wrote works with various media for his *Campanology* series, including the purely instrumental: *Nirvana Symphony*, the fixed media works: *Campanology for musique concrète* (1959) and *Campanology Olympica* (1964), works employing additive synthesis and ring modulation: *Campanology for multi-piano* (1967). In these works, he focused on a single sound-spectrum harmony based on the spectral analysis of temple bell sounds, sometimes combining it with row-oriented dodecophonic techniques. Rather than depicting a totalistic soundscape created by ringing multiple bells as in a Western carillon instrument, he focused on the single bell sound, which he thought of as a fundamental difference between the eastern and western aesthetic regarding bell sounds:

> … the basic philosophy of 'campanology' in the Western world places emphasis on how to combine multiple bells together to form a melody, or in other words, the tuning and the adjusting of musical scales, whereas in Japan, the focus was placed on pursuing a more full and rich sonority through research into alloy proportions and foundry methods.[16]

This can be the reason why there are no such techniques as Change Ringing in the eastern tradition[17], as there usually is only one huge bell–범종(梵鐘) located in each temple in Asia. To emphasize this complex spectrum of a single Japanese bell in the first 5 minutes of *Nirvana Symphony*, Mayuzumi uses only one vertical bell chord over the entire range of the orchestra,

---

[15] Yoshihiko Shimizu, "The Creative Quest into Temple Bell Sonorities: Works of *Musique Concrète* by Toshiro Mayuzumi," *Contemporary Music Review*, 27/1-2 (2018), 36.

[16] Shimizu, "The Creative Quest into Temple Bell Sonorities," 38.

[17] Because of their large sizes (the largest bell in Korea, 성덕대왕신종(Bell of King Seongdeok, 聖德大王神鐘), is of 3.75m height, 2.27m diameter, and 0.11-0.25m wall thickness), they have strike notes between 50 and 110 Hertz that are usually lower than Western bells, and have very long sustaining beatings (맥놀이, 脈動) over one minute.

which is subdivided into three groups of instruments. In this movement he alternates three sub-harmonies in antiphonal choral-like texture. Here group I is made up of 2 piccolos, flute, 2 clarinets, glockenspiel, and sleigh bells, group II contains strings (other instruments including piano are added in the latter section playing pointillistic fragments), and group III includes brass instruments–3 horns, 2 trombones, 1 tuba, 2 double basses, and a gong. These groups are also separated from one another in the performance space. By this spatialization of each modal group, Mayuzumi intends for the audience to experience the sound as if they are listening inside a gigantic virtual temple bell.

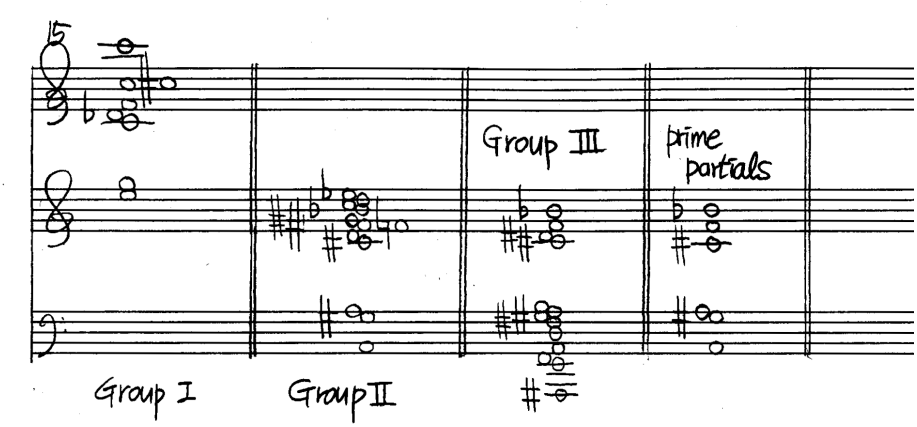

Figure 2. Bell spectrum in three groups in Toshirō Mayuzumi's *Nirvana Symphony*. Score reduction from the first movement by the author.

Figure 2 shows the chords of Group I, II, and III, which are played altogether at the last measure. In the first movement, these chords are played alone or together, sometimes transformed into chords from other groups, creating a variety of harmonic colors. Mayuzumi emphasizes specific pitches by doubling or using those pitches as common tone pitches between different groups. For example, in figure 2, A2, G-sharp3, A3, C-sharp4, F4, B-flat4 are played by both group II and III, and thus function as the lower six prime eigenfrequencies of a bell.

The French Spectralists and Iannis Xenakis (1922–2001)

Mayuzumi's notion of capturing space and time, the "frozen time" harmony[18], and organizing them in a musical time-space can be frequently read in the writings by spectralist composers as well as Xenakis, whose music was one of the major influences on Murail's, as Grisey expounded the importance of temporal manipulations in spectral music: "By skeleton of time we mean the temporal divisions that the composer uses to organize sounds. … it is here à question of approaching the immediate perception of time in its relationships with the sound material."[19] The idea of captured space and time, can be analyzed as the "outside-time" entity of Xenakis's approach: "I propose to make a distinction in musical architectures or categories between outside-time, in-time, and temporal. A given pitch scale, for example, is an outside-time architecture, for no horizontal or vertical combination of its elements can alter it."[20] Although Xenakis never employed spectral objects in his music, his use of gigantic vertical chords / harmonic fields created by sieves from the algebra of set operations in his later cellular automata compositions closely shares some of the approaches of école spectrale. "This can be explained by an observation which I made: scales of pitch (sieves) automatically establish a kind of global musical style, a sort of macroscopic "synthesis' of musical works, much like a 'spectrum of frequencies, or iterations', of the physics of particles."[21] It is also worth noting that it is unlikely to be a coincidence that these composers have strong connections with early electronic music,

[18] Takemitsu, *Confronting Silence*, 22-23.
[19] Gérard Grisey, "*Tempus ex Machina*: A composer's reflections on musical time," *Contemporary MusicReview* 2:1, (1987): 239-275.
[20] Iannis Xenakis, *Formalized Music: Thought and Mathematics in Music* (Hillsdale: Pendragon, 1992), 183.
[21] Xenakis, *Formalized Music*, Preface.

since the spectra of sounds and their analysis are not approachable without computer technology.[22]

Jonathan Harvey (1939–2012)

Jonathan Harvey's *Mortuos Plango Vivos Voco* is one of the earliest compositions that scientifically employs bell sounds both on micro and macro levels from momentary vertical harmonies to the larger formal structure. This acousmatic composition begins with the recorded bell sounds of the great tenor bell at Winchester Cathedral. As the music unfolds, Harvey modulates from one spectrum to another by fixing a common pivotal tone and shifting the other partials with voice leading oriented glissandi. Formally, this bell chord is used as a "bell-tonics" hierarchically, which is analogous to the traditional western tonal system.[23] Each section is based on these pivot pitches. In the later part of the piece, this bell chord is gradually transformed into a singing boy's choir, which is the recording of Harvey's own son's voice, who used to sing at the cathedral as a treble chorister. Harvey used this human voice and bell sounds as contrasting forces, which finally unites into one sound: "The "dead" bell is the mortuous, the "living" boy the vivos. They are one."[24]

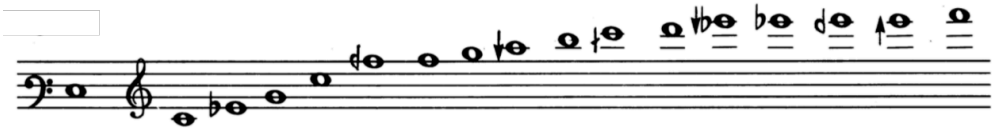

Figure 3. The bell spectrum from Havey's *Mortuous Plango*.[25]

[22] Many scholars count Stockhausen's Stimmung (1968) as the first spectral composition, and it was also written in the electronic studio in Cologne, where Ligeti also stayed and found inspiration for his quasi-spectral micropolyphonic works. See [add citations for this info]

[23] Jonathan Harvey, "Mortuos Plango, Vivos Voco: A Realization at IRCAM" *Computer Music Journal* 5, no. 4 (Winter, 1981): 22.

[24] Jonathan Harvey, *In Quest of Spirit: Thoughts on Music* (Berkeley: University of California Press, 1999), 61.

[25] Jonathan Harvey, ""Mortuos Plango, Vivos Voco," 23.

The idea of using the intervallic structure of a spectral model, "intervallicism seen in a spectral light" in Harvey's work and "a way to incorporate transformational (in the intervallic sense) procedures into spectral music" in Murail's explanation[26], shows a way to reconcile scientific data with traditional musical craft.

Proto-Spectral Forebearers and Magnus Lindberg

The pseudo-spectral usages of harmony within the fixed gamut or register (c.f., no transposition or octave displacement, with fixed pitches in the entire musical register) can be foreseen in the French Spectralist's teacher Messiaen, i.e., Messiaen's modes, and then Messiaen's musical forebearer, Anton Webern. Webern's usages of tone rows were based on this pseudo-spectral viewpoint of seeing intervallic variations within the timbre-harmonic field or the overtone series (c.f., registrally symmetrical harmonic field of op. 21), as he had perspicaciously foreseen the advent of microtonality,[27] which also later become a crucial element of much spectral music. Another important composer that is a part of this lineage is Witold Lutosławski (1913–1994), whose compositional techniques thoroughly integrate the idea of the harmonic field, which is a theoretical precursor of harmonic *objets* of spectralists, and hugely influential on the music of later Finnish pseudo-spectralist composers such as Esa-Pekka Salonen (1958–) and Magnus Lindberg (1958–).[28] These influences can be heard in the various interval based melo-harmonic manipulations of quasi-spectral materials in Magnus Lindberg's music. Magnus

[26] Tristan Murail, "After-thoughts," *Contemporary Music Review* 24/2-3 (2005): 270, quoted in Christopher Gainey, "Hearing Timbre-Harmony in Spectral Music" (PhD diss., The University of British Columbia, 2019), 93.
[27] Anton Webern, *The Path to the New Music*, ed. Willi Reich and trans. by Leo Black et al. (Pennsylvania: Theodore Presser Co. / Universal Edition, 1963), Originally published as *Wege zur neuen Musik* (Vienna: Universal Edition, 1960).
[28] Steven Stucky, "Tanglewood Celebrates Composer Steven Stucky In Its Festival of Contemporary Music," accessed May 1, 2017, https://www.bostonglobe.com/arts/music/2016/07/13/steven-stucky-celebrated-peers-and-students-tanglewood/6WKAJG78z3FVB6rK0SigFJ/story.html.

Lindberg uses 12-tone chords with Lutosławski-influenced intervallic manipulations[29], which is analyzed by a computer and registrally re-arranged based on the overtone series. This program was developed by Gérard Assayag to analyze a chord and to find the virtual fundamental.[30] Yiorgos Vassilandonakis refers to this sound, which appeared in his *Corrente* as bell sounds with a virtual fundamental:

> … characteristic overtone structures of bell sounds with fundamentals on C and B … as revealed by the virtual fundamental generator software. These are very resonant structures, comprised of out-of-tune partials that clash with each other because of the presence of a minor 3rd low in the structure.[31]

Some Applications of Spectral Techniques

In my own work, I used Harvey's bell spectrum as both a vertical punctuational chord and a formal backbone for my solo piano work, *Le tombeau de Harvey*, in much the way that Harvey would use what he called "Schenkerian hierarchical thinking."[32] The tonal overview of this piece draws a big arc, from lower to upper and back to the low partials of Harvey's bell spectrum. I use frequencies from Harvey's bell spectrum as carrier and modular frequencies to create FM harmonies upon which each local level phrase is based. In this sense, Harvey's concrete bell spectrum functions as the 'skeleton' of the piece, while instantaneous FM-

[29] Read Witold Lutosławski, "*Lutosławski on Music*," ed. Zbigniew Skowron Lanham (Maryland: Scarecrow Press, Inc., 2007) and Steven Stucky, "Lutoslawski and His Music" (Cambridge: Cambridge University Press, 2009) for more information about Lutosławski's 12 notes harmonic field.

[30] Read, Edward Paul Martin, "Harmonic Progression in the Music of Magnus Lindberg" (DMA diss., University of Illinois at Urbana-Champaign, 2005), 24 for more details.
Order No.3202139, University of Illinois at Urbana-Champaign, 2005.

[31] Original article from the author's personal website but now has removed. Used with a permission.

[32] Jonathan Harvey, "Spectralism," ed. Joshua Fineberg, *Contemporary MusicReview* 19, no.3 (2000): 11.

synthesized surface level bell harmonies function as the 'musical flesh,' to borrow from Grisey's language.[33]

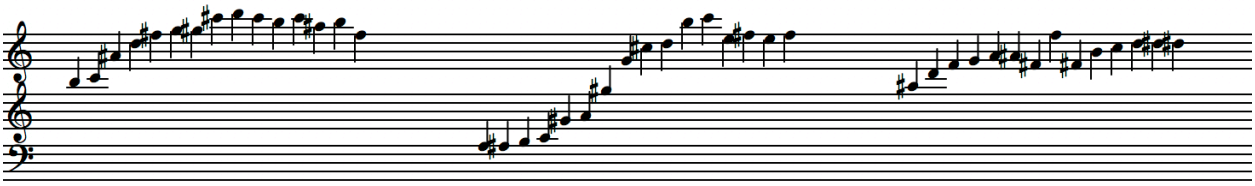

Figure 4. regional FM bell harmonies used in *Le tombeau de Harvey* created by carrier and modulating frequencies from Harvey's bell spectrum.

In *Le tombeau de Harvey*, the quarter-tone frequencies are quantized to either the nearest equal tempered note or duplicated to form 1. a minor 2nd interval 2. a major 7th interval chord, or 3. a minor 9th interval chord to be played by the piano. (e.g., F-half sharp4 is converted to 1. F4 if the original quarter-tone is close to F4 than F-harp4, 2. F4 and F-sharp4, 3. F4 and F-sharp5, or 4. F-sharp4 and F-5.) This idea of quarter-tone quantization was inspired by Grisey's usages of microtones in his *Partiels*, in which he represented quarter-tone pitches as minor 9th interval dyads and octave transposed them to the lower register to increase harmonic tension. Chris Arrell explains Grisey's approaches in quarter-tones in his analysis of Partiels:

> Grisey sometimes rounds quarter-tones to the nearest half-steps above and below when transferring down an octave. In the ninth chord, for example, the 11th partial (A quarter sharp) becomes both A and B-flat, … the 13th partial (C-quarter sharp) rounds to both C natural and C-sharp (Rehearsal 9).[34]

Harvey explains the idea of using a spectral model as a larger musical form as a 'spectral form,' in which the whole piece is like the unfolding in time of what is in fact one brief moment,

[33] Grisey, "*Tempus ex Machina*."

[34] Chris Arrell, "The Music of Sound: An Analysis of Partiels by Gérard Grisey" in *Spectral World Musics: Proceedings of the Istanbul Spectral Musics Conference*, ed. Robert Reigle and Paul Whitehead (Istanbul: Pan, 2008), 322. An octave transposition for sounds intensification is also used in his other pieces, for example *Quatre chants pour franchir le seuil*. Please read Jean-Luc Hervé's analysis for more details.

the timbre of the bell.[35] Tristan Murail expresses this approach as a "rigorous formal plan, within a well-defined framework (the universe of the bell), possessing well-known archetypal correspondences:"[36]

> The bell's spectrum also serves as a formal model. … More precisely, the length of each section (in seconds) is equal to 200 divided by the ratio of the pivot pitch's frequency to the frequency of the fundamental (C3). This gives the following list of durations: 100, 33, 75, 37, 50, 30, 84, and 200.[37]

FM Harmony and Bell ethos in the Music of Harvey and Murail

The bell-like timbral characteristics of FM harmony, discovered by John Chowning in the late 1960's, influenced many spectral composers including Harvey and Murail significantly. Harvey's father observed Jonathan's attachment to bell-like sonorities from his childhood period:

> He loved Skriabin and Fauré, he loved harmonies which were complex and resonant and ways of writing for the piano which would sometimes blur: complex spectral *objets sonores* making for what he would call bell effects.[38]

Harvey used his own version of FM harmonies in a number of works including *Advaya, Ashes Dance Back,* and *White as Jasmine*, which Michael Downes called an 'equal addition compression' technique.[39] Downes explains this technique, which Harvey called an 'n/m' compression, in greater detail. I reduced Downes' analysis to a simpler version of FM formula by removing the intermediate calculation stages. This result shows Harvey's harmony in the form of an FM spectrum having the modular frequency as

---

[35] Harvey, *In Quest of Sprit*, 60.

[36] Tristan Murail, "Villeneuves-lès-Avignon Conferences, Centre Acanthes, 9–11 and 13 July 1992," trans. Aaron Berkowitz and Joshua Fineberg, *Contemporary Music Review* 24/2-3 (2005): 205.

[37] Murail, 204.

[38] Andrew Whithall, *Jonathan Harvey* (London: Faber, 1999), 1, quoted in Michael Downes, *Jonathan Harvey: Song Offerings and White as Jasmine* (Farnham: Ashgate Publishing Limited, 2009), 6.

[39] Downes, 95.

$$\frac{1}{2} \times fundamental \times \frac{n}{n+m}$$

where n and m are from Harvey's compression ratio m / n. If the fundamental frequency is A (110 Hz) and the compression ratio is 3/7, the resultant spectrum will be the unipolar FM spectrum generated by carrier frequency 110 Hz and modulating frequency 38.5 ($= \frac{1}{2} \times 110 \times \frac{7}{7+3}$). The reason why the result is unipolar is, that Harvey only used additive operations for creating his harmonies.

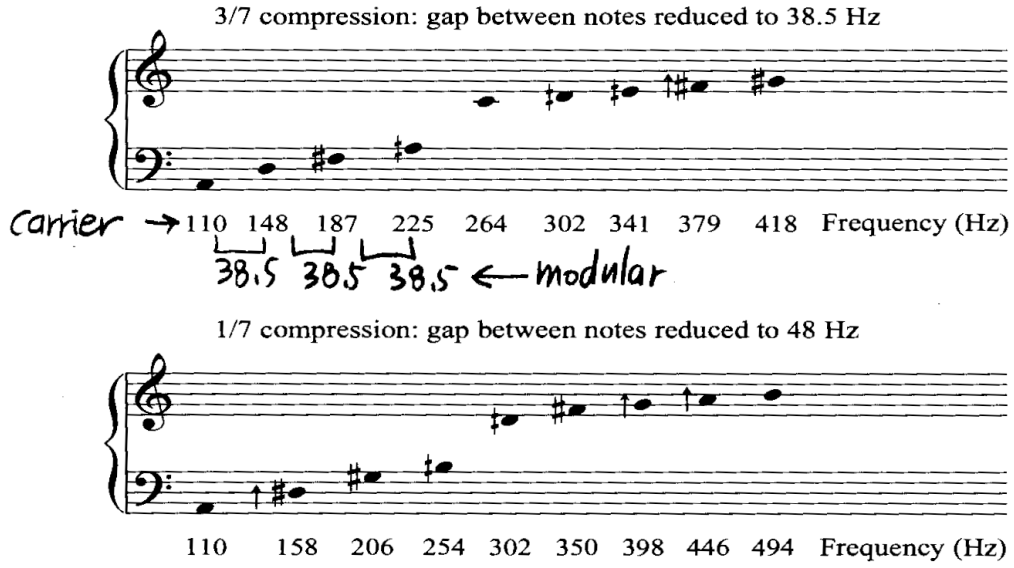

Figure 5. Compressed harmonies from Harvey's sketches. [40]

The 48 Hz from the second spectrum of this figure can be derived from the compression ratio of 1/7 having the equation $\frac{1}{2} \times 110 \times \frac{7}{1+7} = 48.125$.

[40] The original sketches are transcribed by Downes, 96.

Tristan Murail used this kind of frequency modulated harmony as an imaginary bell sound throughout his oeuvre, tried to "mix in, amongst other allusions, a few ethos of bells"[41]:

> The bells of *Gondwana* are imaginary–in contrast to those of *Mortuos plango*. For the beginning of the piece, I wanted to make large bell sonorities heard via the orchestra. … I thought of a mathematical technique used in computer music to produce reasonable convincing bell-like sonorities called 'frequency modulation'.[42]

It is clear that Murail had been interested in and researched the characteristics of bell sounds rigorously, including a small Japanese temple bell sound that he studied at IRCAM with the program IANA. He denotes the principal characteristics of occidental bells as the superposed presence of a major and a minor 3rd, and the spectral profile of a small Japanese bell as 'a bit warped, a bit distorted.'[43]

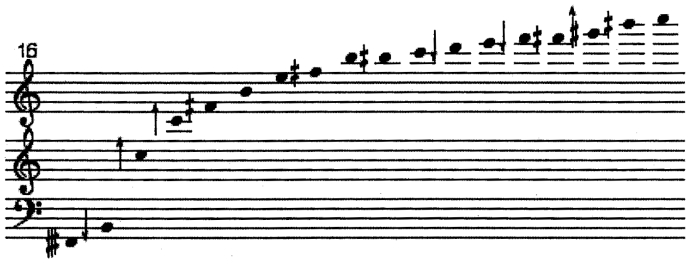

Figure 6. The spectrum of a small Japanese bell,[44] where arrows mean eighth tones and the number of horizontal lines in each sharp denotes a quarter tone.

After the presentation of initial bell sounds with the fixed carrier frequency at C quarter-sharp4 played by the horn, Murail increases the modulator frequency by steps of 4.87 Hz and the index by steps of 1 or 2.[45] Mark Andre-Dalbavie points out that the envelope of these chords whose

[41] Tristan Murail, "Cloches d'adieu, et un sourire... in memoriam Olivier Messiaen," Works, Tristan Murail Official Website, accessed February 5, 2020, https://www.tristanmurail.com/en/oeuvre-fiche.php?cotage=27527.

[42] Murail, "Villeneuves-lès-Avignon Conferences, Centre Acanthes, 9–11 and 13 July 1992," 205.

[43] Murail, 201-202.

[44] Murail, 202.

[45] Tristan Murail, "Target Practice," trans. Joshua Cody, *Contemporary Music Review* 24/2-3 (2005): 169.

model is the percussion/resonance makes him instantaneously think of a bell.[46] Joshua Fineberg, who studied with Murail in his earlier career explains Murail's usage of bell sounds in more detail:

> The idea is to go inside of a bell sound and render audible the normally microscopic structures that make it beautiful. Moreover, by recreating a hybrid with bell-like properties, it is possible to gradually manipulate these structures and make musical objects less and less bell-like in gradual increments.[47]

Murail continued using the ethos related to bell sounds throughout his musical career, for example in his large orchestral works with chorus, *Les sept paroles*, the FM synthesized bell sounds are used as a story teller's tool to provoke and attract listeners' focus: "In order to provide markers for the listener in terms of how the form unfolds, each section is indicated by the sounds of sampled bells."[48]

---

[46] Viviana Moscovich, "French Spectral Music: an Introduction," *Tempo* 200, no. 3 (April 1997): 23.

[47] Joshua Fineberg, *Classical Music, Why Bother? Hearing the World of Contemporary Culture through a Composer's Ears* (New York: Routledge, 2006), 119.

[48] Tristan Murail, "Les sept Paroles," Works, Tristan Murail Official Website, accessed February 5, 2020, https://www.tristanmurail.com/en/oeuvre-fiche.php?cotage=28868.

CHAPTER 2: CHARACTERISTICS OF BELL SPECTRA AND THEIR BACKGROUNDS

2.1 BASIC BELL ACOUSTICS

Historically, researchers use the acoustics of a vibrating circular plate because they are similar to a bell and simpler to conceptualize and analyze mathematically (Rossing describes this process in his article 'The Acoustics of Bells: Studying the vibrations of large and small bells helps us understand the sounds of one of the world's oldest musical instruments.')[49] A circular plate's modal function follows $(\mathrm{J}_m(kr) + \lambda_m \mathrm{I}_m(kr))$ where λ_m is a constant, J_m and I_m are respectively a Bessel and modified Bessel function of the first kind, and the wave number k is related to the frequency f, following the relation $k^4 = 48\pi^2 f^2(1-\sigma^2)\rho/Eh^2$ where E, σ and ρ are Young's modulus, Poisson's ratio and density respectively for the material property with a thickness of h.[50] When a bell is struck, sound is created by the vibration of the physical body of the bell. The mechanical excitation of the bell's wall is transformed into pressure fluctuations in the air, and the motion of air molecules create sound waves. The sound waves (energy transportation by air molecules) then propagate outwards from the sound source eventually reaching and vibrating the listeners eardrums. When a mechanical body vibrates, the vibration includes a theoretically infinite number of mechanical motions. Each specific pattern of vibration creates a pure tone or frequency, and the harmony created by legion of frequencies from different vibrational modes are instantaneously recognized in a global sense as the timbre of the instrument. This notion of "one sound" is a key element of spectral music. Grisey wrote:

---

[49] Thomas D. Rossing, "The Acoustics of Bells: Studying the vibrations of large and small bells helps us understand the sounds of one of the world's oldest musical instruments," *American Scientist*, vol. 72, no. 5 (September-October 1984): 440.

[50] R. Perrin et al., "Chladni's Law and the Modern English Church Bell," *Journal of Sound and Vibration* vol. 102, no. 1 (1985): 11.

"Harmonic and timbral consequencies: […] Integration of harmony and timbre within a single entity. Integration of all sounds (from white noise to sinusoidal sounds)."[51]

In the vibration of an acoustical body, the regions that have the least amount of motion (minimum displacement from the equilibrium position) forms nodes, and the maximum surface displacements form antinodes. The shape and dimension of nodes depend on the spatial orientation and kinetics of the instrumental body. For example, in a vibrating string, nodes and antinodes are points, and in vibrating membranes, they form lines. In circular plates, the material surface vibrates along with largely symmetrical nodal lines, which are either straight (meridian) or circular. The straight lines are called nodal diameter, and the circular lines are called nodal circles. In bell acoustics, the nodal diameter is also called the nodal meridian or azimuthal meridian, and the nodal circle is called the nodal parallel, since it is parallel to the edge of the bell. Each nodal line is associated with a specific vibrational behavior, and the pattern of vibrational movement is called a mode of vibration. A vibrational mode in a bell has to have at least one nodal diameter or nodal circle, and can have infinite combinations of these nodes. In a circular plate, the mode of vibration is notated by a combination of nodal meridian and nodal circle, e.g., (m, n), where m denotes nodal meridian and n denotes nodal circle.

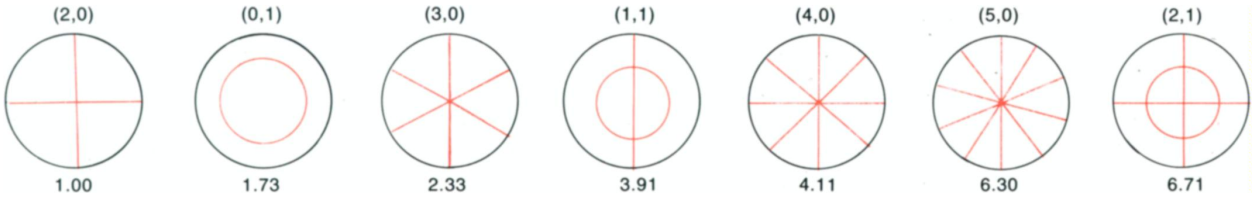

Figure 7a. The first seven modes of vibration in a circular plate with a free edge. The numbers below the plate implies a frequency ratio of the mode.[52]

[51] Gérard Grisey, "Did You Say Spectral?" trans. Joshua Fineberg, *Contemporary Music Review* 19, no.3 (2000): 1.
[52] Rossing, "The Acoustics of Bells," 442.

In campanology, nodal meridians are denoted by roman numerals, and nodal circles are denoted by arabic numbers. Thus, each vibrational mode (eigenmode) is indicated by the combination of a roman numeral and a number, e.g., I-3, II-3, etc. Exceptions are the hum and prime, which are notated as H-2 and P-2 (Lehr) or H-2 and F-2 (Roozen-Kroon)[53]. In this thesis, vibrational modes are indicated by the combination of two numbers with parentheses, e.g., Hum (2,0), Tierce (3,1), etc.[54] If there are two modes which share the same amount of nodal meridians or circles, they are indicated with a # (e.g., Quint–(3,1#)), following the custom of Tyzzer (1930). Note that the meridians here denote half meridians, by measuring half of the bell's surface. The actual nodal meridians of eigenmode is twice more than the notated nodal meridians, since the bell has axisymmetric surfaces. For example, the Prime (2,1) mode has two nodal meridians and one nodal circle on half of the bell's surface, but actually has four nodal meridians and one nodal circle since the bell is axisymmetric. See figure 7b to see the axisymmetric characteristics of bell vibration, and figure 7c for the five lowest bell partials and their names in a typical minor third bell.

Figure 7b. Four nodal meridians and one nodal circle on the whole bell surface (left) and half meridians (right).

[53] P. J. M. Roozen-Kroon, "Structural optimization of bells" (PhD thesis., Eindhoven University of Technology, 1992.)

[54] Notations of bell eigenmodes differ from papers. Roozen-Kroon uses two numbers as here, Lehr uses the traditional way (roman numerals with numbers, e.g., I-2, II-3, etc.), and Schneider uses both full meridians with half meridians in brackets. (e.g., 4,1 [2,1].)

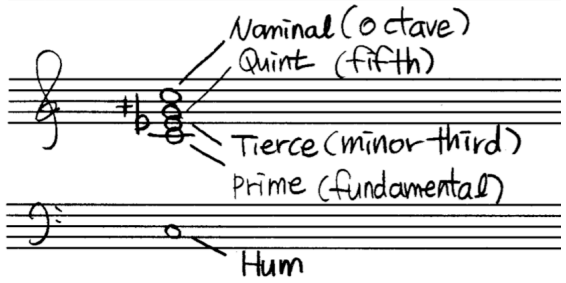

Figure 7c. Five lowest partials and their campanological names of a typical minor third bell.

Each mode of vibration creates a distinct frequency, and this frequency is called a partial, natural frequency, or eigenfrequency. A one dimensional vibrating system creates a series of frequencies in the ratios of a simple integer series–the overtone series. (e.g., the vibration of strings or air columns.) The frequency spectrum created by the oscillations of a 2 or 3 dimensional medium–vibrating systems with more complex profiles– can be mathematically calculated by a group of differential equations derived from structural mechanics. (Please see Appendix A – SIMPLE HARMONIC MOTION and Chapter 3. EIGEN VALUES AND OVERTONE SERIES for more details.) Roozen-Kroon explains this relation of vibrational modes and eigenfrequencies of bell acoustics in her thesis:

> After a bell is excited with a stroke of a clapper or a hammer, the bell starts to vibrate. The vibration of the bell consists of the superposition of an infinite number of excited eigenmodes with distinct eigenfrequencies (assuming the bell to behave in a linearly elastic manner). Every eigenmode vibrates with its own eigenfrequency in a unique mode shape, as an initial amplitude that is determined by the initial conditions of the bell, the excitation process and excitation point, and decays at its own decay rate due to the damping related to the eigenmode.[55]

Since the sound of a bell is a linear combination of a theoretically infinite number of partials, we hear the bell sound as a complex tone with transient responses, in which the dynamic content of the sounds evolves in time. Psychoacoustically, when the ear hears the overtone series, it

[55] Roozen-Kroon, "Structural optimization," 3.

identifies the pitch of the fundamental frequency of the series, and this is possible even if the fundamental is very weak or missing.[56] When a fundamental is missing, our brain calculates the virtual fundamental and recognizes the complex tone as a single tone of this frequency. In other words, for the overtone series, we identify the series as a single pitch of an existing or non-existing fundamental frequency.[57] In musical repertoire, Ligeti used this idea of a virtual fundamental in his unrealized piece, *Pièce électronique No. 3*: "My idea was that a sufficient number of overtones without the fundamental would, as a result of their combined acoustic effect, sound the fundamental."[58] Also, this idea of combination tones (also known as Tartani tones) became the fundamental theoretical background for Hindemith to establish his own musical system based on the level of consonance and dissonance, and the horizontal resolution of tritones.[59] Most recently, Hans Zender used the idea of combination tones as a key algorithm to create a horizontal formal progression by using consecutively calculated combination tones.[60]

Complex tones such as bell sounds have their own psychoaoustic phenomena. Lehr explains the strike tone, the tone that we recognize from the instantaneous bell strike, as a physiological phenomenon. "It is formed in our ears and not in the bell. Note that the strike tone has a pitch one octave lower than that of the fourth overtone, thus the fifth partial. … the first overtone exists in the vibrations of the bell wall, while the strike tone exists in our sense of

---

[56] Rossing, The Science of Sound, 129.

[57] These virtual frequencies are called the combination or difference tones. These phenomena arise solely due to non-linear responses of the human ear and brain. Human hears two frequencies which are within a critical band as a single frequency, the average of the frequencies with a beating, and this is an example of the non-linear hearing phenomena.

[58] Ligeti, *Ligeti in Conversation*, 37.

[59] Paul Hindemith, *The Craft of Musical Composition: Book 1: Theory*, 4th ed., trans. Arthur Mendel (New York: Schott, 1942), 32-43, 80, 87, 97, 104. Hindemith's theory is considered revolutionary in the eyes of the 21st century composers or theorists. For example, his creation of scales (p. 32) is entirely based on the overtone series, and can even be applied to the harmonic fields that are written by Georg Hass or James Tenney.

[60] Read for more details: Robert Hasegawa, "*Gegenstrebige Harmonik* in the Music of Hans Zender," *Perspectives of New Music*, 49, no. 1 (Winter 2011): 207-234.

hearing."[61] Here Lehr explains that the second partial–prime (See figure 7c) is different from the strike tone, although they are the same pitch. This is because the second partial is just a single frequency, but the strike tone is a complex tone made up with a conglomeration of frequencies, which is identified as the same frequency with the prime tone partial. Since usually the strike note coincides with the second partial, prime tone is also called the fundamental tone.

Although there are a number of partials in the spectrum, in our listening process, only partials with high amplitude or in mid-low register contribute to formulate a virtual fundamental or a strike tone. This is because lower sounds mask higher sounds due to the response on the basilar membrane, and also can be more easily heard because of the Fletcher-Munson curves and the critical bandwidth. (e.g., lower frequency has larger ratio of critical bandwidth, means their corresponding basilar membrane covers larger frequency bands.) Rossing explains that the strike note is determined by the three low partials–prime (fundamental, 2nd partial), the twelfth (ninth partial), and the upper octave (double octave, twelfth partial).[62] In campanology, higher partials are regarded as unimportant, and to be important, partials have to be loud and of low order.[63] Although the higher partials are regarded as unimportant to the carillon craftmanship, the main purpose of this research is largely focused on the higher partials which actually formulate the tone-color of bells as a spectral conglomeration/image to our ears. These partials are subsequently generated from the bell profile focused on lower partials, and can be used in musical compositions as harmonic entities; the harmonic profiles of higher partials are unimaginable by any means or tools of musical tradition, but can only be virtually calculated

---

[61] André Lehr, *Campanology textbook : the musical and technical aspect of swinging bells and carillons*. trans, Kimberly Schafter (California: Guild of Carillonneurs in North America, 2005): 20.

[62] Rossing, *The Science of Sound*, 303.

[63] Lehr, 28; Roozen-Kroon, 4; R. Perrin and T. Charnley, "Normal Modes of the Modern English Church Bell," *Journal of Sound and Vibration* 90, no. 1 (1983): 29.

with the help from computer technology. However, they are acoustically plausible with logical coherence, and are not purely imaginary but can exist in the real world with additional bell casting processes with physical resources. This approach is close to the "general framework of artistic attitude" of Xenakis, which has been a strong influence on me: "The techniques set forth here, although often rigorous in their internal structure, leave many openings through which the most complex and mysterious factors of the intelligence may penetrate."[64]

The first ratios of lower partials of the minor third bell (which is the typical western bell) was empirically designed around 1500 by bell founders, which were close to 1:2:2.4:3:4. Since the prime and tierce of these bells formed a ratio of 2:2.4, these bells became known as minor third bells.[65] The first well-tuned carillon was designed and cast in 1644 by the bell founders François and Pieter Hemony, in cooperation with Van Eyck, who perceived and defined 7 partials that should be heard.[66] Van Eyck understood the importance of the curvature and thickness at certain points of a bell's wall, and put these insights into practice when they cast bells. In these bells, the five lower partials have a ratio of 1 : 2 : 2.4 : 3 : 4.[67] It would be helpful to indicate how they tuned bells, since there are important connections between the ways how they tuned the lowest partials and my bell geometric profile and its parametrization. Roozen-Kroon describes the old tuning processes:

> Grinding away small rings of material on the inside of the bell wall the frequencies of the partials are changed. Due to the individual reaction of the partial frequencies to the local changes in wall thickness, the frequency ratios can be changed slightly. Because of the slight inaccuracy inherent to the process of casting, the Hemony brothers casted the

[64] Xenakis, *Formalized Music*, 178.

[65] Albrecht Schneider and Marc Leman, "Sound, Pitches and Tuning of a Historic Carillon," in Studies in Musical Acoustics and Psychoacoustics, ed. Albrecht Schneider (Hamburg:Springer, 2017): 249; One famous bell cast by de Wou, the Gloriosa of Erfurt dating from 1497 already shows the pattern of strong spectral components typical of the minor-third/octave bell with this ratio. Lehr, 250.

[66] Roozen-Kroon, "Structural optimization," 6.

[67] Schneider, *Studies in Musical Acoustics*, 251.

> bells always somewhat thicker than necessary, tuning them afterwards to the correct profile and frequency ratios.[68]

This description provides the clue to the importance of wall thickness and suggest possibilities for tuning the bell into a desired spectral profile. Since in FEM simulation all geometric parameters can be handled as geometric variables in the optimizing process, the way in which the wall thickness of the bell is converted to design variables will affect the geometric flexibility and computation-efficiency of the research output profoundly. The first attempt to build a major-third bell by Van Asperen (1984) by using the FEM was mainly driven by means of wall thickness variations.[69] Schoofs, who successfully realized the first major-third bell in 1985 together with Maas, put six points in his research on which the bell's wall thickness can be adjusted[70], and finally choose two points on the sounding bow (See figure 10) as design variables, which will be discussed later in details.

150 years after the death of Van Eyk and the Hemony brothers, Chladni (1802) realized that the variations in the wall thickness was a crucial factor in adjusting the spectral profile of bells.[71] In 1802, E. F. F. Chladni discovered that the frequencies of a vibrating circular plate with a free edge can be expressed as: $f_{m,n} = v(m + 2n)^p$ where m and n are the numbers of nodal meridians and circles, and v and p are appropriate constants.[72] By using an optimization process with the altered equation $f_{m,n} = v(m + bn)^p$, Perrin et al.[73] discovered optimal data results as

---

[68] Roozen-Kroon, "Structural optimization," 6.

[69] A. J. G. Schoofs, "Experimental design and structural optimization" (PhD diss., Department of Mechanical Engineering, Eindhoven, 1987), 6-10.
This attempted was not succeeded because the range of variation of the bell geometry was too restricted due to the fixed outer contour.

[70] Schoofs, 6-14.

[71] Roozen-Kroon, "Structural optimization," 7.

[72] Rossing, "The Acoustics of Bells," 440.

[73] Perrin, "Chladni's Law and the Modern English Church Bell," 1.

$\log_{10} v = 1.949$ and 2.231, $p = 1.810$ and 1.403, and $b = 0.805$ and 1.407, which are remarkably closed to the original spectral profiles of a Taylor Church Bell in a standard deviation of 0.0194 and 0.0159 respectively.

I used this formula and results in my work, *an air oscillates the earth bells for three days* (2011), to depict the various enigmatic sceneries occurring in the process of firing and cooling potteries. When the potteries enter into a three day cooling process after combustion and vitrification, they make diverse cracking and ringing notes, and this became the main idea of the piece. By using the equation, I generated various types of pseudo virtual bells with diverse chords and timbres. I chose b as [0.8, 1, 1.2, 1.4, 1.618] and p as [0.832, 1, 1.4, 1.618, 1.81, 1.91, 2, 2.28], and most of these numbers are from Perrin's experiment, which have relatively low deviations from the actual acoustical outputs of bell sounds, while some numbers are chosen intuitively. The v value is the fundamental frequency, selected from the B undertone series.

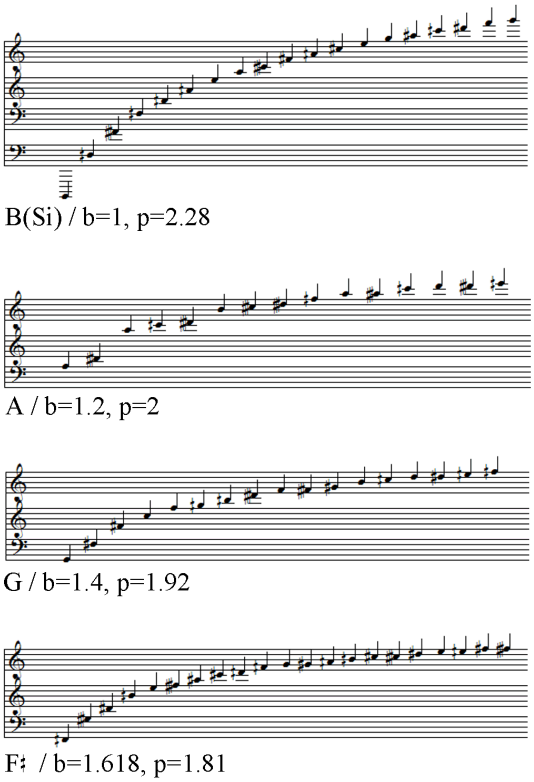

Figure 8. Harmonic fields based on B undertone series as fundamental notes and different B/P values generated by Chladni's Law.

Later, I used a similar Chladni sequence in the harmonic development section in my chamber orchestral work, *Horas*, which finally arrives on the section based on the real FEM bell sounds.

2.2 BELL PROFILE

Schneider introduces the bell geometry profile as follows (figure 9), originally illustrated by Geert van Wou from the 15th century.[74] Here the plate part which closes the bell at the top is called the head, to which the crown part is attached. The bell is installed to the headstock through the canon, which is included in the crown.

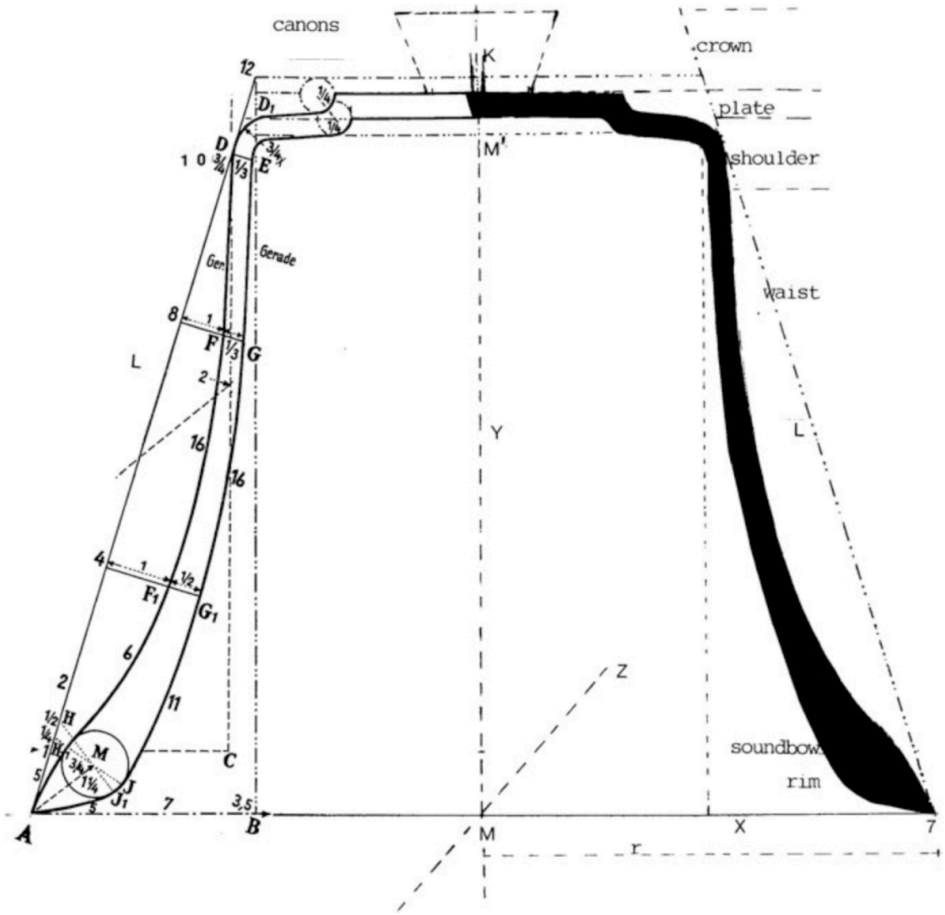

Figure 9. Bell wall profile, Gert de Wou.

More general names of the components of bell are introduced by Lehr, with the names of head, shoulder, waist, hip, lip, and sound bow, whose naming conventions and structural categories I

[74] Schneider, *Studies in Musical Acoustics*, 250, quoted in Klaus W., Ellerhorst, Handbuch der Glockenkunde (Weingarten, Württemberg: Verlag der Martinus-Buchhandlung, 1957).

use for the FEM optimization in this research. A bell can be struck by a clapper, a ball or pear-shaped object made of iron or manganese bronze that is hung inside the bell and attached to an iron shaft.[75] This can be also executed by a hammer outside. In both cases, there is a clapper or hammer hitting the sound bow from inside or outside respectively. The angle at which the clapper or hammer hits the bell is almost perpendicular to the circumferential direction.[76] A swinging bell is excited by a clapper that is triggered by swinging both the bell and clapper back and forth.

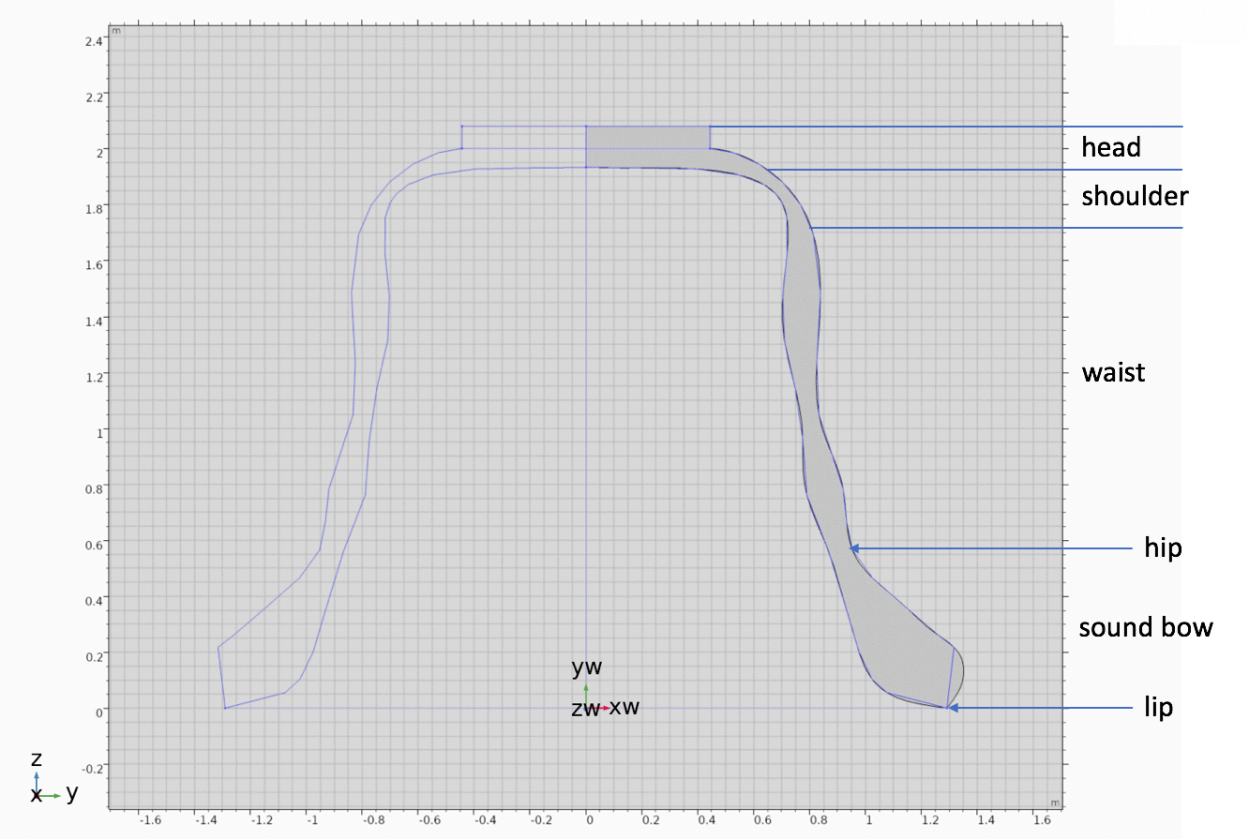

Figure 10. Profile of an optimized bell designed by the author.

[75] Lehr, *Campanology Textbook*, 11.

[76] Roozen-Kroon, "Structural optimization," 25.

2.3 MODAL VIBRATIONS

Perrin and Charnley analyzed and classified the first 134 eigenmodes of an English church bell by using the Finite Element package known as PAFEC (Program for Automatic Finite Element Calculations.)

> The finite element solutions show that there are two broad categories of mode: (1) those primarily in-azimuthal-plane but with some out-of-plane motion; (2) those primarily out-of-plane but with some in-plane motion. The primarily in-plane modes divide into two types which may be described as "ring driven" and "shell driven".[77]

The ring driven modes, which include three important low partials, Hum (2,0), Tierce–Minor third (3,1), and Nominal–Octave (4,1), is named as such because these modes include an antinode very close to the sound bow. The shell driven modes have a nodal circle near the waist, and also take important roles in the bell's timbre, belonging to Prime–Fundamental (2,1), Quint–Fifth (3,1a), and Tenth–Major third (4,1a), and higher eigenmodes. Note that most of these lower partials have only one nodal circle (n = 1). Perrin analyzed that the logarithmic eigenfrequencies result in each classified modal category is close to the linear relationship (as in the overtone series), and converges to the result of Chladni's research. Rossing demonstrated this with the following graph.

[77] Perrin, "Normal Modes of the Modern English Church Bell," 41. Note that he also mentions about other modes, including "Crown driven" modes, which are associated with the low amplitudes, thus are insignificant. (Perrin, 42.)

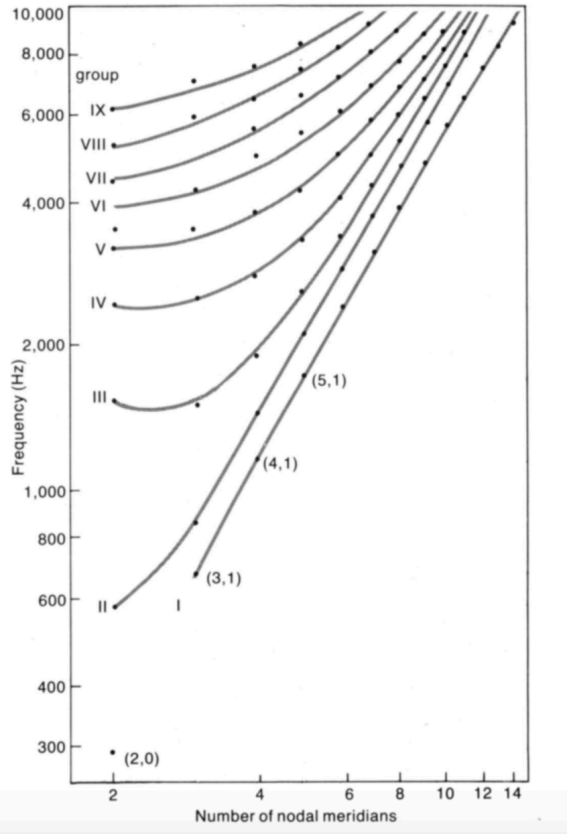

Figure 11. Logarithmic plot graph of eigenfrequencies, classified by each modal group.[78]

Here the roman numerals denote each modal class including the ring driven modes (class I), and shell driven modes (class II).

Table 1 shows the normal modes of vibration for a typical octave minor third bell. The data is from Lehr, Schneider, and Roozen-Kroon. Additional information (ratios and other modal names) is also indicated besides the pure just integer ratios. Lehr denotes that his ratios are measured from a c1 bell with a diameter of 1556 mm and a weight of 2310 kg with a canon, and Schneider and Roozen-Kroon do not indicate a specific data origin, but indicated as octave minor third bells (Schneider), and a traditional North European minor-third bell (Roozen-Kroon). I

[78] Rossing, *The Physics of Musical Instruments*, 443.

assume these are an ideal minor third bell. Also note that the first eleventh and second eleventh only appear on Lehr's table, which is based on a real physical bell.

Partial Name	Eigenmode Code	Carillon Notation	Frequency Ratio
Hum	(2, 0)	H-2, I-2	1
Prime (fundamental)	(2, 1)	F-2, II-2	2
Tierce (minor third, deciem)	(3, 1)	I-3	2.4
Quint (fifth)	(3, 1#)	II-3	3
Nominal (octave)	(4, 1)	I-4	4
major tenth	(4, 1#)	II-4	5 (original ratio), 5.04 (Schneider), 4.913(Lehr)
※Second eleventh (second undeciem)	(3, 2)	III-3	5.284 (Lehr)
※First eleventh (first undeciem)	(2, 2)	III-2	5.413 (Lehr)
Twelfth	(5, 1)	I-5	6
Double octave	(6, 1)	I-6	8
Double eleventh (upper fourth, undeciem)	(7, 1)	I-7	10.66 (Schneider), 10.872 (Lehr)
Upper major sixth	(8, 1)	I-8	13.46 (Schneider), 13.602 (Lehr)

Table 1. The names of the most important lower partials, and their respective modes of vibration
※: Lehr only

Note that the interval of a fourth, which was a prominent spectral feature of Harvey's Winchester bell is only indicated in Lehr's profile. Also note that partials which do not belong to the overtone series can be explained in terms of the undertone series. These partials are the Tierce, Eleventh (fourth), and Upper Major Sixth. Lehr indicated these partials with the ratio of "5:10:12:15:20 or 1/12:1/6:1/5:1/4:1/3,"[79] though he did not explicitly indicate that this follows the undertone series. Although, the undertone series cannot explain the ratio of the major tenth,

[79] Lehr, *Campanology textbook,* 20.

most of the low important modes can be included in the first 9 undertone partials (cents deviation not indicated):

ratio	1/1	1/2	1/3	1/4	1/5	1/6	1/7	1/8	1/9
pitch	G	G	C	G	E-flat	C	A	G	F
mode	Quint	Quint	Prime	Quint	Tierce	Prime	Upper Major Sixth	Quint	Eleventh

Table 2. G undertone series and their respective modes of vibration. Partial names are referring to C (1/3) as their fundamental.

These ratios in the undertone series also matches with the frequency ratios of 1.000:1.200(Tierce):1.500:2.000:2.500:2.667(Fourth):3.000:4.000:5.333(Upper fourth):6.667(Upper sixth), which is from a just-tuned 'ideal bell' that Rossing and Perrin suggested.[80] Note that only 17% of 363 church bells in Western Europe have the hum, the prime, and the nominal tuned in octaves.[81] In addition, the undertone series of the 'ideal bell' ratio suggested here only works for Western European bells, not for Oriental bells, especially ancient Chinese, Korean, and Japanese bells, which are beyond the scope of this paper. The spectral profiles of these bells are very different from Western bells, for example there are ancient Chinese bells which have two distinct strike tones. Rossing introduced these bells, which emit two different tones when struck at the zhéng-gǔ and cé-gǔ strike points. Two different categories of normal vibrational modes are excited separately by striking at these specific positions.[82]

The nodal lines of the first six partials of eigenfrequencies (Hum, Prime, Tierce, Quint, Nominal, and Major tenth) are depicted in Figure 12. Note that the bright area denotes the node

[80] T. D. Rossing and R. Perrin, "Vibration of Bells," *Applied Acoustics*, no. 20 (1987): 60.

[81] A. Lehr, *The Designing of Swinging Bells and Carillon Bells in the Past and Present* (Asten: Athanasius Kircher Foundation, 1987), quoted in Neville H. Fletcher and T. D. Rossing, *The Physics of Musical Instruments*, 2nd ed. (New York: Springer, 2010), 687; Read Appendix C for a distribution of various tunings among Western European church bells of the 363 church bells by Lehr.

[82] T. D. Rossing, "Acoustical Comparison of Ancient Chinese Bells with Western Bells," in *Two-Tone Set-Bells of Marquis Yi*, ed. Chen Cheng Yih (Singapore: World Scientific Publishing Co. Pte. Ltd., 1994), 384.

with the minimum displacement, and the dark area denote the antinode with the maximum displacement.

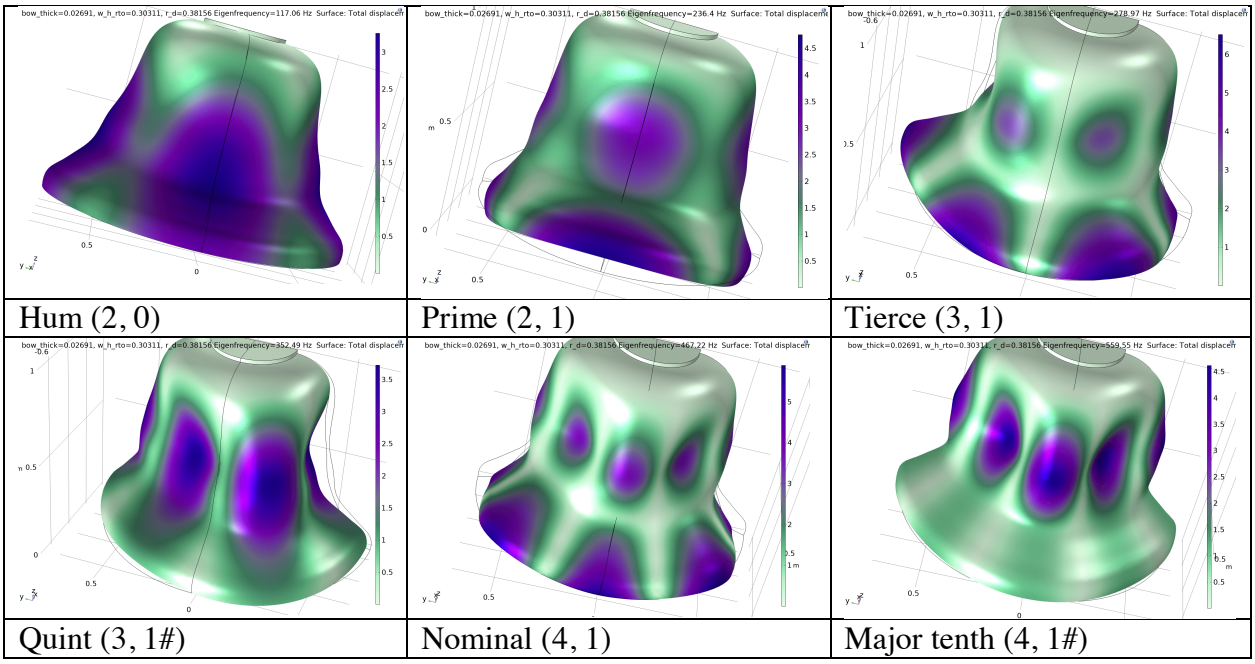

Figure 12. The first important six vibrational modes of a church bell.

Note that Tierce and Nominal have active vibrations on the sound bow, while Prime, Quint and Major tenth do not show the same vibrational behavior. This is because the nodal circle of Prime, Quint and Major tenth is positioned at the middle of the bell waist, while Tierce and Nominal have the nodal circle at the right above the sound bow, the very low part of the bell. For this reason, the Tierce and Nominal are classified as Group I (ring-driven mode), while Prime, Quint and Major tenth are classified as Group II (shell-driven mode). Group III has two nodal circles, one at the same height with Group I and the other at the position of Group II.[83]

Another acoustical feature of bell sounds is beating. There exist two perfect fourth interval partials (a ratio of 4/3) in the bell spectra of Lehr and the Winchester Cathedral of

[83] Read Rossing (1987) for more details.

Mortuos Plango, one is first eleventh (2, 2)–Group 3 and the other is the second eleventh (3, 2)–Group 3. Jonathan Harvey analyzes this as a phenomenon from the secondary strike notes, which build the overtone series of the fourth (F harmonic series, in Harvey's spectrum), having the partials in 5th, 7th, 9th, 11th, 13th, 17th order of F. I want to clarify that the F harmonic series that Harvey suggests are in octave displacements, meaning not in the original register of the natural overtone series. The phenomena of multiple fundamentals of bell spectra can be explained by the modal groups. As one can see in Figure 11, the partials in each group larger than the fourth meridian are converging to the overtone series linearly in the logarithmic frequency graph. This means each group form the overtone series based on different fundamentals, unless the fundamentals of each group are in a relation of prime number integer series. If the fundamentals of each group form an increasing prime number series, the overall output spectrum becomes the overtone series. (e.g, group 1 in 1, 2, 3, 4, …, group 2 in 2, 4, 6, 8, …, group 3 in 3, 6, 9, 12, … etc.) By deploying the overtone series from different fundamentals, one can create pseudo bell sounds without using actual bell acoustics. Likewise, Ligeti used overtones of multiple fundamentals from different natural horns and combined them together to create the ancient bell-like soundscape in his Hamburg concerto.

2.4 EIGENVALUES AND THE OVERTONE SERIES

The overtone series can be induced by using a differential equation, and eigenvalues and eigenvectors derived from the simple motion of string. A general way of inducing the overtone

series is using the 1-D wave equation.[84] From the 1-D wave equation $\frac{\partial^2 \mathrm{v}}{\partial \mathrm{x}^2} - \frac{1}{v^2}\frac{\partial^2 \mathrm{v}}{\partial\, \mathrm{t}^2} = 0$ where v is the instantaneous transverse displacement amplitude of the string and v is the longitudinal speed of wave, we can get two differential wave equations.[85]

$$\frac{\partial^2 \mathrm{v}}{\partial \mathrm{x}^2} = \frac{1}{v^2}\frac{\partial^2 \mathrm{v}}{\partial\, \mathrm{t}^2}$$

We try a product solution for the wave equation, i.e. displacement v at the point x at time t as v = U(x)T(t), where U(x) contains only spatially x-dependent terms and T(t) contains only temporary (i.e. time) dependent terms. By substituting v with U(x)T(t), we can explicitly carry out the differential equation:

$$\frac{\partial^2 \mathrm{U(x)T(t)}}{\partial \mathrm{x}^2} = \frac{1}{v^2}\frac{\partial^2 \mathrm{U(x)T(t)}}{\partial\, \mathrm{t}^2}$$

$$\mathrm{T(t)}\frac{\partial^2 \mathrm{U(x)}}{\partial \mathrm{x}^2} = \mathrm{U(x)}\frac{1}{v^2}\frac{\partial^2 \mathrm{T(t)}}{\partial\, \mathrm{t}^2}$$

$$\mathrm{T(t)}\frac{\mathrm{d}^2 \mathrm{U(x)}}{\mathrm{dx}^2} = \mathrm{U(x)}\frac{1}{v^2}\frac{\mathrm{d}^2 \mathrm{T(t)}}{\mathrm{dt}^2}$$

$$\frac{1}{\mathrm{U(x)}}\frac{\mathrm{d}^2 \mathrm{U(x)}}{\mathrm{dx}^2} = \frac{1}{v^2}\frac{1}{\mathrm{T(t)}}\frac{\mathrm{d}^2 \mathrm{T(t)}}{\mathrm{dt}^2} = k^2$$

Where k is the wavenumber, the number of radians per unit distance.

By using k, this equation can be separated into two differential/wave equations.

$$\frac{\mathrm{d}^2 \mathrm{U(x)}}{\mathrm{dx}^2} = -k^2 \mathrm{U(x)}$$

$$\frac{1}{v^2}\frac{\mathrm{d}^2 \mathrm{T(t)}}{\mathrm{dt}^2} = -k^2 \mathrm{T(t)}$$

Since $v = f\lambda$ (frequency × wavelength) $= (\omega/2\pi)(2\pi/k) = \omega/k$,

[84] For a derivation of the wave equation, please read CHAPTER 1. SAMPLE WAVE PROBLEMS, written by C. C. Mei from the course materials of Wave Propagation Course (2.062J), MIT Open Course Ware website [https://ocw.mit.edu/courses/mechanical-engineering/2-062j-wave-propagation-spring-2017] (accessed April, 2019.)

[85] This part is written based on Professor Steve Errede's "Acoustical Physics of Music PHY406" course materials which I attended in the fall of 2015 at the University of Illinois.

$$\frac{d^2U(x)}{dx^2} + k^2U(x) = 0$$

$$\frac{d^2T(t)}{dt^2} + \omega^2 = 0$$

Because the displacement amplitude at the ends of the string is zero (fixed ends), we have a boundary condition for fixed ends U(x=0) = U(x=L) = 0, where L is the length of the string. In general, there are only two allowed spatially periodic standing wave solutions to this equation – either $\sin kx$, or $\cos kx$. The boundary condition here allows only the $\sin kx$ type solution, because $\sin 0 = 0$, and $\sin kL = 0$ if and only if $kL = n\pi, n = 1, 2, 3, 4, \ldots$ Denoting $k_n = n\pi/L$, we see that the allowed standing wave solutions to the U(x) wave equation are of the form:

$$U_x(x) = A_n \sin(k_n x) = A_n \sin(n\pi x/L)$$

The boundary condition determines the frequencies of the eigenmodes/normal modes of vibration. Since $\lambda = 2\pi/k, \lambda_n = 2\pi/k_n = 2\pi L/n\pi = 2L/n, n = 1,2,3,4, \ldots$ Since $f = v/\lambda$, then $f_n = v/\lambda_n = nv/2L, n = 1,2,3,4, \ldots$

The fundamental frequency is generated when $n = 1$ and this vibrational standing wave eigen-mode is also known as the first harmonic, with $f_1 = v/2L$ and $\lambda_1 = 2L$, and the corresponding standing wave solution is $U_1(x) = A_1 \sin(k_1 x) = A_1 \sin(\pi x/L)$.

Another way of deriving the overtone series is by using the eigenvalue problem, which is discovered by Lagrange. This process can be regarded as a simpler version of the finite element procedure, since it discretizes a string into n+1 numbers of a small section.[86] Consider a long thin tight elastic string with fixed ends. If this string is subdivided into $(n + 1)$ number of segments

[86] Rajendra Bhatia, "Vibrations and eigenvalues," *Resonance* 22: 867-872, https://doi.org/10.1007/s12045-017-0540-8, accessed April 2019, https://www.ias.ac.in/article/fulltext/reso/022/09/0867-0872.

with negligible mass, and there are n points of mass m each placed along the string at regular intervals d. n is the number of points excluding the fixed end points. (Figure 13a)

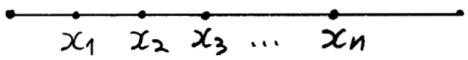

Figure 13a.

The string is pulled in the y-direction, and the points are displaced to positions $y_1, y_2, \ldots y_n$. The tension T is the string tension towards the initial fixed end. Let α be the angle between the string and the x-axis. (Figure 13b)

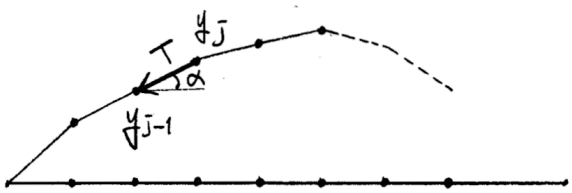

Figure 13b.

The downward tension is $T \sin \alpha$, and if α is small enough then $\sin \alpha$ becomes close to $\tan \alpha$.

$$T \tan \alpha = T \frac{y_j - y_{j-1}}{d}$$

Similarly, the tension in the opposite direction can be calculated.

$$T \frac{y_j - y_{j+1}}{d}$$

The total force exerted on the jth point is the summation of these two components:

$$\frac{T(2y_j - y_{j-1} - y_{j+1})}{d}$$

From Newton's second law of motion, $F = ma = m\ddot{y}$

$$m\ddot{y}_j = \frac{-T(2y_j - y_{j-1} - y_{j+1})}{d}$$

The minus sign indicates that the force is in the downward direction. Since we have n points on the line, we can express this as a matrix vector equation:

$$\begin{bmatrix} \ddot{y}_1 \\ \ddot{y}_2 \\ . \\ . \\ . \\ \ddot{y}_n \end{bmatrix} = \frac{-T}{md} \begin{bmatrix} 2 & -1 & & & & \\ -1 & 2 & -1 & & & \\ & -1 & 2 & & & \\ & & & . & & \\ & & & & . & -1 \\ & & & & -1 & 2 \end{bmatrix} \begin{bmatrix} y_1 \\ y_2 \\ . \\ . \\ . \\ y_n \end{bmatrix}$$

or

$$\vec{\ddot{\mathrm{Y}}} = \frac{-\mathrm{T}}{\mathrm{md}} \vec{\mathrm{B}}\, \vec{\mathrm{Y}}$$

where $\vec{\mathrm{B}}$ is the n × n matrix with entries $b_{ii} = 2$ for all i, $b_{ij} = -1$ if $|i - j| = 1$, and $b_{ij} = 0$ if $|i - j| > 1$. Here T represents the force, so its units are $\frac{mass \times length}{time^2}$. The units of $\frac{-\mathrm{T}}{\mathrm{md}}$ are $\frac{1}{time^2}$. As we did in our previous derivation of the 1-D wave equation, we can separate the temporal element from the displacement element here. (The $\vec{\mathrm{B}}$ matrix represents displacement amplitude factors in y directions.) If we solve the spatially y-dependent part of this equation

$$\ddot{y} = \vec{B}y$$

Again, since there is only a periodic standing wave solution to this equation, we know that the motion of each nodal point in the string is oscillatory, having an unknown displacement amplitude value u.

$$y(x) = (\sin \omega x)\, u$$

If we solve these two equations, we get

$$-\omega^2\, (\sin \omega x)u = (\sin \omega x)\vec{B}u$$

$$\vec{B}u = -\omega^2\, u$$

This means that u is an eigenvector of $\vec{B}$ corresponding to eigenvalue (eigenfrequency) $-\omega^2$. If we substitute $-\omega^2$ with λ, the characteristic equation $Bu = \lambda u$ can be rewritten as

$$-u_{j-1} + 2u_j - u_{j+1} = \lambda u_j, 1 \leq j \leq n$$

and the boundary conditions of fixed ends are

$$u_0 = u_{n+1} = 0$$

The trigonometric identity suggests that

$$-\sin(j-1)\alpha + 2\sin(j\alpha) - \sin(j+1)\alpha = (4\sin^2\frac{\omega}{2})\sin(j\omega)$$

and this suggests that $\lambda = 4\sin^2\left(\frac{\alpha}{2}\right), u_j = \sin(j\alpha)$. From the boundary condition $u_{n+1} = 0 = \sin((n+1)\alpha)$ and, $\alpha = k\pi/(n+1)$. Therefore, the n eigenvalues of $\vec{B}$ are

$$\lambda = 4\sin^2\frac{k\pi}{2(n+1)}, k = 1, 2, 3, \ldots, n.$$

If λ is expressed with ω, this suggests that the string's eigenfrequencies build up the overtone series.

2.5 INHARMONIC BELLS AND NEW HARMONIC PROFILES

In this sub-chapter, I explain how I created just-tuned quinta-chords to which my low bell partials (hum, prime, tierce, quint, and nominal) are tuned. Each bell profile has five low partials that are mutually consonant in the just tuning ratio. (See Figure 14a.) To create multivalent bell tone colours, which are not limited to the equal temperament system, I write how I redefined the idea of consonance, and created consonant quinta-chords to which my bell spectral profiles will be tuned to.

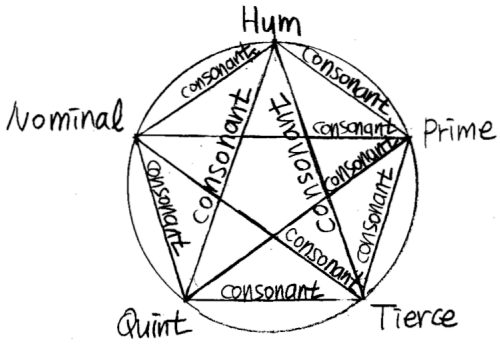

Figure 14a Hum, prime, tierce, quint, nominal partials are mutually consonant to each other.

Inharmonic Bells

As the distribution of various Western European church bells that Lehr suggested (Appendix C) shows, the majority of Western European church bells do not follow the ideal undertone ratios in their lower partials. It is not clear if these non-octave bells are casted intentionally or by a failure. However, as Lehr indicated, these so-called failed octave bells have their own charm:

> They are not false bells. The critical band width is heard; overtones cannot form dissonances with each other as long as they are more than a minor third removed from each other. Again, when two organ pipes form dissonances, the cause is fighting overtones. But since the partials from a bell are themselves [inharmonic] overtones, it is not a question of dissonance.[87]

Here Lehr is describing the idiosyncratic harmonic profile of non-octave bells as a composite timbre created by a single medium, which shares the same idea with the Parisian spectralist composers. These intervals from the lower partials of non-octave bells can be regarded as consonance, depending on how we define the range of consonance.

[87] Lehr, *Campanology textbook*, 50.

Definitions of consonance and dissonance

As Western music history suggests, the idea and ambit of consonance and dissonance have been always variable and arguable, sometimes propounded as even developing or being emancipated by Webern and Schoenberg. Helmholtz defined consonance as

> the coincidence of two of the upper partial tones of the compounds forming the chord. When this is the case the two compound tones cannot generate any slow beats. […] When two such musical tones are sounded together, there will be not only the dissonances resulting from the higher upper partial tones in each individual compound, but also those which arise from a partial tone of the one forming a dissonance with a partial tone of the other, and in this way there must be a certain increase in roughness.[88]

The level of dissonance, or the 'relative distance' increases if the integer ratio between two fundamental becomes larger, which means a higher overtone ratio relation, which in turn creates more beats. Helmholtz suggested consonance intervals in an order of harmoniousness from octave to fifth, fourth, and major and minor third (imperfect consonances). In a musical context, Johann J. Fux, whose "Gradus ad Parnassum (1725)" was studied by both Haydn and Beethoven, considered the unison, third, fifth, sixth, and octave as perfect or imperfect consonances, and second, fourth, tritone, and seventh as dissonances. In counterpoint, a consonant chord has multiple pitches, which are in consonant interval relations with all of the other pitches.[89] Rameau defines consonance as "[…] an interval the union of whose sounds is very pleasing to the ear. The intervals of the third, the fourth, the fifth, and the sixth are the only consonances," and dissonance as "This is the name for intervals which, so to speak, offend the ear."[90] James Tenney

---

[88] Hermann L. F. Helmholtz, *On the Sensations of Tones*, 4th ed., trans. Alexander J. Ellis (Peternoster Row: Longmans, Green, and Co., 1912), 187–188.

[89] A fourth can be regarded as a consonant interval is it is not partaking the lowest pitches of a chord.

[90] Jean-Philippe Rameau, *Treatise on Harmony* (1722), translated by Philip Gossett (New York: Dover, 1971), p. xli. quoted in James Tenney, *A History of 'Consonance' and 'Dissonance,'* (New York: Excelsior Music Publishing, 1988), 65.

(1934–2006) explains this as "[…] aggregates other than dyads had been dealt with at all by earlier theorists, the properties of chords depended entirely on those of their constituent intervals."[91] Schoenberg's definition of consonance is closer to that of Fux, which is the closer and simpler relations to the fundamental tone, while dissonance is defined as those that are more remote, more complicated.[92] Paul Hindemith, whose theoretical background is thoroughly based on acoustical analysis, also has a similar approach to that of Schoenberg:

> To a given tone, the tone an octave higher stands in so close a relationship that one can hardly maintain a distinction between the two. The tone which is only a fifth higher than the given tone is the next mostly closely related, and there follow in order the fourth, the major sixth, the major third, the minor third, and so on.[93]

However, unlike Schoenberg, Hindemith was really thinking about the interval as a qualitative value, having the integer series ratios from the overtone series, not scalar or quantitative unit: "I shall simply follow the suggestions which to the understanding ear lie hidden in the overtone series, and shall thus arrive at a simple and natural construction of the scale." From this premise, Hindemith builds his scale by using the integer ratio and frequencies in the series of C (= 1, 64 Hz) – G (= 3/2, 96 Hz) – F (= 4/3, 85.33) – E (= 5/4, 80) and so on,[94] although he rejected using microtonal intervals including the seventh overtone since it will cause conflicts with the

---

[91] James Tenney, *A History of 'Consonance' and 'Dissonance,'* (New York: Excelsior Music Publishing, 1988), 67. Note that Tenney here tries to emphasize not the inner-relationships between notes in a chord, but tries to emphasize the importance of a fundamental note to which all the pitch members of the chord belongs, and groups them into one harmonious overtone series: "But merely noting the fact of this reversal is still not sufficient to characterize the innovative nature of Rameau's position here, because–in his view–these chords only derive *their* properties from the *son–fodmental–the* "fundamental sound" or "source." Tenney defines consonance and dissonance in five different categories–1. monophonic or melodic, 2. diaphonic, 3. polyphonic or contrapuntal, 4. triadic, 5. timbral. The new concept of 'consonance' in this chapter includes Tenney's CDC (Consonance / Dissonance – Concept) 3, 4, and 5. Read Tenney for more information.

[92] Arnold Schoenberg, *Theory of Harmony*, 3rd ed., trans. Roy E. Carter (Berkeley: University of California Press, 1922), 21.

[93] Hindemith, *The Craft of Musical Composition*, 54.

[94] Hindemith, *The Craft of Musical Composition*, 33–34.

predefined scalar system.[95] This contradicts Webern's prediction, in which the advent of the microtone is a matter of time: "So, a note is, as you have heard, complex–a complex of fundamental and overtones. … there's nothing against attempts at quarter-tone music and the like; the only question is whether the present time is yet ripe for them. … that form the diatonic scale. But what about the notes that lie between? Here a new epoch begins, and we shall deal with it later."[96] American composer Ben Johnston (1926–2019) followed the direction that Webern predicted, and which Partch pioneered later on. Johnston defines consonance intervals as having simpler vibrational ratios. Based on this approach, he employed intervals from prime number integers such as 3, 5, 7, 11, 13 especially in his extended just intonation system, which have a certain amount of cents deviations from equal temperament.[97] Harmonies employing these ratios in Johnston's music sounds lucid and pure, which do not 'distort the tuning of such "overtones" and not taming down the expressive impact they have.'[98]

Threshold

To create just ratio based bell spectra, I define consonant interval in this thesis as the interval which is represented by just ratios smaller than a given maximum integer, within a predefined cents deviation from the equal temperament. Here I will call the cents deviation from just intervals as 'threshold,' following Donnacha Dennehy's term.[99] For example, the equal

[95] Hindemith, *The Craft of Musical Composition*, 37.

[96] Webern, *The Path to the New Music*, 15.

[97] The word 'deviation' would be controversial here, since actually the tones of equal temperament tuning system have cents deviations from the just ratio based tuning.

[98] Ben Johnston, "A Notation System for Extended Just Intonation," in *Maximum Clarity and Other Writings on Music*, ed. Bob Gilmore (Urbana: University of Illinois Press, 2006), 82.

[99] At the forum at the University of Illinois in 2018, and also in a personal conversation with him. Dennehy also mentioned that the term, "threshold" was first used by James Tenney.

temperament major third can be consonant within the threshold of 15 cents, but should be categorized as dissonance within the threshold of 5 cents, since a just major third is 13.7 cents lower than the equal tempered major third. (See Figure 14b.) By employing the idea of threshold, now we can define the concept of dissonance in two categories:

> 1. An interval made up with the ratio of a prime integer which is larger than the maximum predefined consonant ratio (type–1 dissonance, e.g., 17/8 if the largest consonant interval ratio is 16.) or the ratio in a form which the numerator and denominator do not share a common devisor and are larger than the maximum predefined consonant ratio. (e.g., 40/27.) Either numerator or denominator can be divided by any power of 2 to allow for octave transpositions.
>
> 2. A tempered interval which approximate a simple integer ratio but the cents deviation compared with that ratio interval is larger than a given threshold. (type–2 dissonance, e.g., an equal tempered major third within the context of a 10 cent threshold.)

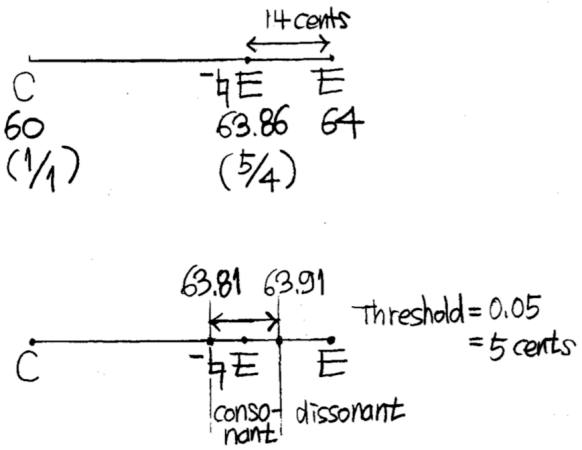

Figure 14b. Equal temperament major third and just major third (upper figure), and the consonance area within the threshold of 5 cents of 5/4 ratio–just tuned major third (lower figure).

The main purpose of utilizing the idea of threshold is mainly to find chords from the scale which includes an unlimited number of intervals. These intervals can be engendered collaterally by either scale–lattice operations or equal division operations. Here the scale–lattice operation denotes a procedure of creating the scale, based on a certain number of ratios, and keeps creating the sub-scales and sub-ratios by using the higher order pitches and ratios. For example, in

Pythagorean C major scalar operation, 3/2 and 2/3 can be the prime low order ratio, and ratios that are collaterally created from this integer ratio including 4/3, 9/8, 16/9, 27/16, 32/17, 81/64, 243/128 are higher order sub-ratios.[100] This ratio discrepancy of large integers (higher order sub-ratios) can come from the employment of both overtone and undertone ratios in the same harmony in the just tuning system. Here the undertone ratio denotes ratios that have a prime number other than 2 as a multiplier in its denominator (e.g., 2/3, 4/7, …etc.,) and the employment of undertone ratios in the overtone ratio-based just scale and vice versa can cause unanticipated problems. Even in the C just major scale, the just major sixth, A, is in the undertone ratio of 5/3 with C. The problem arises between pitches which do not share a common divisor in their denominators. D in a C major scale is in the ratio relationship of 9/8, and the resultant ratio between D (overtone ratio–based pitch) and A (undertone ratio–based pitch) in a C just major scale becomes 40/27, not 3/2. Table 3 demonstrates the just ratios in the C just major scale.

C	D	E	F	G	A	B	C’
1	9/8	5/4	4/3	3/2	5/3	15/8	2

Table 3. Ratios of C just major scale

These integers in just ratios become larger (further from simple integer ratio intervals–more dissonant than consonant), if larger undertone ratios are employed in the tuning system. For example, the ratio between the seventh undertone (8/7) and just major third (5/4) is 35/32, which is a slightly smaller than just major second, 9/8 = 36/32.

[100] Read Ben Johnston, “Scalar Order as a Compositional Resource” in *Maximum Clarity and Other Writings on Music*, 10-31 for a more detailed procedure of expanding sub-order ratios and pitches from a scale.

This shows that employing overtones and undertones in a single scale without a threshold creates type–1 dissonance, and with a small threshold creates type–2 dissonance. For example, in a C just major scale without a threshold, the D minor triad becomes a type–1 dissonance (the ratio of 40/27), and if the threshold is set to 5 cents, D-F-A becomes a type–2 dissonance since the discrepancy between just minor sixth (5/3) and 40/27 is about 22 cents, which is larger than 5 cents.

96TET Scale

The idea of using a threshold can suggest a relatively practical solution with innovative sounds if the threshold is set from 5 to 6 cents. 5 cents is about the minimum amount of frequency that our ear can detect as a frequency change, which is called *just-noticeable difference* (JND): "From 1000 to 4000 Hz, the JND is approximately 0.5 percent of the pure tone frequency, which is about one-twelfth of a semitone."[101] Here one-twelfth of a semitone is 8.33 cents. The frequency resolution Δf in JND remains almost the same when the frequency is lower than 500 Hz, which means that the just noticeable difference will be smaller than 8.33 cents for frequencies lower than 500 Hz. Kollmeier et al. note that the JND is about 3 Hz for these frequencies.[102] If we fix the JND as 3 Hz, for A4 it would be 12 cents, for A3 it would be 24 cents, and for A2 it would be 48 cents. Note that this result is calculated by using pure sine tones. For more complex tones, JND becomes even smaller. For example, for a complex wave such as a human voice between 80 Hz and 500 Hz, the JND goes down to approximately 1 Hz. A 1 Hz change from 500 Hz converts to 3.4 cents. Because of this aspect of psychoacoustical hearing, I

[101] Rossing et al., *The Science of Sound*, 123.

[102] B. Kollmeier, T. Brand, and B. Meyer, "Perception of Speech and Sound," in *Handbook of Speech Processing*, ed., Jacob Benesty, M. Mohan Sondhi, and Yiteng Huang, (Berlin: Springer-Verlag, 2008), 65.

set the threshold of my tuning system to 5 cents. 5 cents is also the cent deviation between the 96 TET minor second (117 cents, between C and C-sharp + a twelfth sharp) and the just minor second interval-15:16, 112 cents.

The 96 TET scale is created by adding equal tempered microtonal pitches to the 12 tone equal temperament (12 TET) system, including a quarter tone above each 12 TET note, a sixth tone above and below each 12 TET note, a twelfth tone above and below, and 41 cents above and below: 12 (12 TET) + 12 (quarter-tones) + 24 (sixth tones) + 24 (twelfth tones) + 24 (41 cents tones). Here the quarter tones are employed for the ratio of 11/8 (11th partial ratio), sixth tones for 7/4 (7th partial), twelfth tones for 5/4 (5th partial / just major third), and 41 cent deviations for 13/8 (13th partial ratio). In 96 TET, I expect our brain can tune the interval to the nearest consonant just intervals with relatively small ratio integer values. Note that the actual quarter-tone and 11/8 just ratio has a discrepancy of 1 cent, a sixth tone + 12 TET major second and 7/8 just ratio has a discrepancy of 2 cents, and a twelfth tone + 12 TET major third and 5/4 has a discrepancy of 3 cents.

Table 4 shows consonant intervals in the 96 tone equal temperament tuning system within the threshold of 5 cents, having the maximum just integer ratio of 16. All intervals in this table are consonant as I have defined it for the purpose of demonstration with a threshold of 5 cents, which do not belong to either type–1 and type–2 dissonance. Note that the ambit of consonance and dissonance in this context can vary based on how a composer defines the threshold and the maximum consonant integer ratio for a given compositional purpose. The numbers in the table denote the MIDI key value with cents values in decimal points (1 cent = 0.01 MIDI key value).

note I	note II	ratio I	ratio II	original note II in just tuning	deviations(cents)
60	60.00	1	1	60	0
60	61.17	15	16	61.12	5
60	61.41	12	13	61.39	2
60	61.50	11	12	61.51	1
60	61.67	10	11	61.65	2
60	61.83	9	10	61.82	1
60	62.00	8	9	62.04	4
60	62.33	7	8	62.31	2
60	62.50	13	15	62.48	2
60	62.67	6	7	62.67	0
60	63.17	5	6	63.16	1
60	63.50	9	11	63.47	3
60	63.59	13	16	63.59	0
60	63.83	4	5	63.83	0
60	64.17	11	14	64.18	1
60	64.33	7	9	64.35	2
60	64.50	10	13	64.54	4
60	65.00	3	4	64.98	2
60	65.33	11	15	*65.37	4
60	65.41	11	15	*65.37	4
60	65.50	8	11	65.51	1
60	65.83	5	7	65.83	0
60	66.17	7	10	66.17	0
60	66.33	9	13	*66.37	4
60	66.41	9	13	*66.37	4
60	66.50	11	16	66.49	1
60	66.67	22(11)	15	66.63	4
60	67.00	2	3	67.02	2
60	67.50	20(10)	13	67.46	4
60	67.67	9	14	67.65	2
60	67.83	7	11	67.82	1
60	68.17	5	8	68.13	4
60	68.41	8	13	68.41	0
60	68.50	18(9)	11	68.53	3
60	68.83	10	6	68.84	1
60	69.33	7	12	69.33	0

Table 4. Consonant intervals within the ratio of integer 16, under 5 cents threshold in 96-TET tuning.

60	69.50	26(13)	15	69.52	2
60	69.67	7	4	69.69	2
60	70.00	16	9	69.96	4
60	70.17	9	5	70.18	1
60	70.33	20(10)	11	70.35	2
60	70.50	11	6	70.49	1
60	70.83	15	8	70.88	5

Table 4, Continued.

Note that there are 28 intervals that can't exist in the 12 TET system, which includes 12/11 (undecimal neutral second), 8/7 (septimal whole tone), 15/13, 7/6 (septimal minor third), 11/9 (neutral third), 13/10, 13/8 (tridecimal neutral sixth), 7/4 (harmonic seventh), … etc.[103]

New Bell Harmonies

For tuning the bell, I decided to use the five lowest modes: Hum, Prime, Tierce, Quint, and Nominal. Harmonies that I decided to use for bell spectral profiles employ the intervals in Table 4 with the just ratio. These five low partials of the bell will be tuned to a pentachord, which are created by the following algorithm:

1. Create all possible 5 pitches chords from 96 TET scale and save them into an array (This will create $_{96}C_5$ numbers of quinta-chords)

2. Compare all intervals in each quinta-chord in the array and check if there is a dissonance–type 1 and 2 (by using a boolean flag)

3. Remove the quinta-chord from the array if the chord includes at least one dissonant interval

Algorithmically, if there is no duplicated pitches in the chord, we can make 329 consonant quinta-chords in the 96 TET system. Table 5 shows the first 12 chords in this setting.

[103] Interval names here are cited from "List of intervals," Huygen-Fokker Foundation Center for Microtonal Music, accessed January 21, 2020, http://www.huygens-fokker.org/docs/intervals.html.

note 1	note 2	note 3	note 4	note 5
60.00	61.41	65.59	67.00	69.50
60.00	61.41	67.00	68.83	70.50
60.00	61.50	65.33	67.83	70.33
60.00	61.50	65.83	67.83	70.33
60.00	61.50	68.50	69.67	70.83
60.00	61.67	64.17	66.67	70.50
60.00	61.67	68.17	69.33	70.50
60.00	61.83	64.33	65.41	68.83
60.00	61.83	66.33	67.50	69.50
60.00	61.83	67.67	68.83	70.33
60.00	62.00	68.50	69.67	70.83
60.00	62.33	68.17	69.33	70.83

Table 5. 12 consonant quinta-chords in 96 TET with threshold 5 cents.

The first chord of Table 5 has the following intervallic ratios: 60:61.41=12:13, 60:65.59=9:13, 60:67=2:3, 60:69.5=13(23):15, 61.41:65.59=7:11, 61.41:67=9:13, 61.41:69.5=5:8, 65.59:67=12:13, 65.59:69.5=5:4, 67:69.5=13:15.[104]

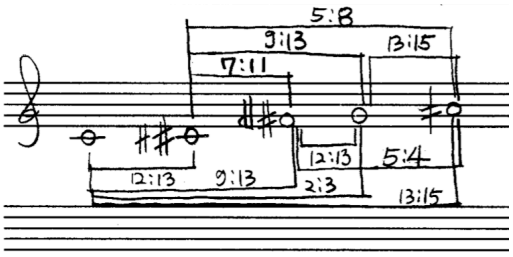

Figure 14c. Consonant intervals in the quinta-chord from Table 5.

[104] To read more about just tuning ratio based harmonies, read Robert Hasegawa, "Just Intervals and Tone Representation in Contemporary Music," (PhD diss., Harvard University, 2008), Tim Johnson, "13-Limit Extended Just Intonation in Ben Johnston's String Quartet #7 and Toby Twining's Chrysaiid Requiem, "Gradual/Tract," (DMA diss., University of Illinois at Urbana-Champaign, 2008).

The accidentals I use here are adopted from Marc Sabat's *Helmholtz-Ellis Accidentals*.[105] Note that the exact usages of microtonal accidentals are different from Marc Sabat's, since in my notation the basic scale without accidentals denote 12 TET C major scale, not a just tuned major scale as in Sabat's system. Also note that the notation of the sixth tone and twelfth tone is switched, following the notation of Austrian composer, Georg Haas (See Figure 15.). This decision was made after consulting with Claudius von Wrochem, the cellist of Kairos Quartett who performed multiple works by Haas. For the 13th partial, I used the same notation from Sabat with altered cents adjustments, 𝅘𝅥𝅯 for 41 cents flat and 𝅘𝅥𝅰 for 41 cents sharp.

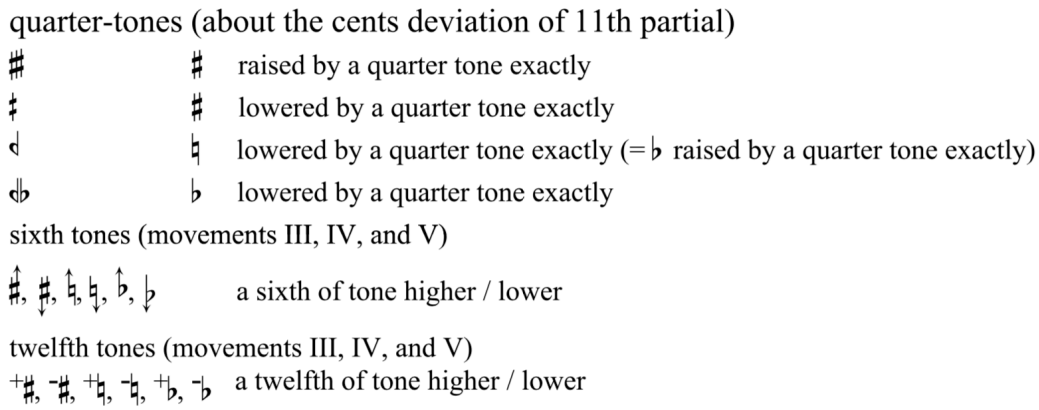

Figure 15. 72 TET microtonal notation in *Unending Rose*

I used harmonies created by this algorithm in my string quartet, *Unending Rose* (2017–2019), and then adopted the same algorithm for creating bell harmonic profiles. Instead of randomly choosing harmonies from 329 (without doubling pitch) or more (with doubling) quinta-chords, I made a certain amount of quinta-chord harmonies intuitively based on voice leading with the original ideal just minor third bell spectrum (Table 1 and 2), and added more quinta-chords by

[105] Marc Sabat, "An informal introduction to the Helmholtz-Ellis Accidentals," *Marc Sabat : music & writings*, accessed January 22, 2020, http://www.marcsabat.com/pdfs/legend.pdf.

"tuning" the inharmonic bell profiles that Lehr suggested as non-octave bells to 96 TET system with consonant ratios under 16 and the threshold of 5 cents. As result, the five lower modes will create a quinta-chord following the spectral physiognomy of the original minor third bell, but the intervallic content of each voice can be altered, but will maintain the consonant quality of just ratios under 16 within the given threshold, 5 cents. Figure 16 shows the 24 quinta-chords that are used as the five lowest eigenfrequencies of virtual bells, and Figure 17 are the quinta-chords that are adopted from Lehr and retuned to 96 TET for virtual bell profiles. See Appendix E for the 2D geometry of 31 virtual bells, which corresponds to these bell harmonies.

Name of the Bell	I-2	II-2	I-3	II-3	I-4
major sixth bell with doubly diminished prime	E_{b3}	B_{b3}	E_{b4}	F_4	C_5
major seventh bell with diminished prime	$C_{\#3}$	B_3	E_{b4}	$F_{\#4}$	C_5
minor octave bell with pure prime	C_3	C_4	E_{b4}	G_4	C_5
minor octave bell with diminished prime	C_3	B_3	E_{b4}	G_4	C_5
major octave bell with pure prime	C_3	C_4	E_4	G_4	C_5
minor ninth bell with augmented prime	B_2	$C_{\#3}$	E_{b4}	G_4	C_5
minor ninth bell with diminished prime	B_2	B_3	E_{b4}	$F_{\#4}$	C_5

Table 6. Non-octave bells that Lehr suggested (Lehr, *Campanology textbook*). Octave transposition performed by the author

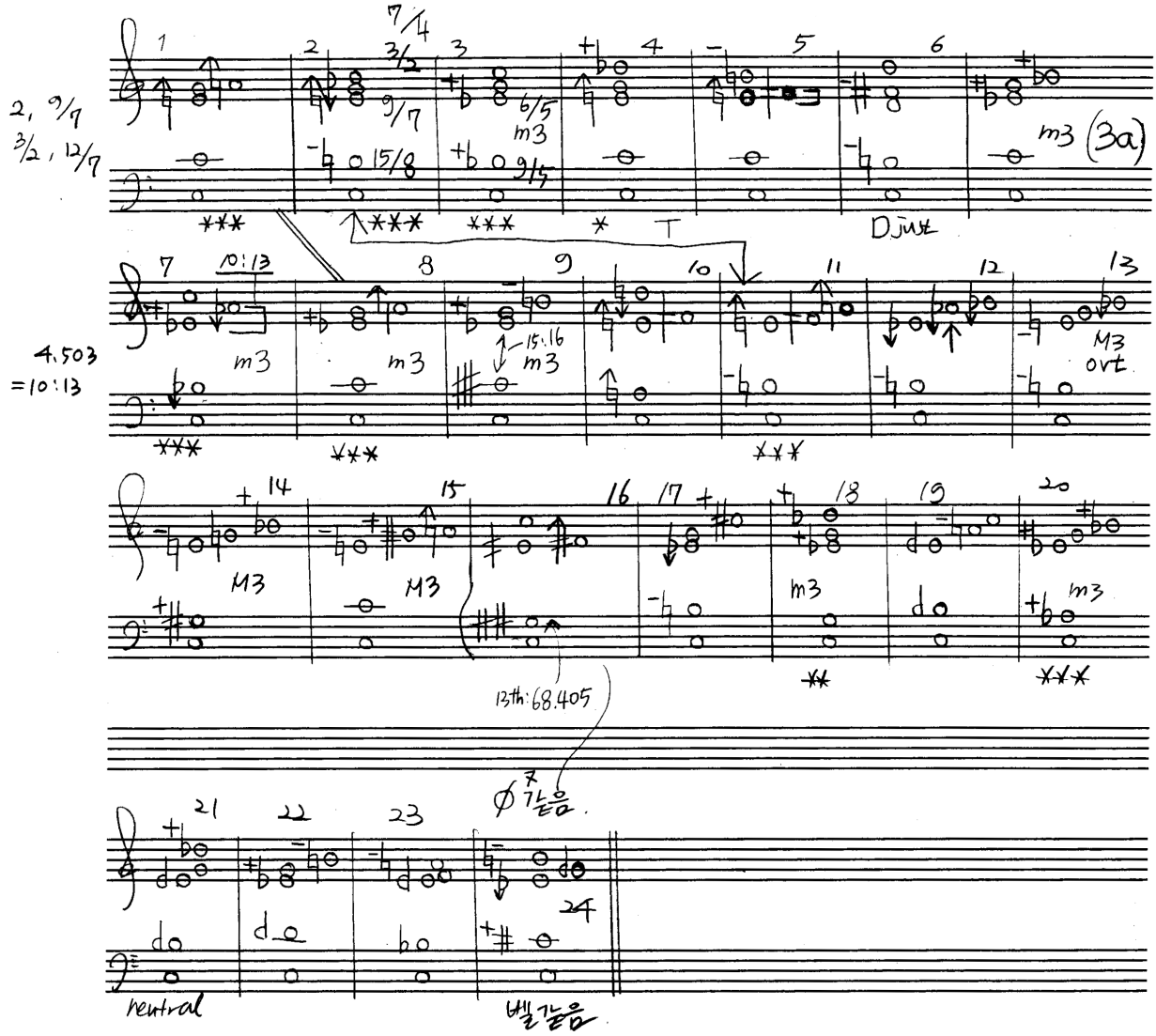

Figure 16. 24 quinta-chords that are used for five low partials for virtual bells. From the original sketch by the author.

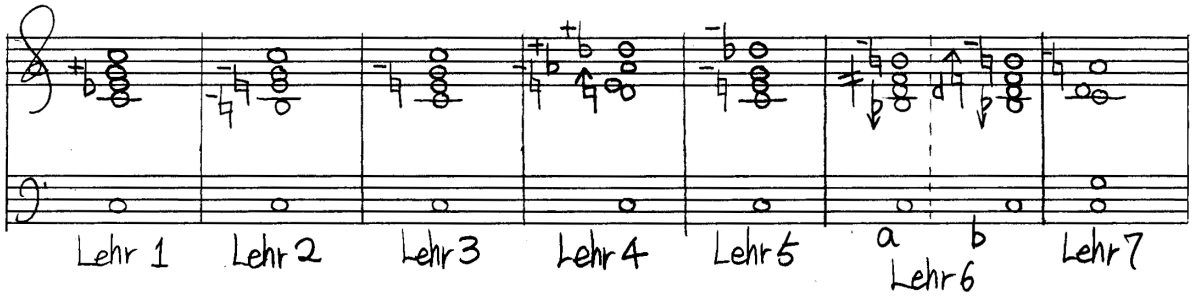

Figure 17. Adopted just tuned quinta-chords from Lehr's inharmonic bell profiles.

CHAPTER 3: FINITE ELEMENT METHOD OF ISOPARAMETRIC 2-D ELEMENTS

3.1 BASIC THEORY

The constitutive relation is

$$\text{stress (force per unit area) } \sigma = E\,\varepsilon$$

where E is Young's modulus, and ε is strain $\varepsilon = \frac{\partial u}{\partial x}$ where ∂u is the displacement of the given point, and ∂x is the infinitesimal length of the x direction. We get $\sigma = E\frac{\partial u}{\partial x}$.

The load that this stress is creating, is $F = A\,\sigma$ where A is the total area.

The problem governing the differential equation in a simple structural analysis is

$$\frac{\partial^2 u}{\partial x^2} = \frac{1}{c^2}\frac{\partial^2 u}{\partial t^2}\ ,\ c = \sqrt{\frac{E}{\rho}} \qquad \textbf{(1.1)}$$

where E is Young's modulus and ρ is the mass density.[106]

This equation can be derived from an element force equilibrium status

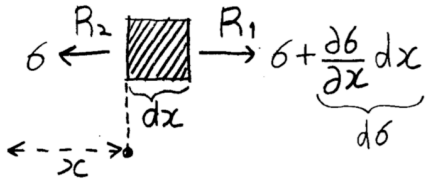

Figure 18. with Area A and mass density ρ.

[106] Most of the physical and mathematical derivations of equations used here are both from my own analysis and from Klaus-Jürgen Bathe's book, "Finite Element Procedures (Jew Jersey: Prentice Hall, 1996)" and its corresponding MIT open courseware (OCW) online lecture "Finite Element Procedures for Solids and Structures" at [https://ocw.mit.edu/resources/res-2-002-finite-element-procedures-for-solids-and-structures-spring-2010] with his own textbook- "Complete Study Guide" written for this course, which is available at [https://ocw.mit.edu/resources/res-2-002-finite-element-procedures-for-solids-and-structures-spring-2010/linear/MITRES2_002S10_linear.pdf] (accessed December, 2018)

d'Alembert's force F can be expressed in terms of the applied force $R_1 - R_2 = F$.

$$F = ma = \rho Aa = \rho A\frac{\partial^2 u}{\partial t^2} \qquad \textbf{(1.2)}$$

$$R_1 = \text{force}\,|_x + \text{force}\,|_{x+dx} = \rho A\,|_x + A\frac{\partial \sigma}{\partial x}\,|_x\,dx\ ,\ R_2 = \text{force}\,|_x$$

Combine the three equations above we obtain

$$A\frac{\partial \sigma}{\partial x}\,|_x\,dx = \rho A\frac{\partial^2 u}{\partial t^2}$$

By applying the stress $\sigma = E\,\varepsilon = E\frac{\partial u}{\partial x}$ then we get

$$\frac{\partial^2 u}{\partial x^2} = \frac{\rho}{E}\,\frac{\partial^2 u}{\partial t^2} \text{ by substituting } \frac{1}{c^2} = \frac{\rho}{E} \text{ we get}$$

$$\frac{\partial^2 u}{\partial x^2} = \frac{1}{c^2}\,\frac{\partial^2 u}{\partial t^2}$$

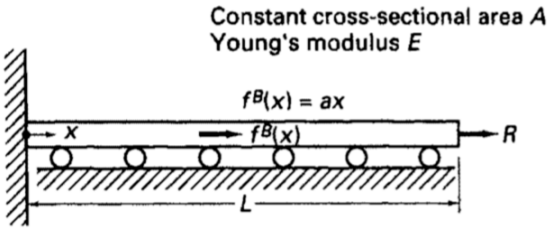

Figure 19. [107]

If a bar (beam) is connected on the wall (Figure 19), the boundary conditions are

1. $u(0, t) = 0$ essential boundary condition
2. $EA\frac{\partial u}{\partial x}(L, t) = R_0$ natural boundary condition

[107] Bathe, 124.

The essential boundary condition means that there is no displacement at the point where x = 0 (on the wall), and the natural boundary condition means that the prescribed boundary force at the right end of the bar $R_0 = A\sigma = AE\frac{\partial u}{\partial x}$ where x=L.

3.2 PRINCIPLE OF VIRTUAL DISPLACEMENT IN THE FINITE ELEMENT METHOD AND GAUSS QUADRATURE

The total potential energy of a rod can be expressed as $\Pi = U - W$ where U is the strain energy of the rod and W is the total potential of the rod.

This equation can be expressed with a variational formulation.

Since U is the strain energy $U = \frac{1}{2} V\sigma\varepsilon = \frac{1}{2} VE(\frac{\partial u}{\partial x})^2$, for a rod

$$U = \int_0^L \frac{1}{2} EA(\frac{\partial u}{\partial x})^2 dx$$

W = total potential of the rod = body force + point force = $\int_0^L u f^B dx + Ru|_{x=L}$ where R is the force applied at the point x = L. Thus, we have

$$\Pi = \int_0^L \frac{1}{2} EA(\frac{\partial u}{\partial x})^2 dx - \int_0^L u f^B dx - R_u|_{x=L}$$

The stationary condition $\delta\Pi = 0$ gives

$$\int_0^L (EA\frac{\partial u}{\partial x})(\delta\frac{\partial u}{\partial x}) dx - \int_0^L \delta u f^B dx - R\,\delta u|_{x=L} = 0$$

(2.1) Principle of Virtual Displacement

This is the Principle of Virtual Work (PVW) / Principle of Virtual Displacement, where δ means "variation in" and δu is an arbitrary variation on u subject to the condition $\delta u|_{x=0} = 0$.[108]

[108] Please read Bathe p. 124-125 for more details.

This can be explained as "A structure is in equilibrium under a set of external loads if after imposing to the structure arbitrary (virtual) displacements compatible with the boundary conditions, the work performed by the external loads on the virtual displacements equals the work performed by the actual stresses on the strains induced by the virtual displacements."[109] In general, this principle is written as the following formula (2.2) by replacing real stress $\int_0^L \mathrm{EA}\frac{\partial \mathrm{u}}{\partial \mathrm{x}}$ with $\int_V \ \underline{\tau}$, variational strain $\int_0^L \delta \frac{\partial \mathrm{u}}{\partial \mathrm{x}}$ with arbitrary virtual strain $\int_V \ \delta \underline{\varepsilon}^{\mathrm{T}}$, variation in displacement $\int_0^L \delta u$ with $\int_V \ \delta \underline{\mathrm{U}}^{\mathrm{T}}$, operating body force $\int_0^L \mathrm{f}^{\mathrm{B}}$ with $\int_V \ \underline{\mathrm{f}}^{\mathrm{B}}$, vibration of the surface displacement (virtual displacement) $\delta \mathrm{u}\,|_{\mathrm{x=L}}$ with $\int_S \ \delta \underline{\mathrm{U}}^{\mathrm{S}^{\mathrm{T}}}$, and the surface force R with $\int_S \ \underline{\mathrm{f}}^{\mathrm{S}}$.

$$\int_V \ \delta \underline{\varepsilon}^{\mathrm{T}} \underline{\tau} \, dV = \int_V \ \delta \underline{\mathrm{U}}^{\mathrm{T}} \underline{\mathrm{f}}^{\mathrm{B}} + \int_S \ \delta \underline{\mathrm{U}}^{\mathrm{S}^{\mathrm{T}}} \underline{\mathrm{f}}^{\mathrm{S}} \, dS \qquad \textbf{(2.2)}$$

Now the equation 2.1 can be derived to the differential equation of equilibrium with the boundary condition at x = L. Writing $\frac{\partial \delta \mathrm{u}}{\partial \mathrm{x}}$ for $\frac{\delta \, \partial \mathrm{u}}{\partial \mathrm{x}}$, recalling that EA is constant and using integration by parts yields

$$-\int_0^L (\mathrm{EA}\ \frac{\partial^2 \mathrm{u}}{\partial \mathrm{x}^2} + \mathrm{f}^{\mathrm{B}})\ \delta \mathrm{u}\ dx + [\ \mathrm{EA}\frac{\partial \mathrm{u}}{\partial \mathrm{x}}\,|_{\mathrm{x=L}} - \mathrm{R}\ ]\ \delta \mathrm{u}_{\mathrm{L}} - \mathrm{EA}\ \frac{\partial \mathrm{u}}{\partial \mathrm{x}}\,|_{\mathrm{x=0}}$$

since the variation of u at x = 0 (where the rod is connected with the wall[110]), $\delta \mathrm{u}_0 = 0$ and

[109] Eugenio Oñate, *Structural Analysis with the Finite Element Method. Linear Statics. Volume 1. Basis and Solids* (Barcelona: International Center for Numerical Methods in Engineering, 2009): 24.

[110] This is because the rod is fixed at the point where u = 0, and also can be confirmed by the essential boundary condition u (0, t) = 0.

EA $\frac{\partial u}{\partial x}\Big|_{x=0} = 0$. The natural boundary condition gives EA $\frac{\partial u}{\partial x}\Big|_{x=L} = R$ and by d'Alembert force

(1.2), $f^B = -\rho A\frac{\partial^2 u}{\partial t^2}$.

By combining these equations, we have the problem governing differential equation (1.1)

$\frac{\partial^2 u}{\partial x^2} = \frac{1}{c^2}\frac{\partial^2 u}{\partial t^2}$, $c = \sqrt{\frac{E}{\rho}}$.

Please read chapter 1.7 "Derivation of the matrix equilibrium equations for the bar using the Principle of Virtual Work" and 1.8 "Derivation of the bar equilibrium equations via the minimum total potential energy principle" in the Oñate book, for more details and variational formulations of the PVW. In summary, Oñate uses the PVW (2.1) and derives the total potential energy for a single bar as

$$\Pi = \frac{1}{2}[\mathbf{a}]^T\mathbf{K}[\mathbf{a}] - [\mathbf{a}]^T\mathbf{q}$$

where **K**, **a**, and **q** are respectively the stiffness matrix, the displacement vector matrix in x and y direction (u, v), and the total equilibrium force vector for the bar. The notation T in the exponent means the transposition of the matrix **a**, and is obtained by interchanging the rows and columns in the **a** matrix. (e.g., if $[a] = [1, -1]$ then $[a]^T = \begin{bmatrix} 1 \\ -1 \end{bmatrix}$)

By adopting the stationary condition $\delta \Pi = 0$, we get

$$\mathbf{K}\,\boldsymbol{a} = \mathbf{q}$$

This is a simplified version of the equation that we encounter in our FEM process.

Usually in analytical studies, problems can be solved by using this stationary condition $\delta \Pi = 0$ and the essential boundary condition $U_0 = 0$ where Π is the total potential energy. Therefore, these conditions are applied to the PVD/PVW and we solve the problem by using the Finite

Element Method. If the PVW can be integrated by parts, we could get a perfect solution by using the Differential Equation of Equilibrium and natural boundary condition. This process is visualized in the Bathe's diagram here (Figure 20).

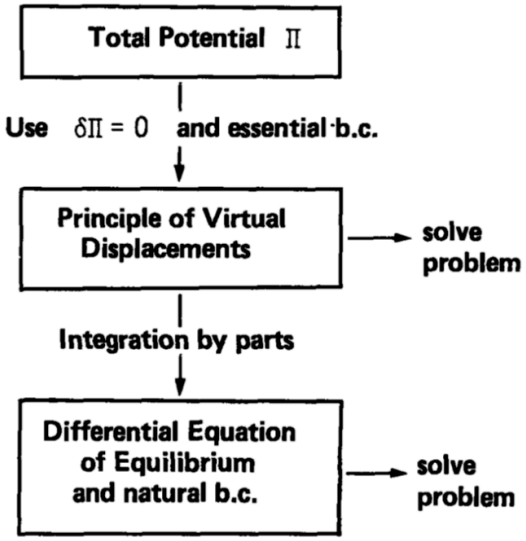

Figure 20. [111]

Oñate introduces this process in eight steps, and these can be summarized as following representation[112]:

1. Selection of a structural model (e.g., 3D solid model, axisymmetric shell model, etc.).
2. Subdivision of the structure into a mesh of non-intersecting domains of finite elements.
3. The calculation of the stiffness matrices $\mathbf{K}^{(e)}$ and the load vectors $\mathbf{f}^{(e)}$.
4. The assemblage of the element stiffness matrices and the load vectors into the overall stiffness matrix $\mathbf{K}$ and the load vector $\mathbf{f}$ for the structure.
5. The global system of linear simultaneous equation $\mathbf{K}\,\boldsymbol{a} = \mathbf{f}$ is solved for the unknown displacement variable $\boldsymbol{a}$.

[111] Bathe, *Complete Study Guide*, 2-8

[112] Oñate, *Structural Analysis*, 38–40. The numerical program-driven computations in FEM are step 3, 4, 5, and 6.

6. The evaluations of the strains and stresses within each element.
7. Solving steps 3, 4, 5, 6 requires a computer implementation of the FEM.
8. Post processing of the results.

Here the stiffness matrix $\mathbf{K}^{(e)}$ means the integration over each element (step 3) and $\mathbf{K}$ is the summation over all elements. In the core FEM computations in steps 3, 4, 5, 6 (The Principle of Virtual Displacement problem-solving step of Figure 20), the integrations of the K matrix are calculated using the Gauss-Legendre quadratures and their corresponding Gauss points without actual integrations. This is due to the complexity of the rational algebraic functions involved in the integrals. Numerical integration appears here as the only option to compute the element integrals in a simple and accurate way.[113] Instead of integrating the whole area of an element, the Gauss quadrature calculates an integral of area as a sum of the given function values at multiple points known as Gauss points, multiplied by predetermined weights. For the integral I of a function f(x) in the interval [-1, 1]:

$$I = \int_{-1}^{+1} f(\xi) d\xi$$

The Gauss quadrature of order q will be

$$I \cong I_q = \sum_{i=1}^{q} f(\xi_i) W_i$$

where W_i is the weight value corresponding to the ith Gauss point located at $\xi = \xi_i$ and q is the total number of Gauss points in the area.[114] "A Gauss quadrature of qth order integrates exactly a polynomial function of degree 2q–1"[115]. For example, for a third degree polynomial function (q

[113] Oñate, *Structural Analysis*, 89

[114] Please read Oñate, *Structural Analysis,* 90 for more details.

[115] Rodolphe Radau, Journal de matlufinatiques vol. 3, (1880): 283 qtd. in Oñate, *Structural Analysis,* 90.

$= 2)$, the Gauss points ξ_q would be ± 0.5773502692 and the prescribed weights at the points is 1.0.

In part 3 and 4, I will demonstrate the process of the calculation of the stiffness matrix **K** of a quadratic isoparametric element, and its integrand by using the Gauss quadrature method. Because of the transformation process from the Master Element Coordinates System to Global (Physical) Coordinates System, we will need the process of incorporating the Jacobian matrices and their determinants. Parts 3 and 4 will show how an overall process of the Finite Element Method is applied in standard or specially developed FEM analysis programs by solving the equilibrium equations for the whole structure $\mathbf{K}\boldsymbol{a} = \mathbf{f}$. These parts are based on the class notes of CEE 570 – Finite Element Methods course taught by Prof. C. Armando Duarte at the Civil Engineering Department at the University of Illinois at Urbana-Champaign, which I attended in Spring 2019.

3.3 SHAPE FUNCTION, MAPPING, AND JACOBIAN MATRICES

The displacement at a point $x = a$ can be written as $u(x = a)$. If we choose the simplest displacement function using polynomials locally defined for an element, the approximate displacement $\hat{u}(x)$ can be written as

$$u(x) \cong \hat{u}(x) = a_0 + a_1 x + a_2 x^2 + \cdots + a_n x^n = \sum_{i=1}^{n} a_i x^i$$

where n is the number of points of the element (e.g., nodes) where the displacement is assumed to be known. This approximate solution can be written in the form

$$u(x) = {N_1}^{(e)}(x){u_1}^{(e)} + {N_2}^{(e)}(x){u_2}^{(e)} + \cdots + {N_n}^{(e)}(x){u_n}^{(e)} = \sum_{i=1}^{n} {N_n}^{(e)}(x){u_n}^{(e)}$$

where $N_1{}^{(e)}(x), \ldots, N_n{}^{(e)}(x)$ are the polynomial interpolating functions defined over the domain of each element e, and $u_i{}^{(e)}$ is the value of the displacement of node i. The function $N_i{}^{(e)}(x)$ interpolates within each element of node i and it is called the shape function of node i.[116] This can be understood as the displacement of each point in an element can be recalculated by averaging displacements of all points and weighing those displacements by using the shape function. For example, the displacement graph of a bar subjected to concentrated end force on point C with a fixed point A, will be the summation of two shape functions for each part of the bar:

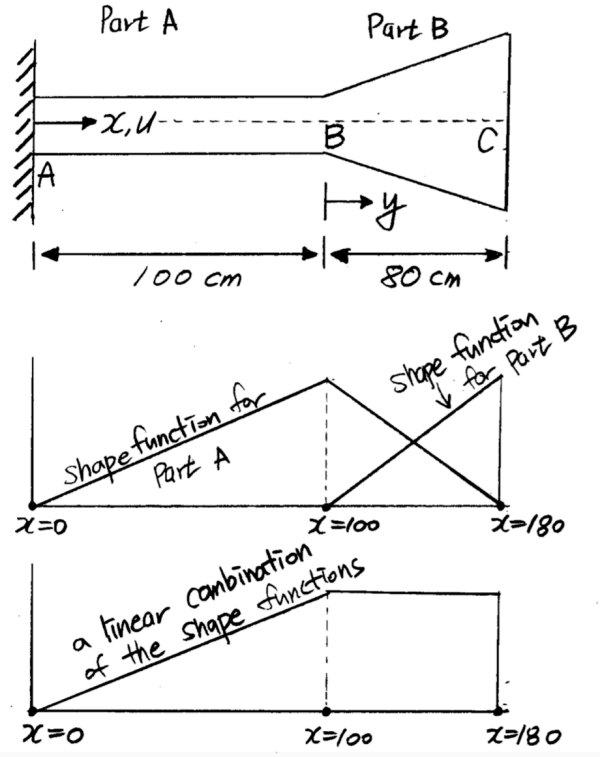

Figure 21. Shape functions of a bar with fixed point. [117]

[116] Oñate, *Structural Analysis*, 45

[117] This problem is originally introduced in the Bathe's OCW online lecture.

Here the shape function for part A is zero at both ends because of the boundary condition and the shape function for part B, and the shape function for part B is zero where the part B area begins (x=100), and becomes 1 at the point where the shape function is originated from. In the actual FEM process, the value of element shape function at each nodal point will be 1 at the given nodal point and 0 at the remaining points. The shape function $N_n{}^{(e)}(x)$ will be multiplied by the displacement of the point $u_n{}^{(e)}$ of all nodes, and the continuous displacement u will be calculated from the summation of $N_n{}^{(e)}u_n{}^{(e)}$. Oñate demonstrates this process with the shape functions for a linear triangular element.

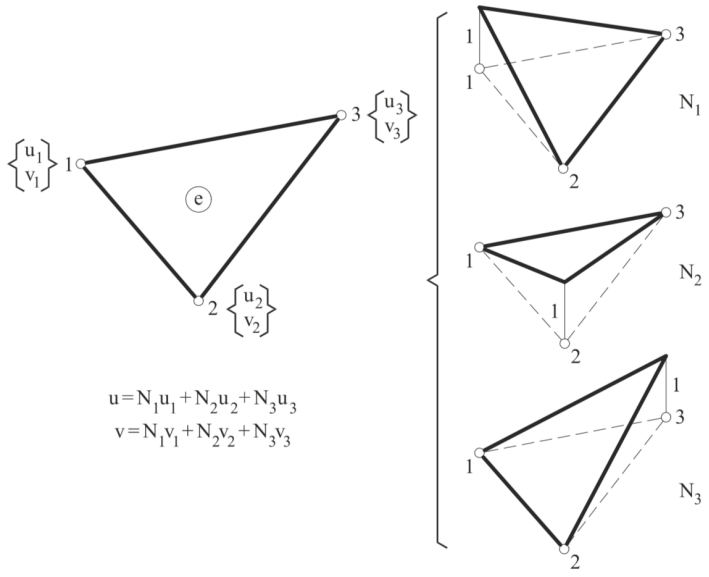

Figure 22. Shape functions for a linear triangular element.

The FE approximation of displacement vector will be

$$u(x, y) = u_1 N_1(x, y) + u_2 N_2(x, y) + u_3 N_3(x, y)$$

and a linear polynomial approximation in 2-D is given by

$$u(x_i, y_i) = \alpha_1 + \alpha_2 x_i + \alpha_3 x_i = u_i$$

where u_i, $i = 1, 2, 3$, are the displacement at node $i = 1, 2, 3$. Solving this for α_i and substituting gives the displacement vector as

$$u = \frac{1}{2A^{(e)}}\left[(a_i + b_i x + c_i y)u_i\right], i = 1, 2, 3$$

where

$$a_i = x_j y_k - x_k y_j, b_i = y_j - y_k, c_i = x_k - x_j \; ; i, j, k = 1, 2, 3$$

and the linear shape function will be

$$N_i(x, y) = \frac{1}{2A^{(e)}}(a_i + b_i x + c_i y), i = 1, 2, 3$$

In parametric formulations, the FE shape functions are defined in a master element and mapped to the actual (global) element using a transformation from (ξ, η) to (x, y) coordinates. In the case of isoparametric elements, the mapping is performed using the same FE shape functions adopted to approximate the displacement over the element.

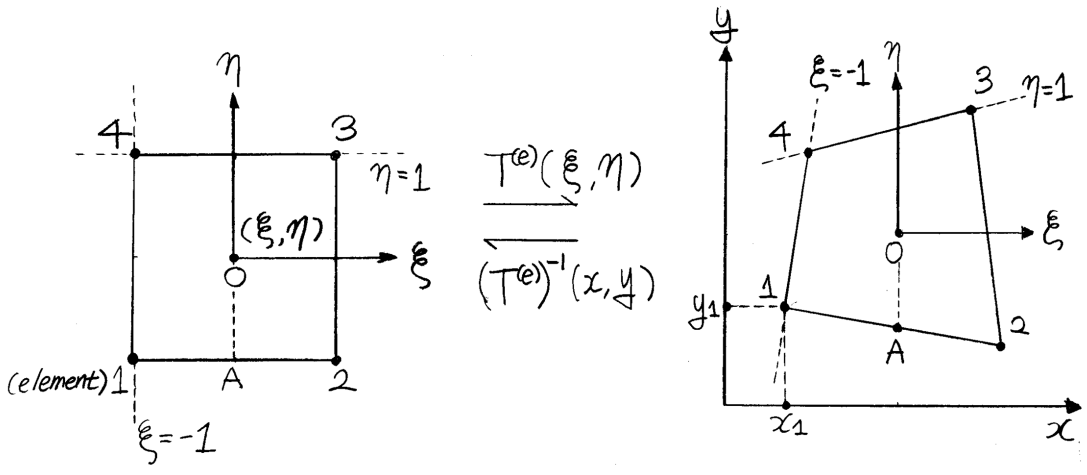

Figure 23. Elements in master coordinate mapped to the global coordinate.

The master element coordinates are notated as (ξ, η), $-1 \leq \xi, \eta \leq 1$, and

$T^{(e)}(\xi, \eta)$ is the transformation from master to global coordinates, and $T^{(e)^{-1}}(x, y)$ is the transformation from global to master element coordinates. The shape functions are

$$x(\xi, \eta) = \sum_{i=1}^{n=4} x_i N_i(\xi, \eta), \qquad y(\xi, \eta) = \sum_{i=1}^{n=4} y_i N_i(\xi, \eta)$$

where x_i, y_i = nodal coordinates, n is the number of shape functions = number of nodes, and $N_i(\xi, \eta)$ is the Finite Element shape functions for an isoparametric 2-D quadrilateral element. The 2-D Lagrange shape functions are obtained from the product of 1-D Lagrange shape functions:

$$N_i(\xi, \eta) = l_I^j(\xi) l_J^k(\eta)$$

where $l_I^j(\xi)$ is 1-D Lagrange polynomial of order I in the ξ direction and $l_J^k(\eta)$ is 1-D Lagrange polynomial of order J in the η direction, and usually I = J, which means the shape function has the same polynomial order in both directions. For quadrilateral elements of order 1,

$$N_i(\xi, \eta) = l_1^j(\xi) l_1^k(\eta), \qquad i, k = 1, 2$$

where

$$l_1^j(\xi) = \frac{1}{2}\left(1 + \xi\xi_j\right), l_1^k(\eta) = \frac{1}{2}\left(1 + \eta\eta_k\right)$$

and (ξ_j, η_k) are coordinates of a node in the master elements. If we apply this to the master element where (ξ_j, η_k) are (-1, -1), (1, -1), (1, 1), and (-1, 1) for node 1, 2, 3, and 4, we get four linear shape functions:

$$N_1(\xi, \eta) = \frac{1}{2}(1 - \xi)\frac{1}{2}(1 - \eta)$$

$$N_2(\xi, \eta) = \frac{1}{2}(1 + \xi)\frac{1}{2}(1 - \eta)$$

$$N_3(\xi, \eta) = \frac{1}{2}(1 + \xi)\frac{1}{2}(1 + \eta)$$

$$N_4(\xi,\eta)=\frac{1}{2}(1-\xi)\frac{1}{2}(1+\eta)$$

The displacement vector $\underline{U}=\{u,v\}^T$ at a point (ξ,η) in the master element is given by

$$u(\xi,\eta)=\sum_{i=1}^{4}u_iN_i(\xi,\eta),v(\xi,\eta)=\sum_{i=1}^{4}v_iN_i(\xi,\eta)$$

In matrix form:

$$\underline{U}(\xi,\eta)=\begin{Bmatrix}u(\xi,\eta)\\v(\xi,\eta)\end{Bmatrix}=\left[\begin{array}{cc:cc:cc:cc}N_1&0&N_2&0&N_3&0&N_4&0\\0&N_1&0&N_2&0&N_3&0&N_4\end{array}\right]\begin{bmatrix}u_1\\v_1\\u_2\\v_2\\u_3\\v_3\\u_4\\v_4\end{bmatrix}=\mathbf{N}\boldsymbol{a}^{(e)}$$

where $\mathbf{N}=[\mathbf{N}_1,\mathbf{N}_2,\mathbf{N}_3,\mathbf{N}_4]$, $\mathbf{N}_i=\begin{bmatrix}N_i&0\\0&N_i\end{bmatrix}$, which means that N is the 2 by 8 combination matrix of four shape functions, and $\boldsymbol{a}^{(e)}$ is the 8 by 1 combination matrix of the nodal displacements in the x and y direction:

$$\boldsymbol{a}^{(e)}=\begin{Bmatrix}{a_1}^{(e)}\\{a_2}^{(e)}\\{a_3}^{(e)}\\{a_4}^{(e)}\end{Bmatrix},\ {a_i}^{(e)}=\begin{Bmatrix}u_i\\v_i\end{Bmatrix}$$

Similarly, for virtual displacements:

$$\delta U(\xi,\eta)=\begin{Bmatrix}\delta u(\xi,\eta)\\\delta v(\xi,\eta)\end{Bmatrix}=\mathbf{N}\delta\boldsymbol{a}^{(e)}$$

$$\delta U^T=[\delta\boldsymbol{a}^{(e)}]^T\mathbf{N}^T$$

where $[\delta\boldsymbol{a}^{(e)}]^T=[\delta u_1,\delta v_1,\delta u_2,\delta v_2,\delta u_3,\delta v_3,\delta u_4,\delta v_4]^T$

The computation of derivatives of FE shape function with respect to global coordinates x, y is based on the chain rule of calculus.

By defining $N_i(x,y) = N_i[\xi(x,y), \eta(x,y)]$, then using the chain rule,

$$\frac{\partial N_i}{\partial \xi} = \frac{\partial N_i}{\partial x}\frac{\partial x}{\partial \xi} + \frac{\partial N_i}{\partial y}\frac{\partial y}{\partial \xi}\ , \qquad \frac{\partial N_i}{\partial \eta} = \frac{\partial N_i}{\partial x}\frac{\partial x}{\partial \eta} + \frac{\partial N_i}{\partial y}\frac{\partial y}{\partial \eta}$$

In matrix form

$$\begin{bmatrix} \frac{\partial N_i}{\partial \xi} \\ \frac{\partial N_i}{\partial \eta} \end{bmatrix} = \begin{bmatrix} \frac{\partial x}{\partial \xi} & \frac{\partial y}{\partial \xi} \\ \frac{\partial x}{\partial \eta} & \frac{\partial y}{\partial \eta} \end{bmatrix} \begin{bmatrix} \frac{\partial N_i}{\partial x} \\ \frac{\partial N_i}{\partial y} \end{bmatrix} = \mathbf{J}^{(e)} \begin{bmatrix} \frac{\partial N_i}{\partial x} \\ \frac{\partial N_i}{\partial y} \end{bmatrix}$$

where $\mathbf{J}^{(e)}$ is the Jacobian matrix of transformation $\mathbf{T}^{(e)}(\xi, \eta)$.

Thus, we have

$$\begin{bmatrix} \frac{\partial N_i}{\partial x} \\ \frac{\partial N_i}{\partial y} \end{bmatrix} = [\mathbf{J}^{(e)}]^{-1} \begin{bmatrix} \frac{\partial N_i}{\partial \xi} \\ \frac{\partial N_i}{\partial \eta} \end{bmatrix} = \frac{1}{|\mathbf{J}^{(e)}|} \begin{bmatrix} \frac{\partial y}{\partial \eta} & -\frac{\partial y}{\partial \xi} \\ -\frac{\partial x}{\partial \eta} & \frac{\partial x}{\partial \xi} \end{bmatrix}$$

where $\left|\underline{\mathbf{J}}^{(e)}\right|$ is the determinant of matrix $\underline{\mathbf{J}}^{(e)}$.

3.4 STIFFNESS MATRIX, LOAD VECTOR, AND GAUSS INTEGRATION

The element strain-displacement matrix **B** can be computed using

$$\varepsilon = \begin{Bmatrix} \frac{\partial u}{\partial x} \\ \frac{\partial v}{\partial y} \\ \frac{\partial u}{\partial y} + \frac{\partial v}{\partial x} \end{Bmatrix} = [\mathbf{B}_1, \mathbf{B}_2, \mathbf{B}_3, \mathbf{B}_4] = \begin{Bmatrix} a_1{}^{(e)} \\ a_2{}^{(e)} \\ a_3{}^{(e)} \\ a_4{}^{(e)} \end{Bmatrix} = \mathbf{B}\boldsymbol{a}^{(e)}$$

$$\mathbf{B}_i = \begin{bmatrix} \frac{\partial N_i}{\partial x} & 0 \\ 0 & \frac{\partial N_i}{\partial y} \\ \frac{\partial N_i}{\partial y} & \frac{\partial N_i}{\partial x} \end{bmatrix} \qquad i = 1, 2, 3, 4$$

where the derivatives of shape functions are computed from the previous process.

The virtual strains can be computed in a similar way:

$$\delta\varepsilon = \begin{Bmatrix} \dfrac{\partial \delta u}{\partial x} \\ \dfrac{\partial \delta v}{\partial y} \\ \dfrac{\partial \delta u}{\partial y} + \dfrac{\partial \delta v}{\partial x} \end{Bmatrix} = \mathbf{B}\delta\boldsymbol{a}^{(e)}$$

where $\delta a^{(e)}$ implies the virtual nodal displacements.

$$\delta\underline{\varepsilon}^T = [\delta\boldsymbol{a}^{(e)}]^T\mathbf{B}^T$$

where $[\delta\boldsymbol{a}^{(e)}]^T$ is $[\delta u_1, \delta v_1, \delta u_2, \delta v_2, \delta u_3, \delta v_3, \delta u_4, \delta v_4]^T$.

The approximation of stress field $\boldsymbol{\sigma}$ in a quadrilateral element can be calculated by using the Hooke's law:

$$\boldsymbol{\sigma} = \mathbf{D}\varepsilon = \mathbf{DB}\boldsymbol{a}^{(e)}$$

where **D** is the elastic material matrix (or constitutive matrix) containing the material data.

$$\mathbf{D} = \begin{bmatrix} d_{11} & d_{12} & 0 \\ d_{21} & d_{22} & 0 \\ 0 & 0 & d_{33} \end{bmatrix}$$

In a plain-stress model for isotropic elasticity, we have $d_{11} = d_{22} = \frac{E}{1-\nu^2}$, $d_{12} = d_{21} = \nu d_{11}$, and $d_{33} = \frac{E}{2(1+\nu)}$ where E is the Young modulus and ν is the Poisson ratio.[118]

For quadrilateral elements (e.g., the evaluation of integrand of the stiffness matrix $\mathbf{K}^{(e)}$), the two-dimensional Gauss-Legendre quadratures are used to numerically integrate functions. The quadratures are defined in the master element as:

[118] Oñate, 122.

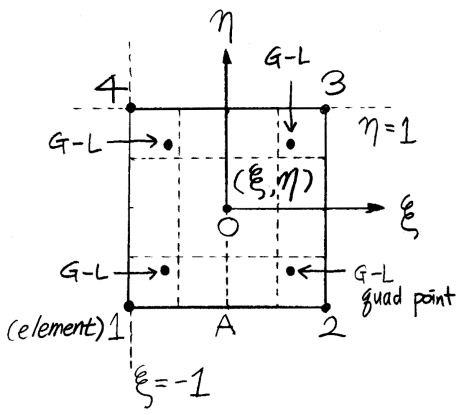

The integral of a function $g(\xi, \eta)$ over the master element is computed using 2-D G-L quadrature as follows.

$$\mathrm{I} = \int_{-1}^{1}\int_{-1}^{1} g(\xi,\eta)d\xi d\eta = \int_{-1}^{1}\left[\sum_{i=1}^{n_i} g(\xi_i,\eta)\,W_i\right]d\eta = \sum_{j=1}^{n_j}\sum_{i=1}^{n_i} g\left(\xi_i,\eta_j\right)W_i W_j$$

where n_i, n_j are number of quadrature points in the ξ and η direction, ξ_i, η_j are coordinates of quadrature points in the master element, and W_i, W_j are quadrature weights in the ξ and η direction. The number of quadrature points in each direction is selected based on the polynomial order in each direction. If p_ξ and p_η are the polynomial order in the ξ and η direction of the shape function respectively, then

$$2n_i - 1 \geq p_\xi, \qquad 2n_j - 1 \geq p_\eta$$

The stiffness matrix, $\mathbf{K}^{(e)}$, and equivalent nodal force vector, $\mathbf{f}^{(e)}$ for any element are obtained via the PVW explained previously.

$$\delta\,\text{virt} = \int_{A^{(e)}} \delta\,\varepsilon^{\mathrm{T}}\sigma\,\mathrm{t}\,dxdy = [\delta\,\boldsymbol{a}^{(e)}]\int_{A^{(e)}} \mathbf{B}^{\mathrm{T}}\mathbf{D}\mathbf{B}\,\mathbf{t}\,dxdy\,\boldsymbol{a}$$

where $A^{(e)}$ is the area of element, $\delta\,\varepsilon^{\mathrm{T}}$ is the virtual strain, σ is the actual stress, and $\boldsymbol{a}^{(e)}$ is virtual nodal displacements.

In the case of a quadrilateral element,

$$\mathbf{K}^{(e)} = \int_{A^{(e)}} \mathbf{B}^{\mathrm{T}} \mathbf{D} \mathbf{B}\, \mathbf{t}\, dA = \int_{-1}^{1}\int_{-1}^{1} \mathbf{B}^{\mathrm{T}}(\xi,\eta)\mathbf{D}(\xi,\eta)\mathbf{B}(\xi,\eta)\ \mathbf{t}|\mathbf{J}(\xi,\eta)| d\xi d\eta$$

Here the derivatives of shape functions $\mathbf{B}^{\mathrm{T}}(\xi,\eta)$ and $\mathbf{B}(\xi,\eta)$can be computed by using the G-L quadrature:

$$\mathbf{K}^{(e)} = \sum_{i=1}^{n_i}\sum_{j=1}^{n_j} \mathbf{B}^{\mathrm{T}}(\xi,\eta)\mathbf{D}(\xi,\eta)\mathbf{B}(\xi,\eta)\ \mathbf{t}|\mathbf{J}(\xi,\eta)|\, W_i W_j$$

We assume $\mathbf{D}$, $\mathbf{t}$, and $|\mathbf{J}|$ are constants. The integrand of $\mathbf{K}^{(e)}$ is a quadratic polynomial in ξ and η (e.g., there product gives ξ^2, η^2, $\xi\eta$ and there derivatives are linear monomials), we need p = 2 for both ξ and η, $2n_i - 1 \geq 2, n_i = 2$, which means that we need two G-L quadrature points for the integrand. The coordinates of the sampling points and their weights for the first eight Gauss quadratures, the coordinate table gives us that ξ and η are $\pm\frac{1}{\sqrt{3}} = 0.5773502692$ and its weight value would be 1.[119] Since in my research I am only computing the eigenfrequencies, this paper will not cover the calculation processes of body forces and surface tractions. For more details, please refer to Oñate or Bathe, and other FEM books such as "The Finite Element Method Its Basis and Fundamentals" by Olgierd (Kidlington, Oxford: Butterworth-Heinemann, 2013).

[119] Please refer the "Table 3.1 Coordinates and weights for Gauss quadratures" on Oñate, 91.

CHAPTER 4: BELL MODEL CONSTRUCTION

4.1 MODEL CONSTRUCTION

The first research in the search for a new bell tone color by using numerical optimization techniques was initiated by Lehr and the bell founder of the Royal Eijsbouts bell casting company in Asten, the Netherlands. Van Asperen (1984) employed the FEM analysis of the eigenfrequencies of axisymmetric structure and implemented an optimization algorithm in the FEM software, DYNOPT. The first prototype of the major third bell was designed by Maas and Schoofs, and finally adapted by the bell founder. Mass used DYNOPT to tune the first five eigenfrequencies of a bell in a just major-third target harmonic profile.[120]

Figure 24a. First carillon with major-third bells made by using the FEM by Royal Bell-Foundry Eijsbouts[121]

[120] P.J.M. Roozen-Kroon, *Structural Optimization of Bells* (Eindhoven: Technische Universiteit Eindhoven, 1992) 8. The first numerical analysis of bell eigenmodes was conducted by Banens in 1972 by using the FEM.
[121] Schoofs, *Experimental design and structural optimization,* 6.17.

Rolf Bader, with whom I communicated with at the earlier stage of my research also wrote to me about his experience with using the FEM in bell optimization processe in the 1970s.

> The FEM of the model was performed by Björn Lau those days. I did my FEM models using the mesh algorithm of Femlab (now Comsol), exported it and then used my C++ and C'# code for doing the models. … I did learn FEM from the old Argyris team in Stuttgart. They developed many elements in the 70s to make the calculations feasible on the old punchcards. Schad and Frick, part of that team, did do a FEM model with spectral harmonic elements, as they expected modes on the bell anyway. They calculated the bells of the rebuilt Frauenkirche in Dresden, which had heavy ornamentations. Therefore, it sounded very much out of tune and had to be melted and recasted again.[122]

For the model construction, I referred mainly to Schoofs' research, parts of Roozen-Kroon's approach (which follows mostly in Schoofs' footsteps), and that of Behzad Keramati Nigjeh et al.[123] Since bells are axis-symmetric, Schoofs designed half of the 2D bell geometry, and rotated it around a central axis to build the 3D bell geometry. Each adjustable value in the geometry was called a design variable, and was set to attain the most efficient result within the available computational resources. Figure 24b is the initial bell geometry that Schoofs suggested, where r_i is the radii of each design point, and t_i is the corresponding thickness.

[122] An email communication with Rolf Bader, between April 19 and July 15, 2019.

[123] Behzad Keramati Nigjeh, Pavel Trivailo, and Neil McLachlan, "Application of Modal Analysis to Musical Bell Design," Paper presented at the *Acoustics 2002 - Innovation in Acoustics and Vibration, Annual Conference of the Australian Acoustical Society*, Adelaide, Australia, November 13-15, 2002.

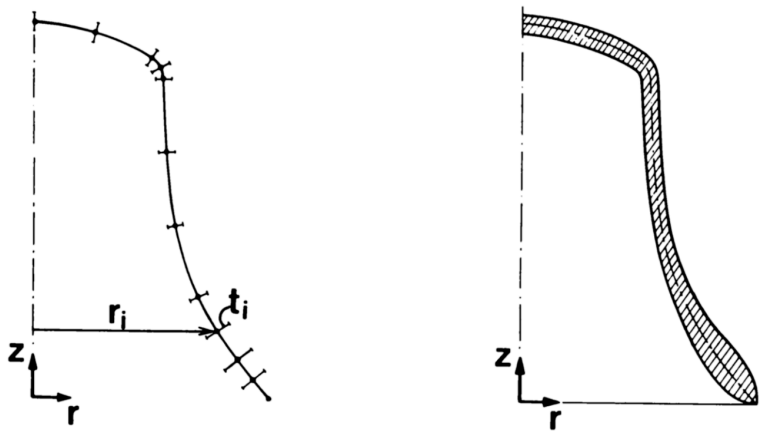

Figure 24b. Initial bell 2D geometry that Schoofs employed for explorative computations.[124]

In Figure 25, the left figure is the sample bell geometry with five design variables that Schoofs suggested in his paper (1987)[125], and the right figure is the final model with seven design points that he used for his optimization process. From the nominal reference curve given in the figure, Schoofs changed the radius of each points by Δn_i, which is proportional to its corresponding design variable x_i: $\Delta n_i = wr_i \times x_i \times r_j$ where wr_i is a weighting factor and Schoofs used 0.05 as a constant for all of his simulations.

[124] A. Schoofs, F. Van Asperen, and P. Maas, "Computation of Bell Profiles Using Structural Optimization," *Music Perception* 4, no. 3 (Spring 1987): 246.
[125] A. Schoofs, *Experimental design and structural optimization*, 6.12.

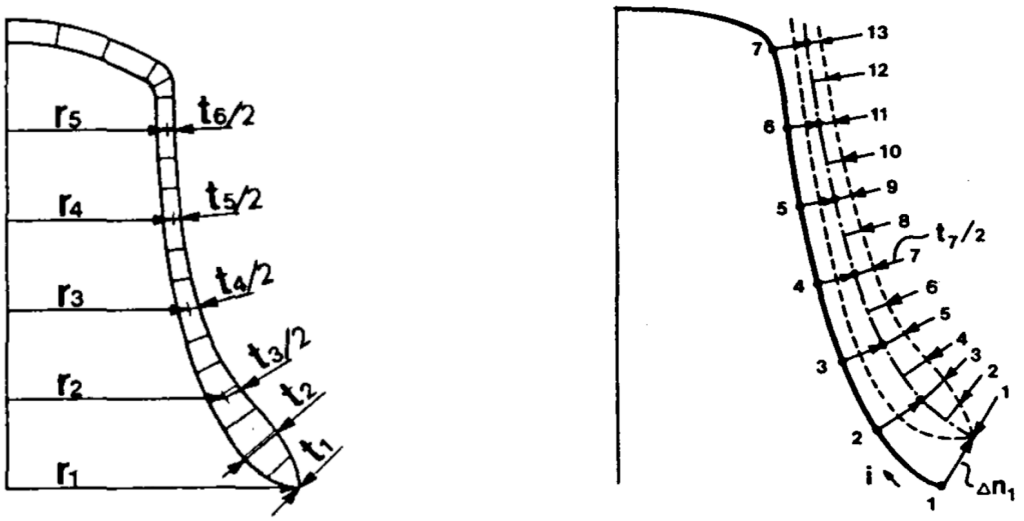

Figure 25. The bell geometry of five design points with six thickness variables (left) and seven design points with 13 thickness variables (right), Schoofs (1987).

For the wall thickness of each basic point, ta_i, Schoofs defined the resultant wall thickness variable $ta_i = tn_j \times (1 + wt_i \times t_i)$ where tn_j is the basic nominal values, wt_i is a weighting factor of 0.1 (only 10% change of the wall thickness will be shifted if the design variable t_i is shifted to 1.0), and t_i is the design variables related to the thickness of the point. Schoofs used five types of the design variable x_i for his bell's wall curve design.

a. $x_i = \alpha,$ $\quad i = 1, 2, \dots, 7$
b. $x_i = \alpha(4 - i)/3,$ $\quad i = 1, 2, \dots, 7$
c. $x_i = \alpha\left(1 - \frac{|4-i|}{3}\right),$ $\quad i = 1, 2, \dots, 7$
d. $x_2 = \alpha,$ $\quad i = 1, 3, 4, 5, 6, 7$
e. $x_3 = \alpha,$ $\quad i = 1, 2, 4, 5, 6, 7$

To limit geometrical variations, the range of x_i is constrained between -3 and 3, and to limit unexpected nonlinearities of geometry, the difference between near two design variables are constrained to be less than 2.0: $-3.0 \leq x_i \leq 3.0$ for all x_i, and $|x_i - x_{i-1}| \leq 2.0, i = 2,3, \dots, 7$. Figure 26 shows the amount of curvature changes depending on variation types, and it's

corresponding changes of the Hum frequency. Note that for type a, the wall curvature will remain the same since each radius point will be changed in the same rate $\Delta n_i = wr_i \times (x_i = \alpha, \text{constant}) \times r_j$, and for type d and e, only certain points of bell radii are varied from the nominal radii. For type b, the upper radii will be narrower and lower radii will be enlarged, and for type c the adjustment will be concentrated on the waist part of the bell.

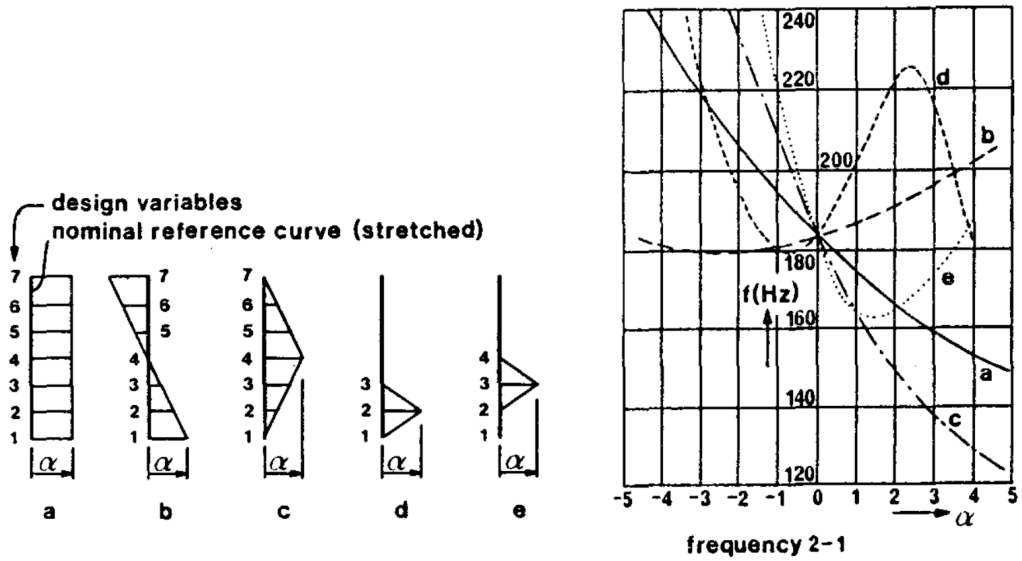

Figure 26. Types of variation of the design variables and its corresponding frequency variations (Schoofs, 1987).

The research of Nigjeh et al. shows direct relationships between the harmonic profile of lower partials and the bell geometry, especially the cone angle (angle between the head and shoulder/waist) and the wall curvature. The eigenfrequency ratios vary drastically as the cone angle decreases, since the geometry loses its characteristic bell shape and becomes closer to a regular cylinder. In the research, Nigjeh also includes the frequency variation of modes depending upon the length and width of a cylinder.

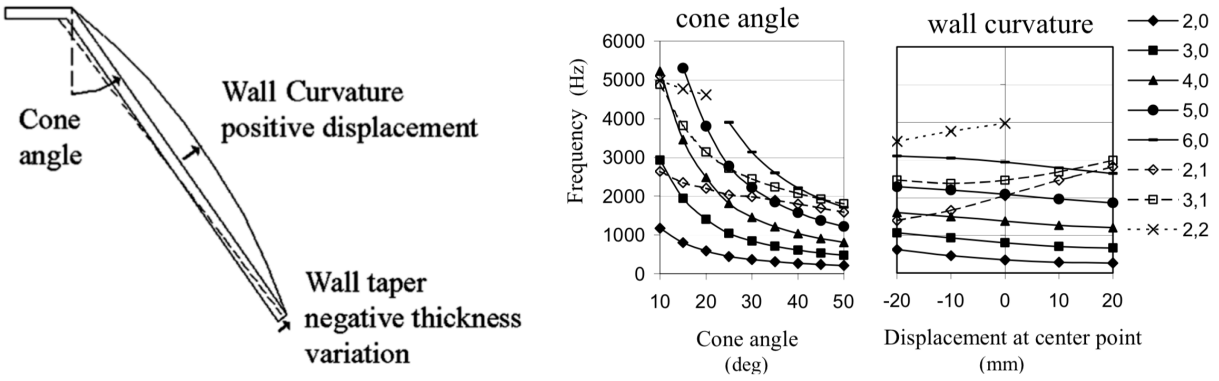

Figure 27. Low eigenfrequency plots for varying cone angle and wall curvature (Nigjeh, 2002). Note that the eigenmode notation is different from what is used here.

Nigjeh's solution for the major third bell differs from Schoofs' solution. While Schoofs achieved the major third harmonic profile mainly by varying radius on each design point, the approach of Nigjeh is more focused on varying thicknesses. Figure 28 shows the different geometric feature between these two approaches.

In my 2D bell geometry, I set up design variables which crucially affected lower bell eigenfrequencies in the models of Schoofs and Nigjeh. These include the bell diameter (radius), bell height, cone angle, wall thickness, and bow thickness. Here the bell height parameter can be removed since the overall ratio between bell diameter and height can be adjustable only by using one parameter and fixing the other. The definition of parameters and 2D bell geometry were not only theoretically defined, but also constantly revised while creating a successful just tuned minor third bell.

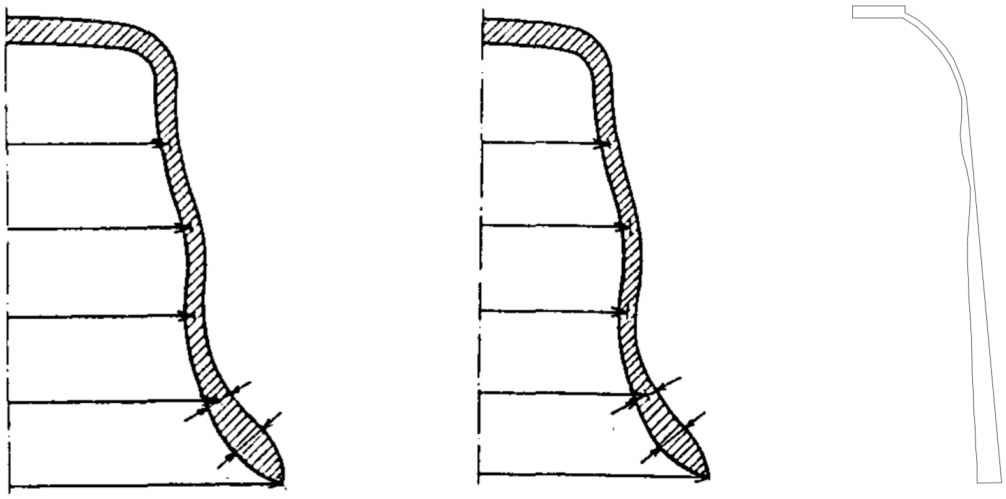

Figure 28. 2D geometries of the major third bell by Schoofs (left and middle, 1987) and Nigjeh (right, 2002).

The thickness parameter in general is quintessential for the tone color of the bell, which can be confirmed from Schoofs' experiment and also from the way how Van Eyk and the Hemony brothers tuned the lowest partials in the 18th century, previously discussed. The radius parameter was required to tune the Hum and Prime ratio to 1:2. It is also a crucial parameter to decide the fundamental frequency of the bell, which is called the fD-parameter, which is the product of the frequency of the hum tone and the diameter of the lip of the bell. Later the overall angle of the bell wall was subdivided to two parameters, the angle of waist (upper part of the bell) and the angle of hip (lower part of the bell), and here the proportion of waist and hip height became adjustable by using the waist-hip ratio parameter. This decision was made mainly to create a just minor third ratio between the Prime and Tierce. From multiple simulations, I discovered that the ratio among the three lowest partials (Hum, Prime, and Tierce) increase drastically when the angle of the hip becomes steeper, close to that of a cylinder, which can also be confirmed from the parametric plot in Figure 27. This is mainly because the Prime (2, 1) and Tierce (3, 1) mode have a nodal circle on the verge between hip and waist, while the Hum (2, 0) mode doesn't have

a nodal circle in the position. It is easy to imagine that the amount of mass, wall thickness, and the position of nodal circle (height of the hip, or the ratio between waist and hip) will largely decide the ratios between these three eigenmodal frequencies. In general, the harmonic profile of each partial really depends on the modal shape of each eigenmode. The positions of nodal circles and nodal meridians, and the amount of mass and stiffness where antinodes are located are crucial for tuning each partial separately. Here the mass of the position where antinodes are located can be controlled by the wall thickness of the area, and in this sense the importance of bow thickness arises.

The Sound bow was one of the major parts that the old bell foundries used for tuning bell tone colors:

> The founder works, instead, with a set of "experience rules" which are learned by years of practice and which allow him to predict what will happen when a particular change in a known bell profile is made. He can, for instance, predict the changes in partial tones that will occur when the bell is made taller, the sound bow is made thicker, or the upper part of the waist is made wider.[126]

Acoustically, the sound bow region is where the maximum vibration occurs[127], and also defines the lower partials of “ring-driven” modes: modes with one nodal circle near the waist in Group I (including Hum, Tierce, and Nominal) and Group III (including First eleventh and Second eleventh). In these modes, one antinode (anti-nodal circle) is located exactly in the middle of the soundbow, and Rossing indicates these modes as the “Most important families [groups]” having an antinode where the clapper strikes: at the soundbow.[128]

---

[126] Andre Lehr, “From Theory to Practice,” *Musical Perception: An Interdisciplinary Journal – A Carillon of Major-Third Bells* 4, no. 3 (Spring, 1987): 271.

[127] Rossing, “The Acoustics of Bells,” 441.

[128] Rossing, “Vibrations of Bells,” 45.

There were also multiple empirical discoveries during the simulations, similar to that of an ancient bell foundry's worker's process. These include the crucial relation between bow thickness and the three lowest partials (Hum, Prime, and Tierce), and the relation between the height of the bell's upper part (shoulder) and the Hum : Quint ratio. Later the radius of the bell's head was added.

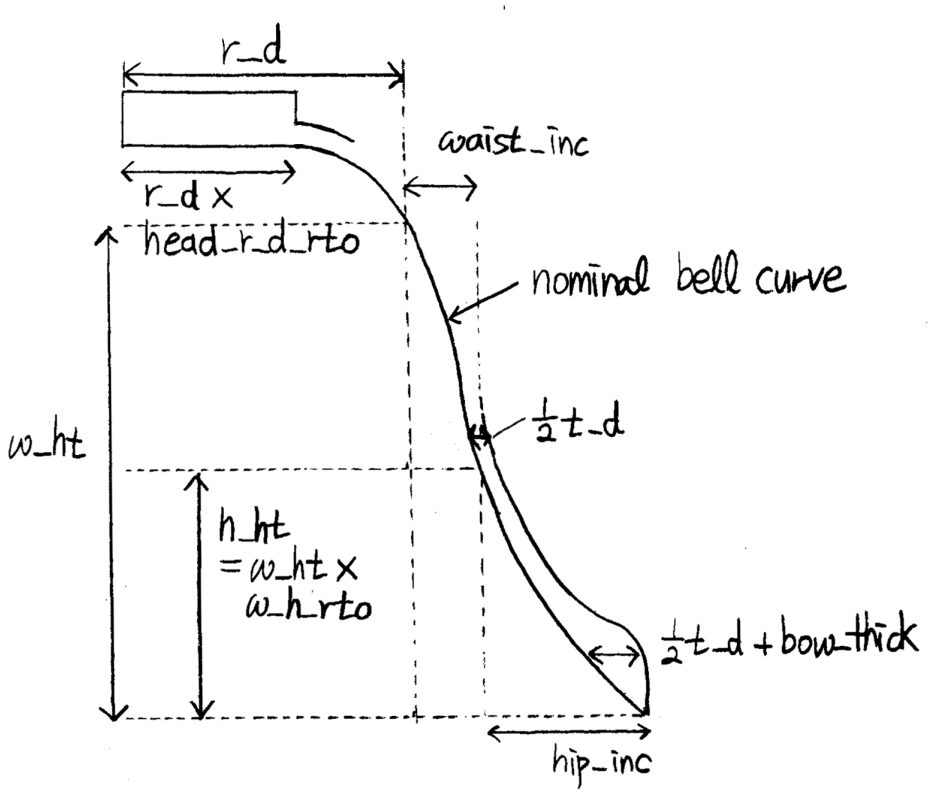

Figure 29. 2D bell nominal curve and adjustable design variables.

variables	value (m3 bell)	default value	description
den	8700	8700	density
y_mod	1.05E+11	1.05E+11	Young mod
p_rto	0.36	0.36	Poisson ratio
r_d	0.36398	0.37	radii (m)
w_ht	0.9	0.9	Constant) waist height (m)
w_h_rto	0.30918	0.35	ratio between waist and hip, waist * rto = hip
h_ht	w_ht*w_h_rto	0.25	hip height (m) = w_ht * w_h_rto
waist_inc	0.02	0.03	default waist increment (m)
hip_inc	0.0325	0.05	default hip increment (m)
t_d	0.067446	0.036	default thickness (m)
bow_thick	0.03719	0.025	bow thickness (m)
head_r_d_rto	0.5	0.5	ratio between head and radius = r_d*head_r_d_rto

Table 7. Design variables

For more precise tuning, local thickness parameters were added to adjust the mass that is concentrated on specific nodal lines. For computational efficiency, the number of additional thickness variables are limited to four, and these are selected based on the number of nodal circles on the bell surface. The additional thickness design points are located in the shoulder, belly (between waist and hip), hip, and the head area.[129]

[129] These points are connected with the Interpolation Curve, "An interpolation curve consists of a curve that interpolates or approximates a sequence of points." in COMSOL Multiphysics: "Chapter 7: Geometry Modeling and CAD Tools," COMSOL Multiphysics Reference Manual, accessed March 17, 2020, https://doc.comsol.com/5.5/doc/com.comsol.help.comsol/COMSOL_ReferenceManual.pdf.

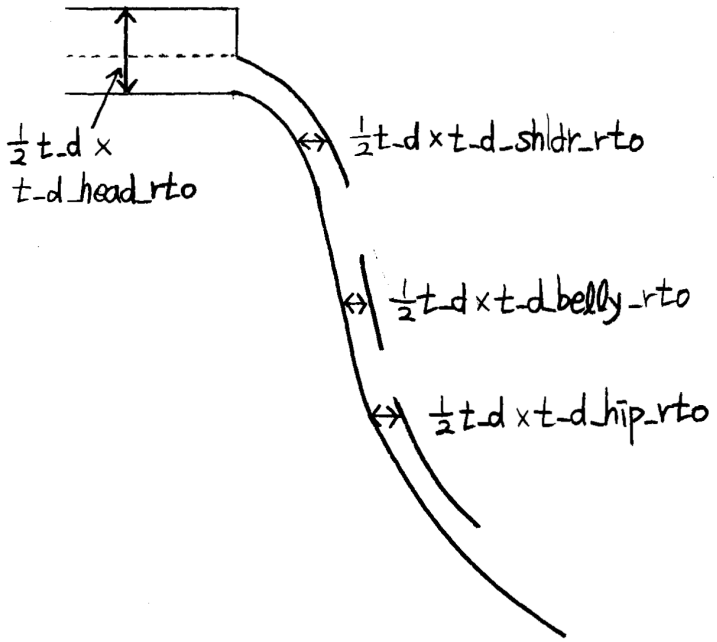

Figure 30. Additional local thickness design variables

variables	value	default value	description
t_d_head_rto	1.176	1.15	top(head) thickness ratio (ratio to t_d)
t_d_shldr_rto	0.37	1	shoulder thickness (ratio to t_d)
t_d_belly_rto	0.53	1	belly thickness (ratio to t_d)
t_d_hip_rto	0.65	1	hip thickness (ratio to t_d)

Table 8. Additional local thickness design variables

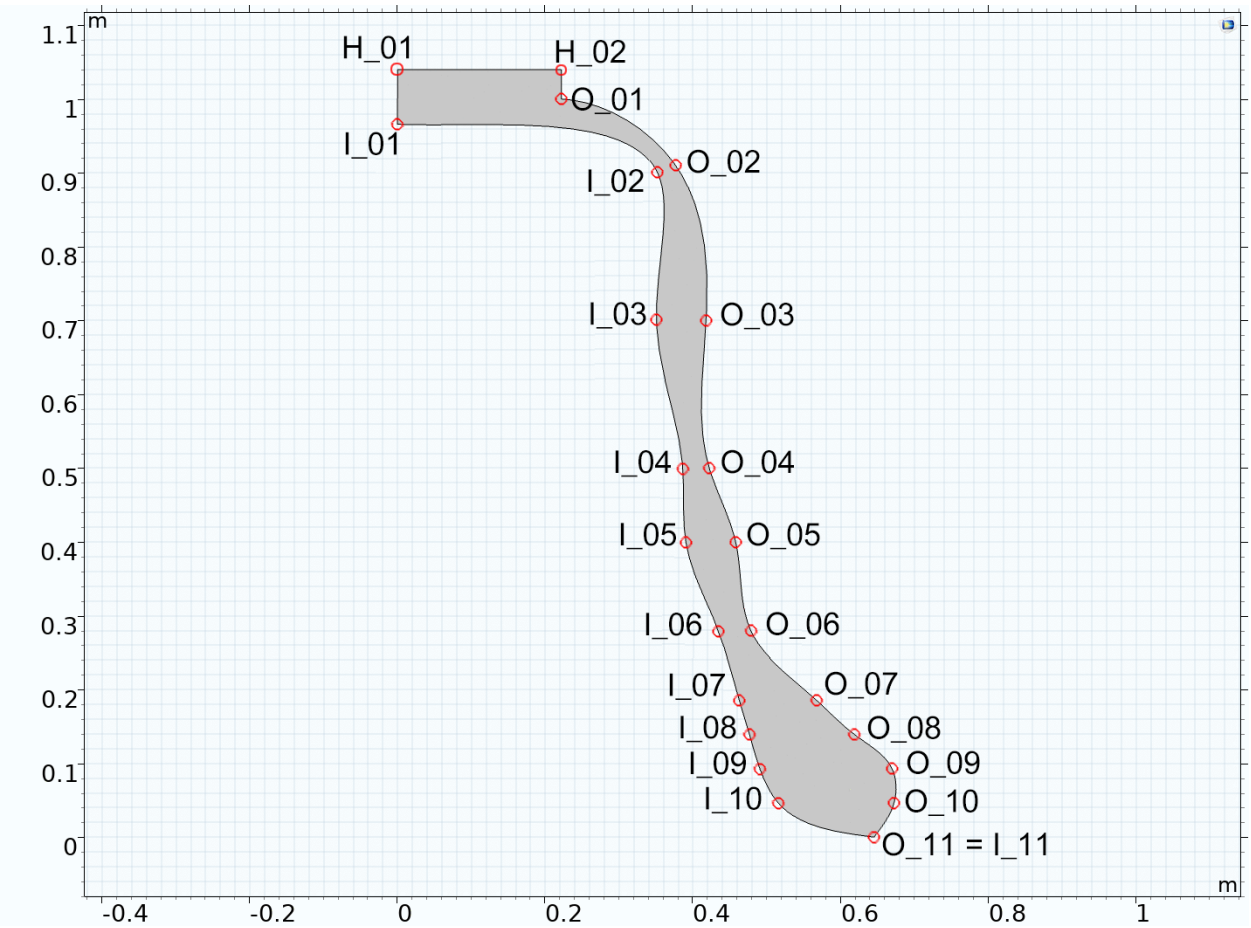

Figure 31. Final bell geometry with 11 adjustable inner and outer points with adjustable head.

Figure 31 shows the final 2D bell geometry that has 11 outer design points and 11 inner design points. Each point is controlled by design variables in Table 7 and Table 8. The parameter values of Figure 31 are from the just minor third bell, bell-Lehr 1 from Figure 17. After building the 2D geometry of the bell, the geometry is rotated around the Y axis (Y=0), and finally 3D tetrahedral Finite Elements are applied to the mesh. Figure 32 shows this procedure. I used a larger mesh in the optimization process for fast computations of the optimization routine, and used fine or extra-fine mesh for measuring 32 low eigenfrequencies of optimized bells for more accurate spectral measurement.

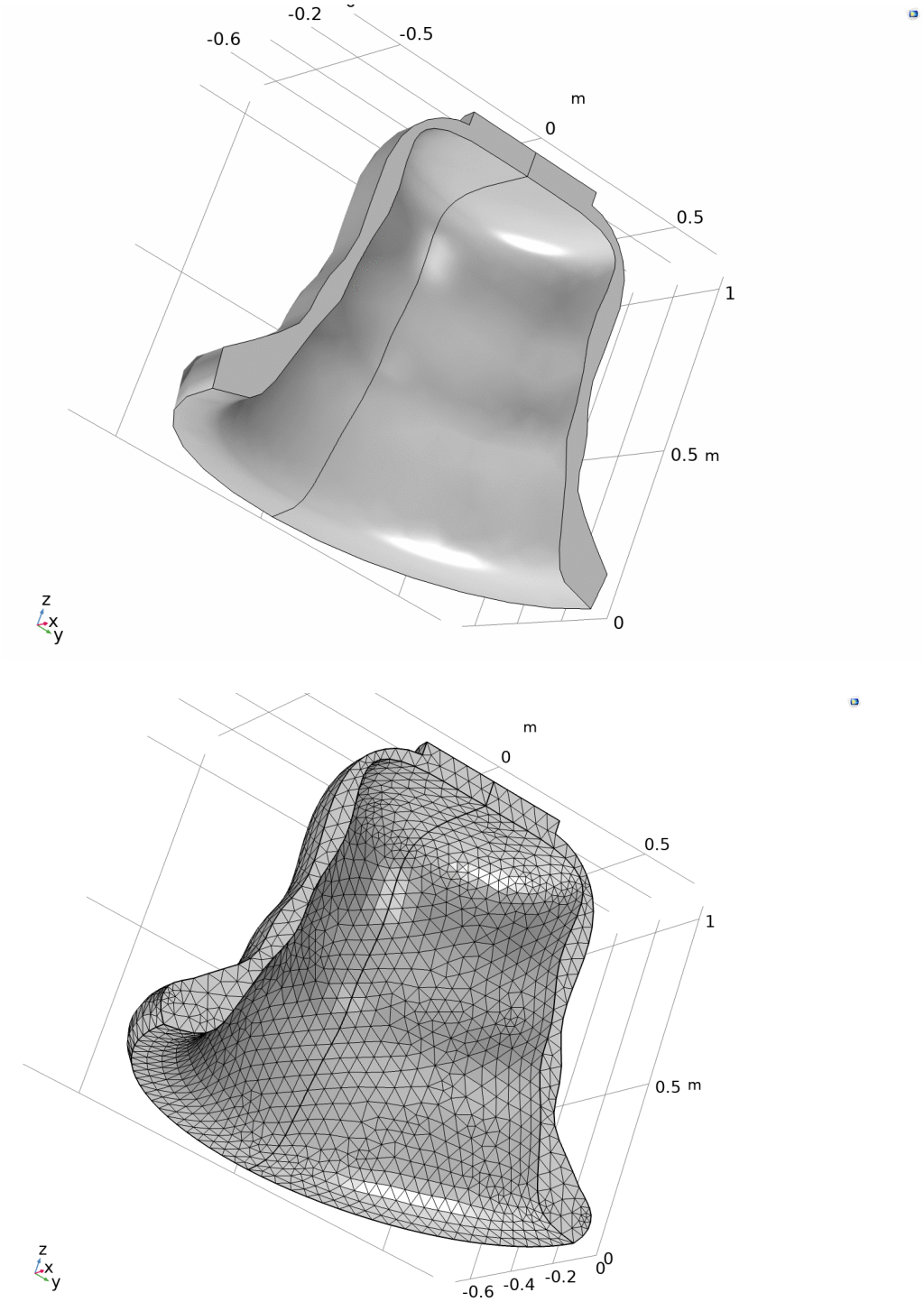

Figure 32. 3D bell geometry after a rotation operation, and with the Finite Elements application.

Note that the overall bell size is fixed to maintain the total height close to 1 meter, although later I added a scalar factor which can proportionally magnify or reduce the overall bell size. The reason for this decision is that the final output that will be employed in my composition is the ratio of lower partials of the bell, not the absolute frequency value of each eigenmode. Although the absolute eigenfrequency values are determined by the physical size of the bell, the overall ratio between partials remain the same regardless of the size and fD-parameter. In other words, the adjustment of the overall bell size transposes the bell harmony and strike tone, while the quality of harmony remains the same.

In order to understand the relationship between bell shape and lower modal frequencies, the 2D bell geometry designing process was continuously accompanied with the frequency analysis due to changes of design variables. Figure 33 shows the frequency changes of six low eigenfrequencies due to variations of six design variables: bow thickness, radius, overall thickness, ratio between waist and hip height, waist angle (waist increment), and hip angle (hip increment). For example, the relation between the bow thickness with tierce and nominal frequency can be easily captured in the first frequency change graph (frequency / bow thickness), and the drastic eigenfrequency ratio changes due to the bell radii can be read in the second frequency change graph (frequency / radii) in which the x-axis denotes the radii change.

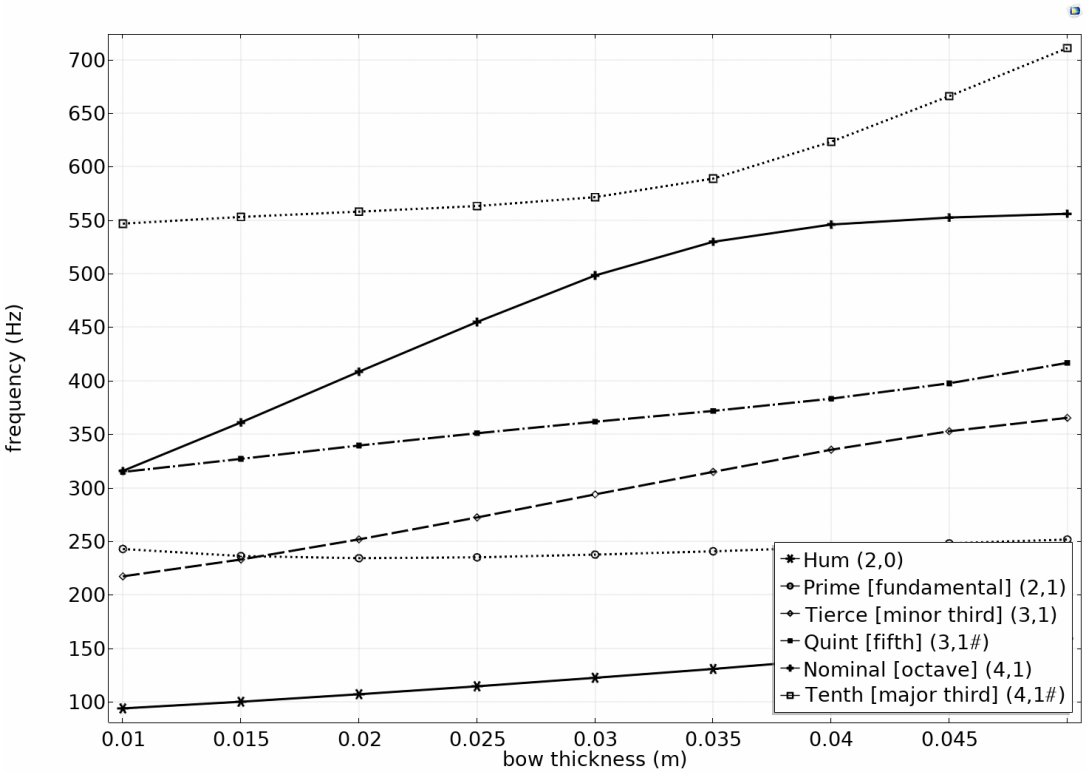

Figure 33. Frequency changes of lower six eigenfrequencies due to variations of six design variables

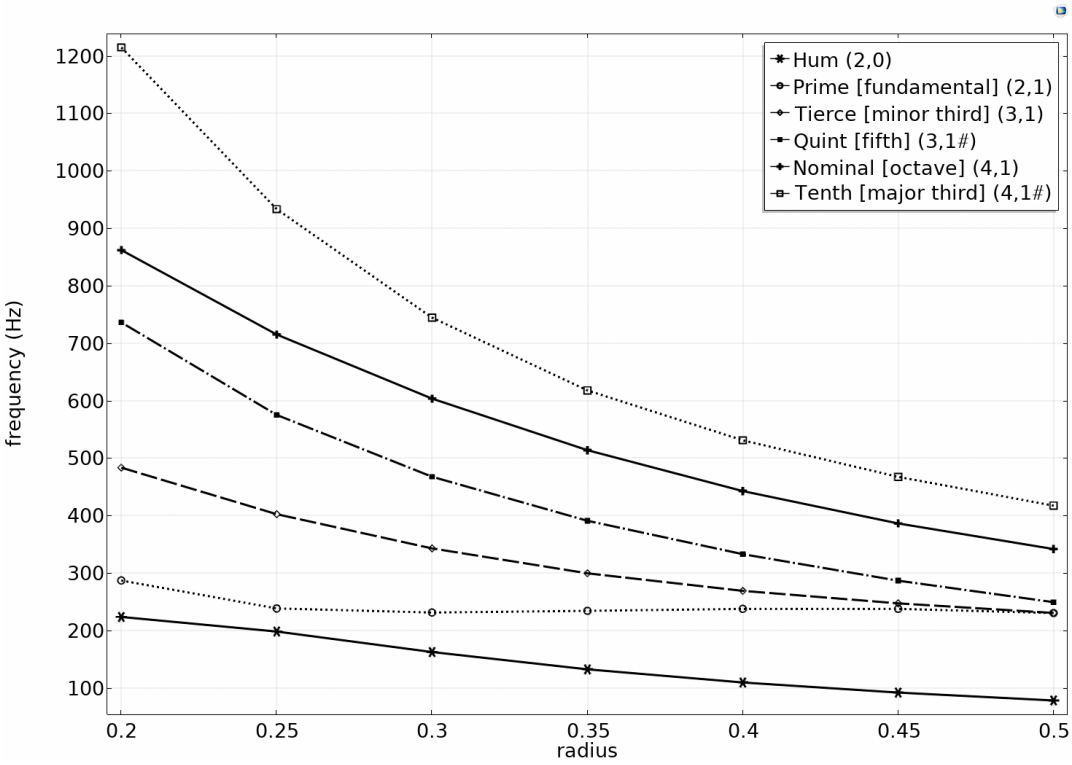

Figure 33, Continued

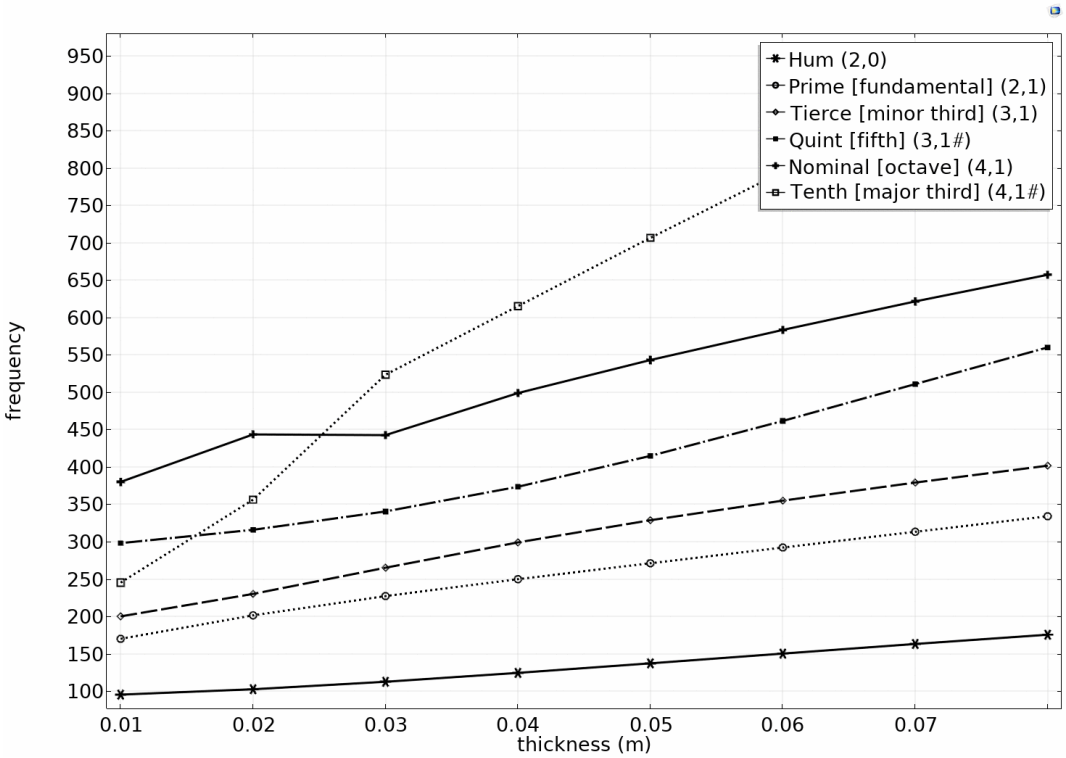

Figure 33, Continued

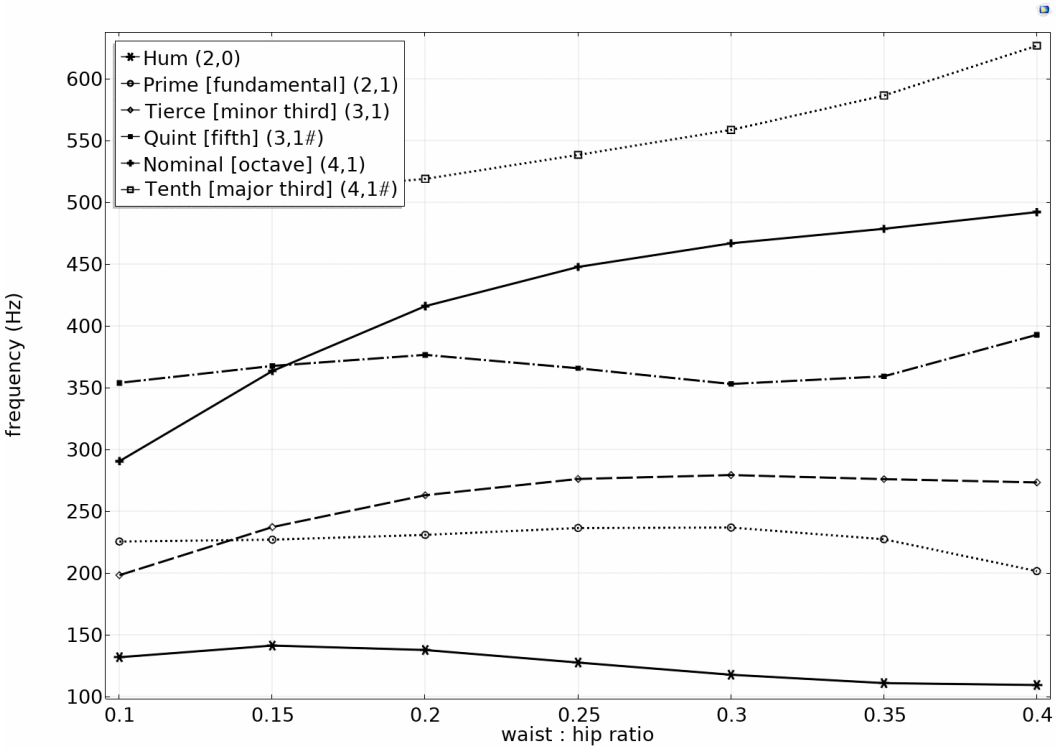

Figure 33, Continued

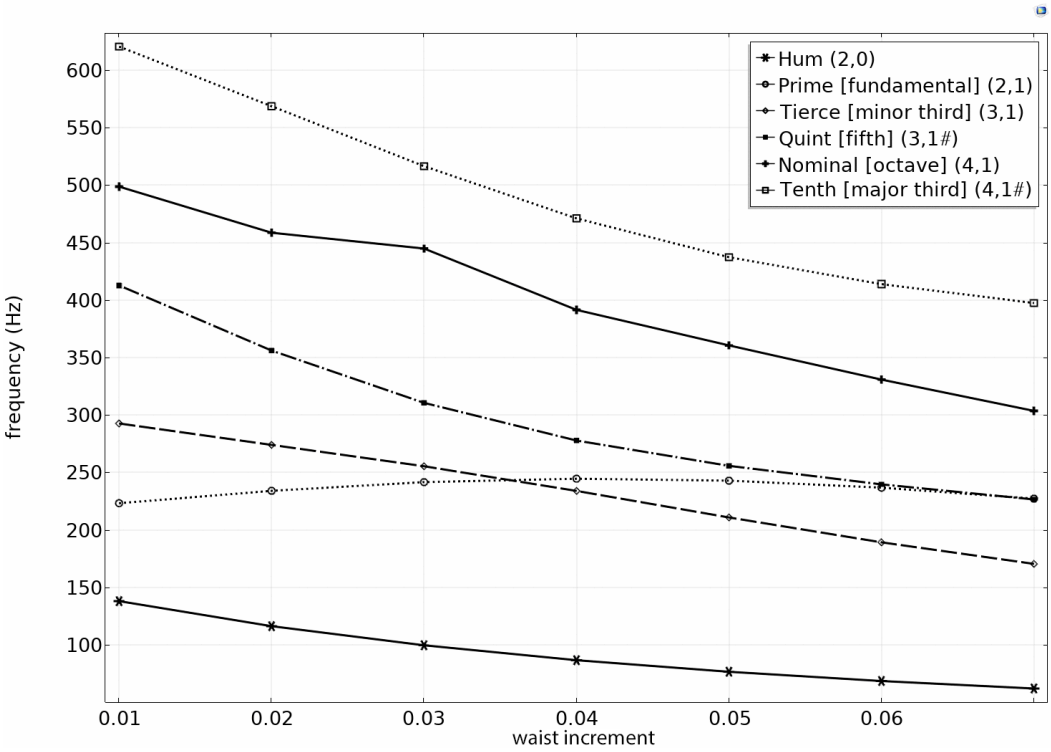

Figure 33, Continued

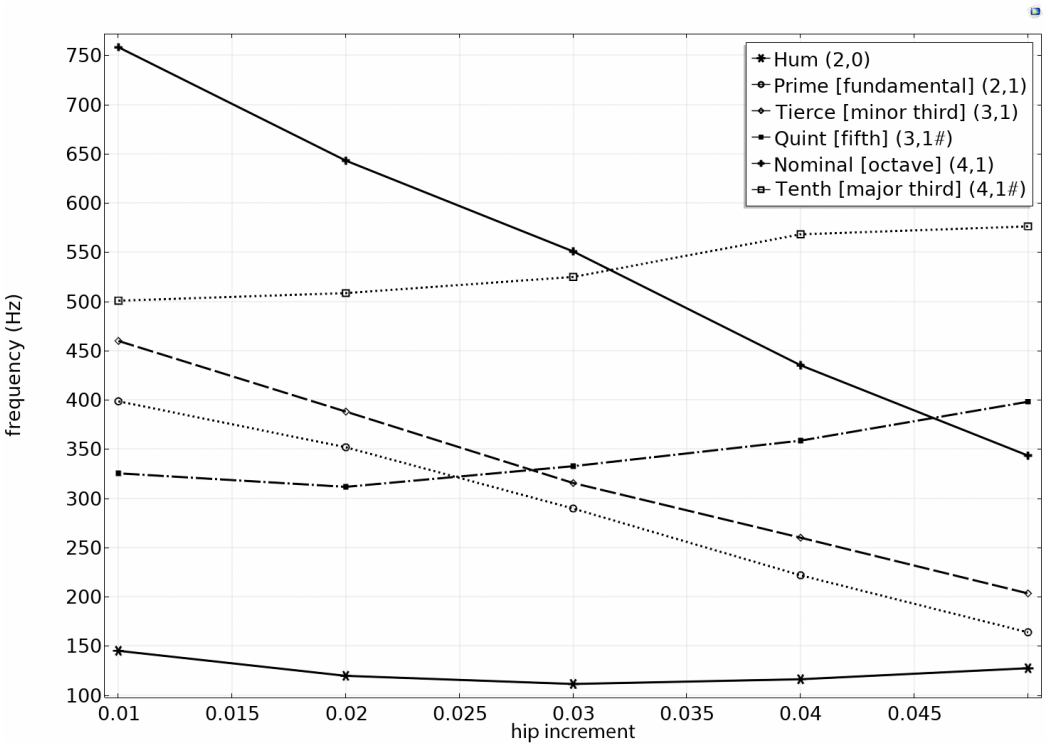

Figure 33, Continued

The minimum and maximum values for each design variable for further optimization modules are decided after performing the frequency examination due to variations of design variables, to keep the range of each eigenfrequency within the desired frequency range (e.g., Tierce higher than Prime, Nominal between Quint and Major tenth, … etc,) and in the range that does not distort the bell geometry so significantly that it will prevent it from materializing a 3D geometric model. Table 9 and 10 show the minimum and maximum values for each design variable.

	radii	bow thickness	waist-hip ratio	waist increment	hip increment	thickness
minimum value	0.25	0.02	0.16	0.02	0.0325	0.028
default	0.379	0.025	1/3.25	0.021	0.038	0.034
maximum value	0.45	0.05	0.42	0.033	0.045	0.07

Table 9. Minimum and maximum values of design variables [in meter].

	thickness	head-thickness ratio	shoulder-thickness ratio	belly-thickness ratio	hip-thickness ratio
minimum value	0.028	1	0.3	0.3	0.4
default	0.034	1.176	0.37	0.53	0.65
maximum value	0.07	1.3	1	1	1

Table 10. Minimum and maximum values of additional local-thickness design variables [in meter].

The material property of the bell, including density, Young modulus, and Poisson ratio are determined more freely. The density value of the bell is decided by the bell material, which is usually made up of an alloy including copper, bronze, tin, or iron. The value of density together with Young modulus and Poisson ratio are decided by averaging the parameters from

experiments by Schneider et al.[130], Niejgh et al. (2002), and Carvalho et al. (2014)[131], while freely adjusting the values during the first minor third bell creation process. (See Table 11.)

	Young modulus, E	Poisson ratio, ν	Density, ρ
Schneider	1.05×10^{11}Pa	0.36 or 0.37	8,392 kg/m^3
Niejgh	9.4×10^{10} Pa	N/A	8,400 kg/m^3
Carvalho	9.0×10^{10} Pa	0.34	8,700 kg/m^3

Table 11. Material properties from Schneider, Niejgh, and Carvalho

No exact values for these variables are necessary, since this is not for casting a real bell, but to create realistic virtual bells having the desired lower eigenfrequencies. In the optimization process these variables were initially included as design variables, but finally excluded and used as constants since the effects on the final lower partial ratios were negligible. For the entire process I set density = 8,700 g/m^3, Young modulus E = 1.05×10^{11}Pa, and Poisson ratio ν = 0.36.

4.2 VERIFICATION

For the verification of my research model, I implemented a small virtual bell of the Gert de Wu church bell (Figure 9) with my 2D parameters and design variables. Alexander Siebert et al. conducted a research of eigenfrequency analysis of a bell with a typical rib (a vertical part of the bell) in the shape of German Gert de Wu church bell, mainly to analyze the effects created by

[130] Albrecht Schneider et al., "Finite-element transient calculation of a bell struck by a clapper," *The Journal of the Acoustical Society of America*, no. 119 (May 2006): 3290, https://doi.org/10.1121/1.4808852.

[131] Miguel Carvalho and Vincent Debut et al, "Physical Modeling and Dynamical Simulation of a 13th Century Bell," In *Proceedings of the 9th International Conference on Structural Dynamics*, EURODYN, 2014.

bell ornamentations[132]. I only used the geometry and eigenfrequency data without the ornamentation from the research, and compared it with the output spectrum of my bell model. Siebert implemented a bell with a typical Gert de Wu rib in a relatively reduced size, having a maximum diameter of 250 mm and a total height of 220 mm following the typical carillon bell rib of Fleischer (1996)[133].

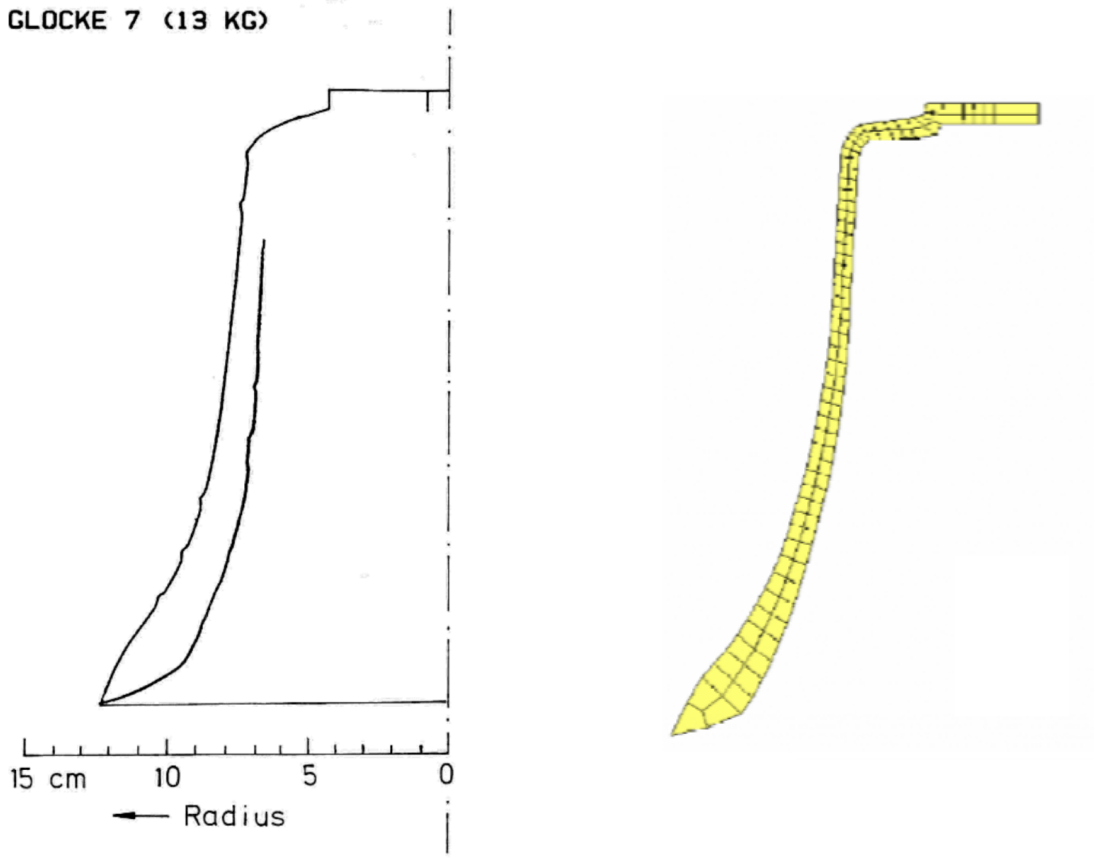

Figure 34. The 2D geometry of a typical Gert de Wu church bell rib from Fleischer (1996, Left) and its FEM implementation with 12,500 3D elements by Siebert (2006, Right).

[132] Alexander Siebert, Gunther Blankenhorn, and Karl Schweizerhof, "Investigating the vibration behavior and sound of church bells considering ornaments and reliefs using LS-DYNA," In *Proceedings of the 9th International LS-DYNA Conference*, Detroit, USA, Pub. LSTC, Livermore, California, 2006.

[133] H. Fleischer, "Schwingung und Tonhöhe von Glockenspielglocken, Forschungs und Seminarberichte ausdem Gebiet Technische Mechanik und Flächentragwerke," In *Technical report*, Institut für Mechanik, Universitätder Bundeswehr, München, 1996.

First, I created an approximate geometry of the Fleischer bell (Figure 35, left), and then optimized the geometry to attain the closest eigenfrequencies to the Fleischer bell (Figure 35, right). Since it is not the original intention of this research to implement the exact geometric data of a pre-existing bell, the verification process was focused on the possibility of creating an approximate bell shape of a pre-existing bell and its optimization. After creating the closest output bell shape (Figure 35, left), the design variables are optimized to tune the lower eigenfrequencies to the spectral profile of the Siebert bell (Figure 35, right). Here I used the same material property data from Siebert's simulation: Young modulus = 9.5×10^{10}Pa, Poisson's ratio = 0.3, and density = 8,450 kg/m^3.

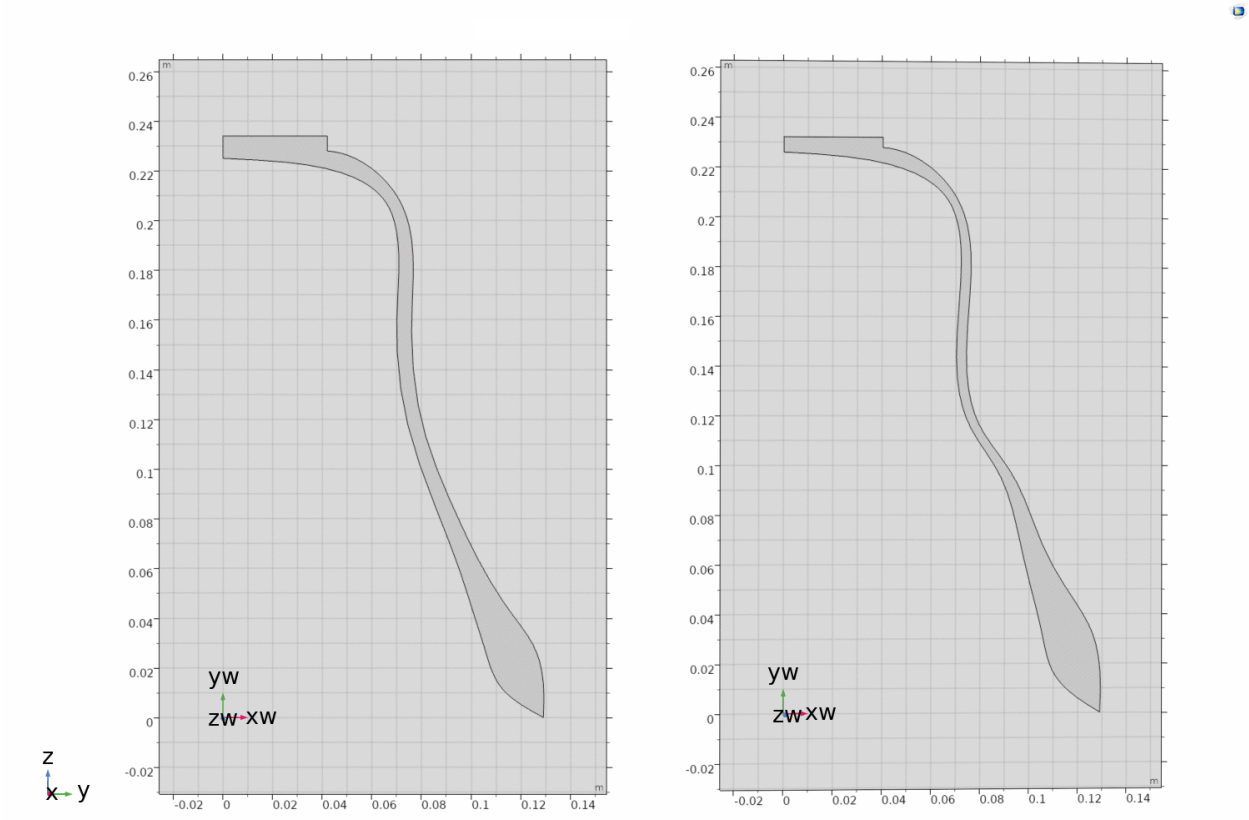

Figure 35. 2D bell geometry with approximate parameters (left), and after optimization (right).

	Fleischer	FEM bell	deviation(%)	Optimized bell	deviation(%)
Hum	265.5 (Hz)	321.12 (Hz)	20.95	279.68 (Hz)	5.34
Prime	555.7	531.95	4.27	535.60	3.61
Tierce	679.2	708.36	4.29	697.56	2.7
Quint	774.8	1072.30	38.4	780.33	0.71
Nominal	1137	1372.00	20.67	1177.40	3.55

Table 12. Comparison of frequencies between the original Fleischer bell, the bell with approximate 2D geometry, and the optimized bell.

The optimized bell has a very close spectral profile to the Flescher bell. Note that the curvature on the waist of the optimized bell was created to tune the lower eigenfrequencies. Since the curvature of my bell geometry is not controlled by a curvature value but adjusted by x coordinate values of multiple design points located in the waist and hip area, the final geometry differs from the original Fleischer bell. Note that the differences of eigenfrequencies between the Flescher bell and my bell with approximate parameters were caused not by the FEM element shape or size (which also usually create errors), but by the differences of bell curvature and local thickness values.

4.3 OPTIMIZATION–THEORETICAL BACKGROUND

The optimization process is a searching process for the optimal value of a given function-optimization function or problem. Similarly to many other computational algorithms, the optimization algorithm was largely developed to solve various problems that occurred during the World War II period with regard to logistics, food supply, and economics: “My own contributions grew out of my World War II experience in the Pentagon. During the war period (1941–45), I had become an expert on programs and planning methods using desk calculators. …

I saw that Leontief's model had to be generalized. His was a steady-state model, and what the Air Force wanted was a highly dynamic model, one that could change over time."[134]

In the optimization process, the derivatives of objective functions need to be used, to optimize the input/control values properly so that the algorithm chooses larger or smaller gradients toward the minimized result of the objective function (minimum problem). This is called the gradient method, which solves the optimization problem with the search directions defined by the gradient (derivative) of the function at the given evaluation point. In this method, the algorithm recursively uses local derivatives of the function on multiple evaluation points, to find a new point which has a closer value to the optimal result. The point where the function has the local minimum needs to be surrounded by near-zero gradients and the direction of gradient value should be changed by bypassing the point. In other words, the point should be located on a dent/dint in the function graph. The problem arises since there could be multiple dents on the 2D geometry of function, and a local minimum on a dent does not guarantee that it is the global minimum value. (See Figure 36.)

There exist various optimization algorithms depending on application software, for example COMSOL Multiphysics supports optimization algorithms including the Constraint Optimization by Linear Approximation (COBYLA) method, the Nelder-Mead method, and the Monte Carlo method.[135] One of the algorithms that I employed in my research is the Nelder-Mead method, which uses the concept of a simplex and gradient, which was originally developed by George B. Dantzig after WW II in response to logistical problems, by introducing the concept

[134] George B. Dantzig and Mukund N. Thapa, *Linear programming 1: Introduction* (New York: Springer-Verlag, 1997), 23.

[135] "Optimize Engineering Designs with the Optimization Module," Product: Optimization Module, COMSOL, accessed February 3, 2020, https://www.comsol.com/optimization-module.

of Linear Programming. Dantzig introduces the concept of optimization and linear programming as following:

> Mathematical programming (or optimization theory) is that branch of mathematics dealing with techniques for maximizing or minimizing an objective function subject to linear, nonlinear, and integer constraints on the variables. …Linear programming is concerned with the maximization or minimization of a linear objective function in many variables subject to linear equality and inequality constraints.[136]

The Simplex Method is a problem-solving model for optimal allocation of scarce resources,[137] and through an algorithm it solves linear programs by moving along the boundaries from one vertex (extreme point) to the next.[138]

Dantzig suggests the fundamental concept of the Simplex Algorithm as following:

> The Simplex Method is applied to a linear program in standard form …The objective is replaced by a new objective w (instead of z), which is the sum of the artificial variables. Now at this point the Simplex Algorithm is employed. It consists of a sequence of pivot operations, referred to as Phase I, that produces a succession of different canonical forms with the property that the sum of the artificial variables decreases with each iteration. The objective is to drive this sum to zero.[139]

Here the linear program in standard form denotes a linear polynomial function, which has z as its minimum value: $c_1x_1 + c_2x_2 + \cdots + c_nx_n = z$ (Min). The Nelder-Mead method is a widely used optimization algorithm, and uses local optimal points made up with multiple evaluation points which constitutes a simplex (e.g., line, triangle, etc.) The area of simplex becomes smaller and moves toward the optimal point as the algorithm moves on: "In the Nelder-Mead method the simplex can vary in shape from iteration to iteration. Nelder and Mead introduced this feature to allow the simplex to adapt its shape to the local contours for the

[136] Dantzig, *Linear programming,* 1.
[137] "Brewer's Problem," Algorithms, Part II, Princeton University, Coursera, accessed February 3, 2020, https://www.cs.princeton.edu/~rs/AlgsDS07/22LinearProgramming.pdf.
[138] Dantzig, *Linear programming,* 63.
[139] Dantzig, *Linear programming,* 78.

function, and for many problems this seems to be effective. …The Nelder-Mead method uses a small number of function evaluations per iteration and it is the most widely used direct search method."[140] By using the algorithm, it analyzes the gradient and finds a better evaluation point from the design space and recursively create a smaller simplex to arrive on the optimum, where the solution point can be determined by a location where the gradient finally becomes zero.[141] Note that it is not guaranteed of finding the global optimal value because the local optimum doesn't always match with the global optimum.

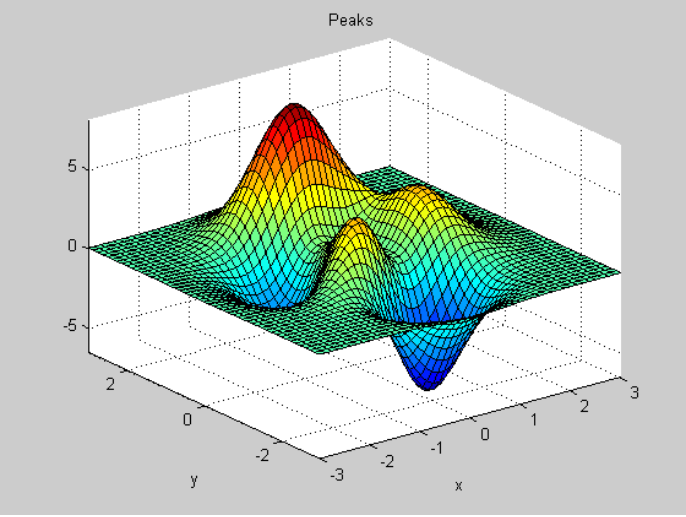

Figure 36. This figure suggests that there could be multiple local minima based on different initial evaluation points.[142]

[140] K.I.M. McKinnon, "Convergence of the Nelder-Mead Simplex method to a non-stationary point," *Society for Industrial and Applied Mathematics* 9, no. 1 (May 1996): 148.

[141] Robbie Balcombe, "Introduction to Design Optimization in COMSOL Multiphysics," Video Gallery, COMSOL, accessed February 3, 2020, https://www.comsol.com/video/introduction-to-design-optimization-in-comsol-multiphysics.

[142] Stuart Kozola, "Tips & Tricks: Getting started using optimization with MATLAB," Optimization Tips & Tricks, File Exchange, MathWorks, accessed February 3, 2020, https://www.mathworks.com/matlabcentral/fileexchange/21239-tips-tricks-getting-started-using-optimization-with-matlab?focused=90fa1646-70f5-b9cf-8e55-5ca2c2e0a9d4&tab=example.

The optimization model is a complex problem-solving model and there is a large body of research on this subject in mathematics and computer science. Since there is a limit on the computation and number of evaluation points within the localized design space, the optimization model is not efficient for a function with a wide range of gradient fluctuations. Fortunately, the low eigenfrequencies of a bell have relatively low gradients without directional changes (e.g., positive to negative and vice versa), the optimization algorithm works relatively efficiently for my bell optimization process. In the process, the initial values/conditions are crucial for finding the global optimal result, likewise in the general optimization process. For more details, please read Dantzig for the Simplex algorithm, and Nelder (1965) for the Nelder-Mead method.[143]

4.4 OPTIMIZATION–APPLICATION

For fast computations in the optimization process, Schoofs used partial derivatives of the frequencies with respect to the wall thickness in his experiment. The frequencies here are represented by linear functions, which are the approximation of resulting frequencies in the range of 2 %. The regression equations are in the order of three or four, and can be expressed as $\mathrm{f_i}(\mathrm{r},\mathrm{t}) = \mathrm{fr_i}(\tilde{\mathrm{r}}) + \mathrm{ft_i}(\tilde{r},\tilde{\mathrm{t}})$ by using the derivatives of the frequencies with respect to the component of the thickness parameter, $\tilde{\mathrm{t}}$. Schoofs used a linear polynomial for $\mathrm{ft_i}(\tilde{r},\tilde{\mathrm{t}})$: $\mathrm{ft_i}(\tilde{\mathrm{r}},\tilde{\mathrm{t}}) = \mathrm{r_1 t_1} + \mathrm{r_2 t_2} + \cdots + \mathrm{r_{nt} t_{nt}} + \mathrm{r_{nt+1} g_1(r) t_1} + \cdots + \mathrm{r_{nt+nt} g_{nt}(\tilde{r}) t_{nt}}$, where $\mathrm{g_j}(\tilde{\mathrm{r}}), \mathrm{j} = 1,2,\ldots,\mathrm{nt}$ are common polynomials in the components of $\tilde{\mathrm{r}}$ (radii). The linear polynomial $\mathrm{fr_i}(\tilde{\mathrm{r}})$ is in the order of three, having β_0 as the lowest order constant and x^3 as the maximal order variable. The estimated value of $\mathrm{ft_i}(\tilde{\mathrm{r}},\tilde{\mathrm{t}})$ can be calculated by differentiating the model with

[143] John A. Nelder and R. Mead, "A Simplex Method for Function Minimization," Computer Journal 7, no. 4 (January 1965): 308–313.

respect to the component of $\tilde{t}$: $\frac{\partial ft_i}{\partial t_j} = r_j + r_{nt+j} g_j(\tilde{r}),\ \ j = 1, 2, \ldots, nt$, and the approximation of regression equation will be attained by differentiating ft_i and discretely integrating it back: $\hat{f}_i = fr_i + \sum_{j=1}^{nt} (\frac{\partial ft_i}{\partial t_j}) t_j$.[144] In the optimization profess, Schoofs calculated the frequency (3, 1)–Tierce first, since it is the most important frequency in bell design.

For the object function, Schoofs used seven lowest frequencies in his thesis:

$$S^2(\underset{\sim}{x}_j) = [\sum_{i=1}^{7} w_i^2 \{c_i(\underset{\sim}{x}_j) - c_i^*\}^2 + w_8^2 \{fD(\underset{\sim}{x}_j) - 200\}^2] / \sum_{i=1}^{8} w_i^2$$

$$j = 1, 2, \ldots, r \qquad (6.3.14)$$

where w_i are weighting factors, $c_i(x_j)$ are frequency ratios in cents on computed design points, c_i are the corresponding target frequency ratios, and $fD(x_j)$ is the fD-parameter.[145] Since Schoofs used fixed value:1 for all weighting factors, the object function can be rewritten as following:

$$\frac{(C_{Hum} - C_{Hum*})^2 + (C_{Prime} - C_{Prime*})^2 + (C_{Tierce} - C_{Tierce*})^2 + \left(C_{Quint} - C_{Quint*}\right)^2}{8}$$

$$+ \frac{(C_{Nominal} - C_{Nominal*})^2 + (C_{Twelfth} - C_{Twelfth*})^2 + (C_{Double\ octave} - C_{Double\ octave*})^2}{8}$$

$$+ \frac{(fD - 200)^2}{8}$$

The ideal fD parameter ($hum\ tone\ frequency \times\ bell\ diameter$) is set to 200, since it is an optimal value for large traditional minor-third bells. In his other paper (1987), Schoofs didn't use the fD value, and only used the four lowest partials for optimization: $F(\tilde{x}) = \sum_{j=1}^{4} \left\{ \frac{\omega_5}{\omega_j} - (\frac{\omega_5}{\omega_j})_{ideal} \right\}^2$.[146] Since the ω_j–each low eigenfrequency is in the denominator having ω_5 in its

[144] Read Schoofs (1987) for the full polynomial expression, and more details.

[145] Schoofs (1987), 6.35.

[146] A. Schoofs, F. Van Asperen, and P. Maas, "Computation of Bell Profiles Using Structural Optimization."

numerator, the lower frequencies will have more effects on the result of equation. (e.g., $400_{\text{Nominal}}/100_{\text{Hum}}$ has more proportion than $400_{\text{Nominal}}/300_{\text{Quint}}$ in the object function.)

In my optimization process, the five lowest frequencies–Hum, Prime, Tierce, Quint, and Nominal are used for the object function, without using the fD value. No weighting factor is added to specific eigenfrequencies. Instead of using a specific target frequency for each eigenfrequency, the four lowest just ratios are employed in the object function.

$$F = \left(\frac{\frac{\omega_{\text{prime}*}}{\omega_{\text{hum}*}}}{\frac{\omega_{\text{prime}}}{\omega_{\text{hum}}}} - 1 \right)^2 + \left(\frac{\frac{\omega_{\text{tierce}*}}{\omega_{\text{hum}*}}}{\frac{\omega_{\text{tierce}}}{\omega_{\text{hum}}}} - 1 \right)^2 + \left(\frac{\frac{\omega_{\text{quint}*}}{\omega_{\text{hum}*}}}{\frac{\omega_{\text{quint}}}{\omega_{\text{hum}}}} - 1 \right)^2 + \left(\frac{\frac{\omega_{\text{nominal}*}}{\omega_{\text{hum}*}}}{\frac{\omega_{\text{nominal}}}{\omega_{\text{hum}}}} - 1 \right)^2$$

For a typical just minor third bell, the object function will be:

$$F_{\text{just m3 bell}} = \left(\frac{\frac{\omega_{\text{prime}*}}{\omega_{\text{hum}*}}}{\frac{2}{1}} - 1 \right)^2 + \left(\frac{\frac{\omega_{\text{tierce}*}}{\omega_{\text{hum}*}}}{\frac{12}{5}} - 1 \right)^2 + \left(\frac{\frac{\omega_{\text{quint}*}}{\omega_{\text{hum}*}}}{\frac{3}{1}} - 1 \right)^2 + \left(\frac{\frac{\omega_{\text{nominal}*}}{\omega_{\text{hum}*}}}{\frac{4}{1}} - 1 \right)^2$$

For the desired frequency ratios, I used the just ratios in Figure 16 and 17. The optimal value for the object function is set to 0.01. For efficient computation in the given resource, I subdivided the optimization process into two steps: 1. optimization of the overall shape and 2. optimization of local thickness parameters for more precise tuning, including shoulder, belly, hip, and head. (Figure 30.) A large number of bells could be optimized within the object function value 0.01 by using only the first step of optimization, while some bells needed a fine tuning by using the second step optimization. If the object function value could not reach to 0.01 within 2000 trials, the optimization was terminated. Table 13 shows the object function values after the optimization process.

Object function	0.003	0.000001	0.001064	0.00068	0.00406	0.013963	0.000000132
Bell No.	Bell 001	Bell 002	Bell 003	Bell 004	Bell 005	Bell 006	Bell 007

0.0067752	0.0009	0.010364	0.00043747	0.0063908	0.00003	0.008	0.01
Bell 008	Bell 009	Bell 010	Bell 011	Bell 012	Bell 013	Bell 014	Bell 015

0.01546	0.0026779	0.0031483	0.0005132	0.0087595	0.0016744	0.000931	0.0014
Bell 016	Bell 017	Bell 018	Bell 019	Bell 020	Bell 021	Bell 022	Bell 023

0.004154	0.00053	0.000062	0.002434	0.018675	0.0000677	0.003335	0.043105
Bell 024	Lehr 001	Lehr 002	Lehr 003	Lehr 004	Lehr 005	Lehr 006	Lehr 007

Table 13. Object function result value for each bell

4.5 RESULT

Here I will show bell 002 (just major third bell with just major seventh nominal), which has one of the lowest object function values after optimization. The 3D geometry of the bell, object function value, optimal design variables, and 32 resultant eigenfrequencies are calculated after further structural analysis by using an extra-fine mesh after the optimization. See Appendix E for the 2D geometry of 31 virtual bells.

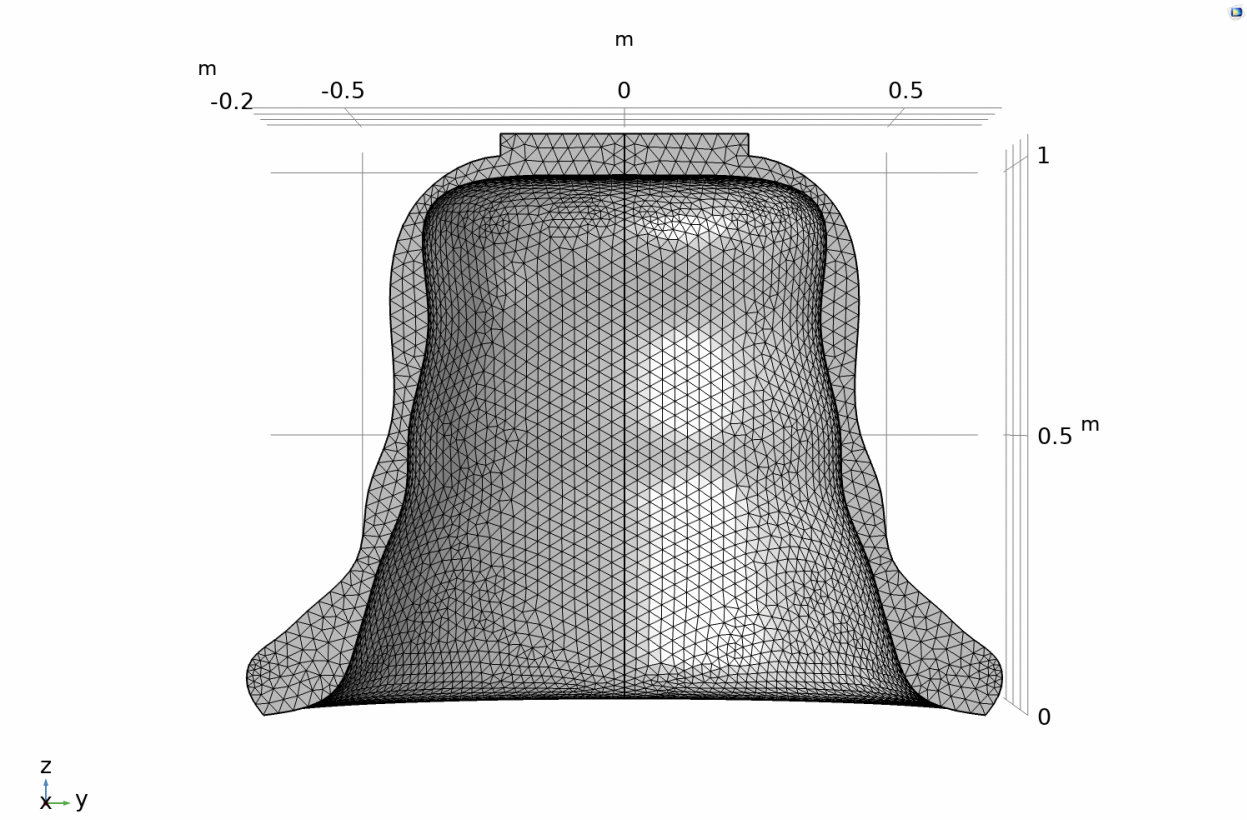

Figure 37. Bell 002–3D Geometry with the object function value, 0.0000017053 (1.7053E-6)

radius	bow thickness	waist-hip ratio	waist increment	hip increment	head ratio
0.36398	0.03719	0.30918	0.02	0.0325	0.5

thickness	head thickness ratio	shoulder thickness ratio	belly thickness ratio	hip thickness ratio	objective function
0.067446	1.176	0.37	0.53	0.65	0.0000017053

Table 14. Bell 002–Design variables

Prime/Hum	Tierce/Hum	Quint/Hum	Nominal/Hum
15/8	9/7 (18/7)	3/2 (3)	7/4 (7/2)

Table 15. Bell 002–Tuning ratios

186.131	348.59	478.367	555.725	590.217	651.616	790.231	807.68
813.651	826.96	920.21	933.31	962.716	1053.137	1100.752	1219.176
1235.305	1237.332	1367.006	1374.52	1387.648	1415.535	1451.532	1502.969
1544.283	1576.417	1623.871	1675.565	1680.141	1692.894	1710.862	1796.892

Table 16. 32 eigenfrequencies of Bell 002 [Hertz]

4.6 TRANSFIGURATION OF BELL

A creation of linear harmonic progressions by means of a gradual shift and morphology of instrumental shapes/materials in order to create mobile harmonic progressions was one of the original motivations of this research. Creating a continuous harmonic progression of frequency spectra has been a huge task for spectral composers from its advent. This originates from the fundamental departure of spectral music, which is based on static spectra, including compressed/expanded spectra (Grisey's *Vortex Temporum*), FM harmony (Murail's *Gondwana*, Chowning's *Stria*, etc.), instrumental timbre (Grisey's *Partiels* and Murail's *Désintégrations,* etc.), overtone spectra of the human voice (Murail's *L'Esprit des dunes*, Harvey's *Speakings*, etc.), the pure overtone series (works by Tenney and Haas), and artificially altered overtone spectra (Lindberg's *Kinetics*, *Fresco*, and *Marea*, etc.) A gradual change of the ratio between carrier and modular frequencies in FM was strategically employed to achieve a continuous harmonic progression, by Tristan Murail and Heinrich Taube in their pieces *Gondwana* and *Aeolian Harp* respectively.[147] Lindberg used an interpolation technique, by applying the idea of the passing tone or the passing group of Messiaen, on the level of large harmonic fields.

By using the gradual transfigurations of virtual bells, here I want to present an original musical "passing spectra" by using the physical modeling and its resultant acoustical data. In this example, the beginning harmony is from Bell 018 (perfect fifth prime with just minor 3rd tierce and just minor 9th nominal), and the final arrival harmony is from Bell 013 (just major third

[147] In fact, this ratio change in FM can be regarded as a pseudo-acoustic version of a transfiguring instrument; the inharmonicity created by a non- integer ratio between carrier and modular frequency emulates a modeling of the multi-dimensional modal vibrations of a virtual instrument and their gradual transfiguration, which engenders the gradual shift of timbre.

tierce with just major seventh prime and harmonic minor seventh nominal). Figure 38 shows the geometries of Bell 018 and 013.

Figure 38. 2D geometries of Bell 018 (left) and 013 (right).

Intermediate harmonies are calculated by creating intermediate bells' geometry between these two. This means that there could be an arbitrary number of intermediate stages of shape between these two bells, and here I created five intermediate bells between the Bell 018 and 013. Each of the intermediate bell has its own spectral profile, which is calculated by using the structural analysis. Table 17 shows the five intermediate bells and their design parameters, and Figure 39 shows how the 2D geometry of Bell 018 is transfigured into the Bell 013. For this experiment I interpolated linearly, but any other kind is possible as well.

radii	0.32308	0.32797	0.33286	0.337745	0.34263	0.34752	0.35241
bow thickness	0.04344	0.04156	0.03968	0.0378	0.03592	0.03404	0.03216
waist-hip ratio	0.40364	0.38493	0.36623	0.34752	0.32881	0.31011	0.2914
waist inc.	0.02	0.02	0.02	0.02	0.02	0.02	0.02
hip inc.	0.039051	0.037959	0.036867	0.03578	0.03468	0.03359	0.0325
thickness	0.064237	0.064519	0.064801	0.065083	0.065365	0.065647	0.065929
bells	Bell 018	in-bell 1	in-bell 2	in-bell 3	in-bell 4	in-bell 5	Bell 013

Table 17. Five intermediate bells between Bell 018 and Bell 013

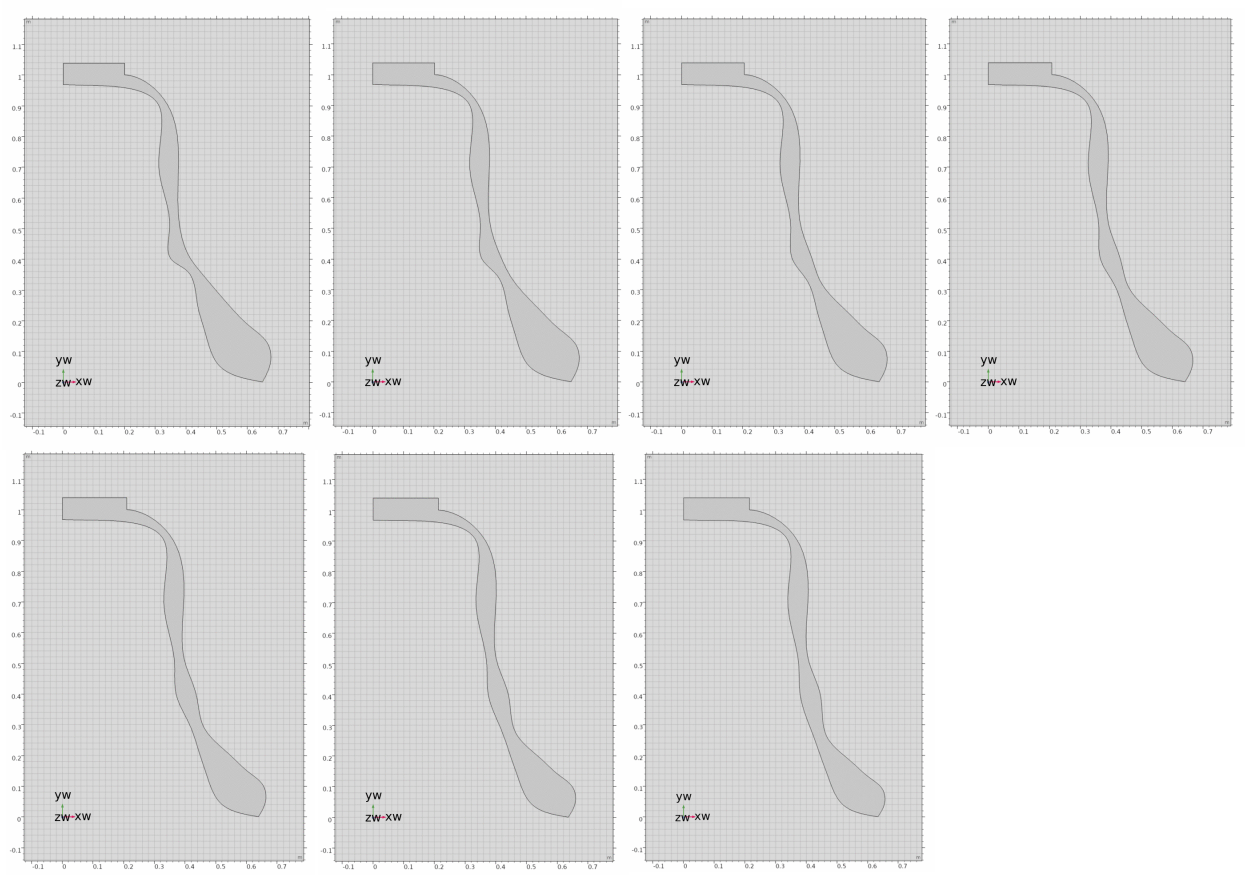

Figure 39. Transfiguration of bell geometry from Bell 018 to Bell 013.

1218.87	1236.92	1249.77	1257.48	1247.47	1217.50	1190.6
1158.46	1149.18	1139.32	1128.85	1128.05	1132.10	1135.6
1155.79	1106.18	1112.79	1121.67	1118.46	1105.67	1093.4
1076.26	1098.92	1066.95	1050.92	1035.57	1018.11	1000.7
1073.39	1071.52	1063.83	1033.05	1005.53	979.42	957.31
1043.49	1022.72	999.57	974.84	950.94	926.94	904.19
904.00	882.57	863.07	844.90	836.06	835.74	835.05
885.93	877.03	862.01	844.31	828.43	811.37	796.92
853.24	843.13	833.95	835.52	826.72	808.54	796.09
822.49	830.27	833.59	823.96	814.91	805.32	791.64
693.63	689.35	679.72	667.17	654.67	654.43	654.12
691.37	658.60	646.95	651.73	653.89	641.17	627.49
614.36	636.65	632.65	610.63	592.27	575.77	561.68
509.10	498.74	489.86	482.27	476.29	471.12	468.05
313.49	315.95	320.53	326.35	333.43	340.93	349.33
206.81	203.36	199.71	196.04	192.67	189.37	186.52
Bell 018	in-bell 1	in-bell 2	in-bell 3	in-bell 4	in-bell 5	Bell 013

Table 18. 16 eigenfrequencies of intermediate bells between Bell 018 and Bell 013 [Hertz]

Figure 40 shows the changes of each lower modal frequency after computing 16 eigenfrequencies for each intermediate bell. Note that most of the eigenfrequencies are not linearly changing (e.g., linear interpolation) due to the transfiguration of the bell.

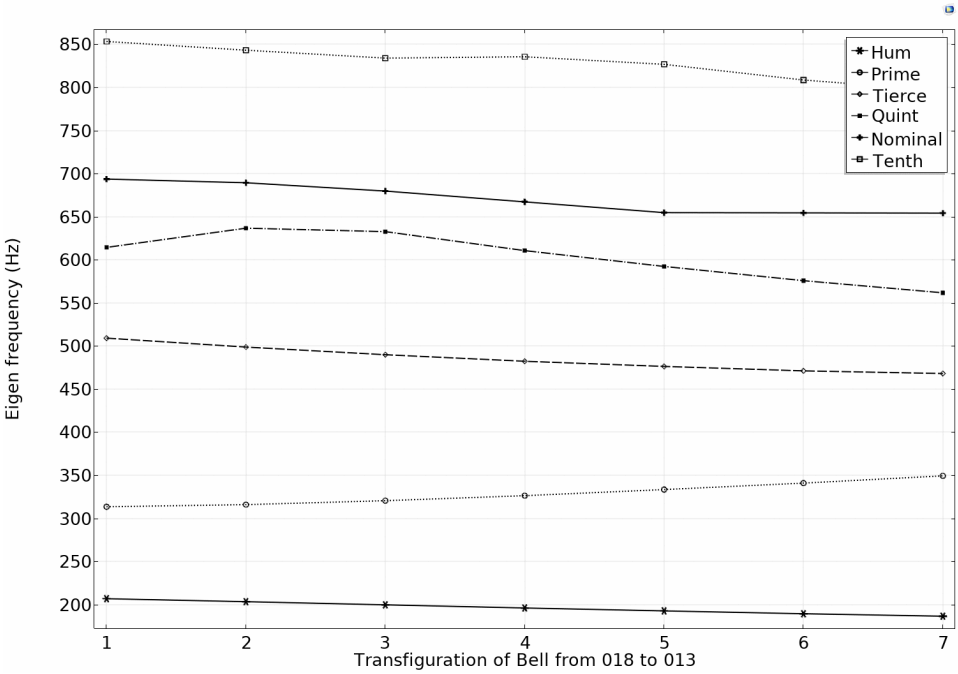

Figure 40. Frequency changes of lower six eigenfrequencies due to the transfiguration.

Since I will use the relative ratios of harmonic profiles, the eigenfrequencies are converted to ratios with respect to the prime frequency (Table 19).

5.894	6.082	6.258	6.414	6.475	6.429	6.383
5.602	5.651	5.705	5.758	5.855	5.978	6.088
5.589	5.440	5.572	5.722	5.805	5.839	5.862
5.204	5.404	5.342	5.361	5.375	5.376	5.365
5.190	5.269	5.327	5.270	5.219	5.172	5.132
5.046	5.029	5.005	4.973	4.936	4.895	4.848
4.371	4.340	4.322	4.310	4.339	4.413	4.477
4.284	4.313	4.316	4.307	4.300	4.285	4.273
4.126	4.146	4.176	4.262	4.291	4.270	4.268
3.977	4.083	4.174	4.203	4.230	4.253	4.244
3.354	3.390	3.404	3.403	3.398	3.456	3.507
3.343	3.239	3.239	3.324	3.394	3.386	3.364
2.971	3.131	3.168	3.115	3.074	3.040	3.011
2.462	2.452	2.453	2.460	2.472	2.488	2.509
1.516	1.554	1.605	1.665	1.731	1.800	1.873
1.000	1.000	1.000	1.000	1.000	1.000	1.000
Bell 018	in-bell 1	in-bell 2	in-bell 3	in-bell 4	in-bell 5	Bell 013

Table 19. 16 eigenfrequency ratios with respect to the prime frequencies

Finally, I added a stepwise motion of the fundamental (a passacaglia of descending 1.5 interval–just ratio of 10:11–from E to G) to add a dramatic tension to the chord progression. Once this chord progression is notated as MIDI cent values (Table 20), they are musically notated in Figure 41. Note that the chords in Figure 41 are quarter-tone quantized. Depending on different compositional purposes including performance contexts, the level of microtonal precision can be varied. To convey the transparent quality of just-tuned bell harmonies, it would be more effective if the lower frequencies can be deployed in a tuning system of higher resolution, such as 72 TET or 96 TET.

82.72	81.76	80.74	79.68	78.34	76.72	75.10
81.84	80.48	79.14	77.80	76.60	75.46	74.28
81.80	79.82	78.74	77.70	76.44	75.04	73.62
80.56	79.70	78.00	76.58	75.12	73.62	72.08
80.50	79.28	77.96	76.28	74.60	72.94	71.32
80.02	78.46	76.88	75.26	73.64	72.00	70.32
77.54	75.92	74.34	72.80	71.40	70.20	68.96
77.18	75.80	74.32	72.78	71.26	69.70	68.14
76.54	75.12	73.74	72.60	71.22	69.64	68.12
75.90	74.86	73.74	72.36	70.96	69.56	68.02
72.96	71.64	70.20	68.70	67.18	65.96	64.72
72.90	70.84	69.34	68.30	67.16	65.62	64.00
70.86	70.26	68.96	67.18	65.44	63.74	62.08
67.60	66.02	64.54	63.08	61.66	60.28	58.92
59.20	58.14	57.20	56.32	55.50	54.68	53.86
52.00	50.50	49.00	47.50	46.00	44.50	43.00
Bell 018	in-bell 1	in-bell 2	in-bell 3	in-bell 4	in-bell 5	Bell 013

Table 20. 16 note harmonies represented in MIDI cents

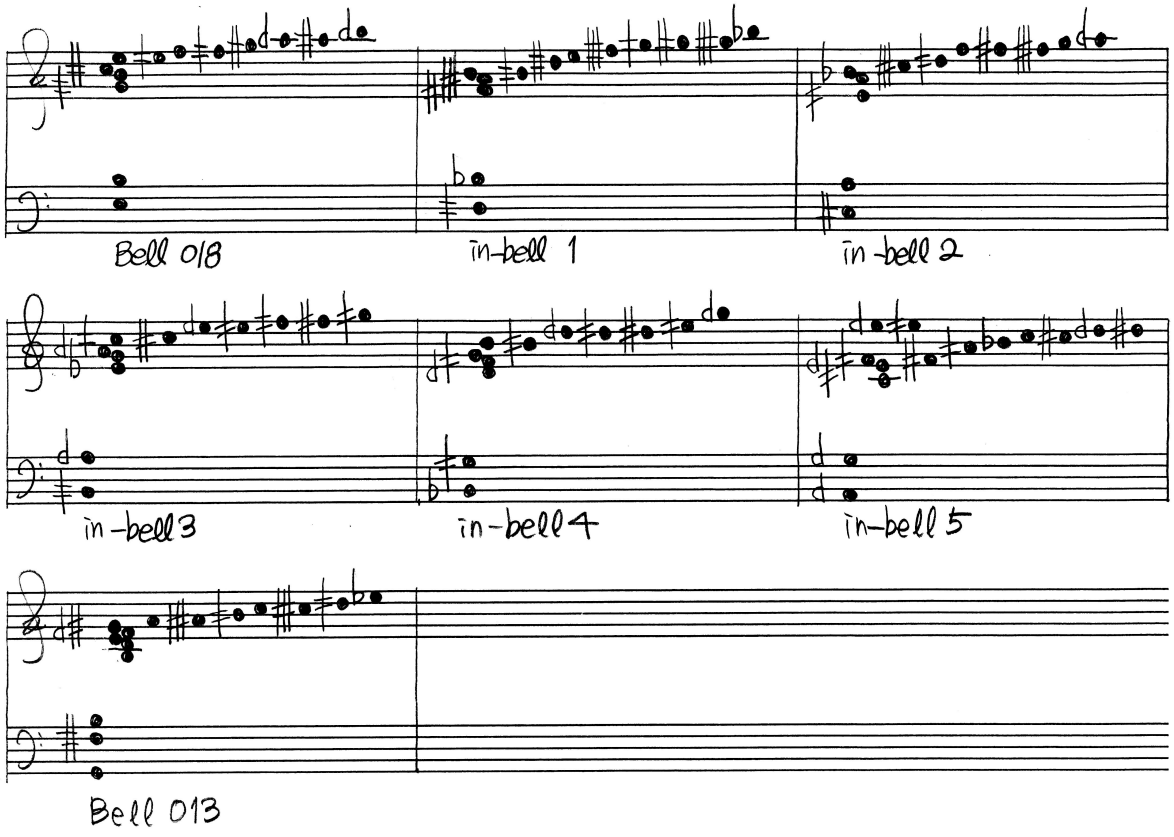

Figure 41. Mobile chord progression created by the bell transfiguration.

CHAPTER 5: CONCLUSION

Creating harmony that is structurally based on a physical or mathematical model is relatively new territory and has not been actively explored because of its multidisciplinary nature. This also differs from FFT-based analysis of recorded sounds–*objet sonore*, as the sounds are created by using mathematical or physical/acoustical formulae[148]. The power of this approach is that creators can make sounds which can surpass the limitation of sensible materials, by using the dynamical system as a rudder with which to navigate an infinite sonic time-space, while maintaining its natural, realistic, and plausible quality, as if the sound-space can exist in another multiverse. It can also remove the total randomness of arbitrary parameters, or chaotic collages of out-of-nothing improvisations, which can be easily deployed in a musical space and become out of the control of the creator; this can cause antipathy from the audience, or lose the balance between consonance and dissonance, with the resulting output being an intolerable amount of cacophony regardless of the level of the art. In other words, the systematic model in music can work as a virtual tool-kit that the creator can integrate with his/her imagination, with sounds, and time in a playful manner in the musical space.[149] Thus, the sounds that are created within this imaginary boundary will become closer to nature or universe, be them beautiful or ugly, orderly or chaotic, spiritual or visceral, and finite or infinite–what Xenakis described as "the collision of hail or rain with hard surfaces, or the song of cicadas in a summer field."[150] The FEM was one way of inspiring the creation of bell sounds, that humans have been casting and developing for

[148] This is the area where the Systematic Musicology is mainly focused on.

[149] In music history after 20th century, the musical system was mostly defined by the composer or the composer's collective experiences based on which he/she makes musical decisions. This collective experience can also be regarded as musical system in a global sense, likewise an AI composer creates music based on the knowledge and decisions that have been accumulated in its existential history.

[150] Xenakis, *Formalized Music*, 9.

thousands of years, even dating back to the second millennium before Christ. China had a thriving bell culture even from the Shang dynasty, c.1520-c.1030 BC.[151] Since this research only covered the spectral, and not the dynamic response–amplitude profile of bells (which can be done by measuring the average displacement of each eigenmode material surface, and normalizing it with respect to other modal displacements), further research can be conducted to cover the overall data from virtual bells besides modal frequency result. Of course, the creation of virtual instruments does not need to be limited to campanology, but can be expanded to other unexplored imaginary instruments with any possible physical shape: a thousand unborn sounds that are not vibrating yet.

[151] Andre Lehr, "The Two-Pitch Chinese Bell During the Shang and Chou Dynasty," National Carillon Museum, Ostaderstraat 23, NL-5721 WC Asten, accessed Feb 23, 2020, http://www.campaners.com/pdf/pdf596.pdf.

POSTFACE

This research was not really a structurally initiated or robustly planned project. Every direction of study was determined and guided by personal interests and curiosity. I had never predicted that the final arrival of my studies was to be virtual bells. I was looking for the physical body of sounds, a device that can give life to an imaginary earth on which I can stand, presenting a balance of freedom and constraints, as Stravinsky once suggested in his *Poetics of Music* lectures.[152] Through the body of sounds, I wanted to express musical pathos and logical or spiritual drama. During the journey, I was always tied to the question of "why" and "how" of sound, as in Zen Buddhism question (Hwadu–話頭 or kōan–公案), "What is this (이뭣고 / 是甚麼)?" Whenever I encountered questions, the answers were heading toward the ethos of bell sounds, either directly or indirectly. To resolve riddles for 10 years of journeying, I had to study areas that were completely unknown to me, some of which I did not even know existed. From the winter 2018 to spring 2019, while I was studying the FEM and searching for a programming language to implement the virtual bell geometry, I had to question everyday if my research direction was correct and if I had the ability to conduct the studies. However, I continually and slowly pressed on, and almost miraculously arrived at a stage I had never expected.

From another perspective, this research probably began as a reaction to the tradition of total serialism, and in the direction of an absolute (but personal) integration. As Alexander Goehr (1932–) points out, the main body of mid 20th century classical music was dominated by the philosophy of objectivity: "Choice, taste, and style were dirty words. […] All this may well be

[152] "My freedom will be so much the greater and more meaningful the more narrowly I limit my field of action and the more I surround my-self with obstacles," Igor Stravinsky, *Poetics of Music in the Form of Six Lessons* (Cambridge: Harvard University Press, 1947), 70.

seen as a kind of negative style precept: a conscious elimination of sensuous, dramatic or expressive elements […] What was relevant was the drive to an objective and anonymous ideal in which the composer does not imagine his music but sets up matrix structures and performs operations on them from which the music results. […] This search for anonymity, for a common language, should have led, if only through a reductio ad absurdum."[153]

Still it is quite ironic that Boulez's pitch multiplication[154], a technique which is designed to eliminate the slightest tonal gravity into the sounds of conglomeration of serial matrices (again, by Goehr: "relegating the row itself from the foreground of music into the position of a not-to-be-heard matrix determining long-term relationships")[155], share a striking similarity with the bell sounds, toward which I began this journey from the opposite direction from Boulez. This is because Boulez's pitch multiplication, which reinforces the lower intervallic relationships and their sounds, creates a similar sonic result with sounds that are articulated by multiple modal vibrations, within each modal group the vibrational quality is close to the linear harmonic series having lower "artificially-tuned" inharmonicities (e.g., the Tierce interval.)

This irony truly demonstrates that music can only be personal, and there exists no music that is composed by universal law; only sound (space in time) and time (time in space) are universal, or they are the only objective phenomena, which are created and perceived subjectively. Thus, all ideas and techniques that are introduced and deployed in this thesis are

---

[153] Alexander Goehr, "A Letter to Pierre Boulez," in *Finding the Key: Selected Writings of Alexander Goehr*, ed. Derrick Puffett (London: Faber and Faber Limited, 1998), 4-6.

[154] Read Pierre Boulez, "*Boulez on Music Today*," trans. Susan Bradshaw and Richard Rodney Bennett (Cambridge: Harvard University Press, 1971) or Lev Koblyakov, *Pierre Boulez: A World of Harmony* (New York: Routledge, 1990) for more details.

[155] Goehr, "A Letter to Pierre Boulez," 10.

just one way of creating music based on my choices to make virtual bells, by studying campanology and the Finite Element Method.

The bell sound is the sound of enlightenment in Buddhist literature, which embraces an infinite amount of complexity within an instantaneous moment. A sound that is created by nature, but also is tuned and controlled by humans: an ideal synthesis of nature and science. Once the sound is released, it begins its dying process immediately, which is the only truth in Buddhism, the river of Heraclitus. I am very glad that I could study this strikingly beautiful phenomenon, and with it, write music.

BIBLIOGRAPHY

Arrell, Chris. "The Music of Sound: An Analysis of Partiels by Gérard Grisey." In *Spectral World Musics: Proceedings of the Istanbul Spectral Musics Conference*. Edited by Robert Reigle and Paul Whitehead. Istanbul: Pan, 2008: 318-333.

Bader, Rolf. *Nonlinearities and Synchronization in Musical Acoustics and Music Psychology*. Hamburg: Springer, 2013.

Benade, Arthur H. Fundamentals of Musical Acoustics. 2nd ed. New York: Dover Publications, Inc., 1990.

Balcombe, Robbie. "Introduction to Design Optimization in COMSOL Multiphysics." Video Gallery, COMSOL. Accessed February 3, 2020. https://www.comsol.com/video/introduction-to-design-optimization-in-comsol-multiphysics.

Bathe, Klaus-Jürgen. Finite Element Procedures. Jew Jersey: Prentice Hall, 1996.

Bhatia, Rajendra. "Vibrations and eigenvalues." *Resonance* 22: 867-872. https://doi.org/10.1007/s12045-017-0540-8. Accessed April 2019. https://www.ias.ac.in/article/fulltext/reso/022/09/0867-0872.

Boulez, Pierre. *Boulez on Music Today*. Translated by Susan Bradshaw and Richard Rodney Bennett. Cambridge, Massachusetts: Harvard University Press. 1971.

"Brewer's Problem." Algorithms, Part II, Princeton University, Coursera. Accessed February 3, 2020. https://www.cs.princeton.edu/~rs/AlgsDS07/22LinearProgramming.pdf.

Burt, Peter. *Overtones of Progress, Undertones of Reaction: Toshiro Mayuzumi and the Nirvana Symphony*. Accessed Dec 20, 2019. https://web.archive.org/web/20060903144412/http://www.research.umbc.edu/~emrich/Burt.html.

Carvalho, Miguel, Vincent Debut, Jose Antunes, and Elin Figueiredo, "Physical Modeling and Dynamical Simulation of a 13th Century Bell." Proceedings of the 9th International Conference on Structural Dynamics. EURODYN, 2014.

"Chapter 7: Geometry Modeling and CAD Tools." COMSOL Multiphysics Reference Manual. Accessed March 17, 2020. https://doc.comsol.com/5.5/doc/com.comsol.help.comsol/COMSOL_ReferenceManual.pdf.

Dantzig, George B and Mukund N. Thapa. *Linear programming 1: Introduction*. New York: Springer-Verlag, 1997.

Downes, Michael. *Jonathan Harvey: Song Offerings and White as Jasmine*. Farnham: Ashgate Publishing Limited, 2009.

Fineberg, Joshua. *Classical Music, Why Bother? Hearing the World of Contemporary Culture through a Composer's Ears*. New York: Routledge, 2006.

Fleischer, Helmut. "Schwingung und Tonhöhe von Glockenspielglocken, Forschungs und Seminarberichte ausdem Gebiet Technische Mechanik und Flächentragwerke." In *Technical report*, Institut für Mechanik, Universitätder Bundeswehr, München, 1996.

Goehr, Alexander, "A Letter to Pierre Boulez." In *Finding the Key: Selected Writings of Alexander Goehr*, edited by Derrick Puffett. London: Faber and Faber Limited, 1998.

Grisey, Gerard. "Did You Say Spectral?" Translated by Joshua Fineberg. *Contemporary Music Review* 19, no.3 (2000): 1-3.

Grisey, Gerard. "Tempus ex Machina: A composer's reflections on musical time." Translated by S. Welbourn. *Contemporary Music Review* 2 (1987): 239-275.

Harvey, Jonathan "Mortuos Plango, Vivos Voco: A Realization at IRCAM," *Computer Music Journal* 5, no. 4 (Winter, 1981): 22-24.

Harvey, Jonathan. *In Quest of Spirit: Thoughts on Music*. Berkeley: University of California Press, 1999.

Harvey, Jonathan. "Spectralism." edited by Joshua Fineberg. *Contemporary MusicReview* 19, no.3 (2000): 11-14.

Hasegawa, Robert Tatsuo. "*Gegenstrebige Harmonik* in the Music of Hans Zender." Paper presented at the annual meeting for MTSNYS, Buffalo, NY, April 9, 2011.

Hasegawa, Robert Tatsuo. "Just Intervals and Tone Representation in Contemporary Music." Order No. 3312377, Harvard University, 2008. https://search.proquest.com/docview/304600764?accountid=14553.

Helmholtz, Hermann L. F. *On the Sensations of Tones*, 4th ed. Translated by Alexander J. Ellis. Peternoster Row: Longmans, Green, and Co., 1912.

Hervé, Jean-Luc. "*Quatre chants pour franchir le seuil*," translated by Bob Gilmore. In *Contemporary Compositional Techniques and OpenMusic*, edited by Rozalie Hirs and Bob Gilmore. Paris: Editions Delatour France / Amsterdam School of the Arts, 2009.

Hindemith, Paul. *The Craft of Musical Composition: Book 1: Theory*. 4th ed. Translated by Arthur Mendel. New York: Schott, 1942.

Howlea, V.E. and Lloyd N. Trefethen. "Eigenvalues and musical instruments" *Journal of*

Computational and Applied Mathematics 135 (2001): 23–40.

Johnson, Tim. "13-Limit Extended Just Intonation in Ben Johnston's String Quartet #7 and Toby Twining's Chrysaiid Requiem, "Gradual/Tract," DMA diss., University of Illinois at Urbana-Champaign, 2008.

Johnston, Ben. "A Notation System for Extended Just Intonation." In *Maximum Clarity and Other Writings on Music*. edited by Bob Gilmore. 77-88. Urbana: University of Illinois Press, 2006.

Johnston, Ben. "Scalar Order as a Compositional Resource." In *Maximum Clarity and Other Writings on Music*. edited by Bob Gilmore. 10-31. Urbana: University of Illinois Press, 2006.

Kozola, Stuart. "Tips & Tricks: Getting started using optimization with MATLAB." Optimization Tips & Tricks, File Exchange, MathWorks. Accessed February 3, 2020. https://www.mathworks.com/matlabcentral/fileexchange/21239-tips-tricks-getting-started-using-optimization-with-matlab?focused=90fa1646-70f5-b9cf-8e55-5ca2c2e0a9d4&tab=example.

Lehr, André. *Campanology textbook: the musical and technical aspect of swinging bells and carillons*. Translated by Kimberly Schafter. California: Guild of Carillonneurs in North America, 2005.

Lehr, André. "From Theory to Practice." *Musical Perception: An Interdisciplinary Journal – A Carillon of Major-Third Bells* 4, no. 3 (Spring, 1987): (267-280).

Lehr, André. *The Designing of Swinging Bells and Carillon Bells in the Past and Present*. Asten: Athanasius Kircher Foundation, 1987. quoted in Fletcher, Neville H. and T. D. Rossing. *The Physics of Musical Instruments*, 2nd ed. New York: Springer, 2010.

Lehr, André. "The Two-Pitch Chinese Bell During the Shang and Chou Dynasty." National Carillon Museum, Ostaderstraat 23, NL-5721 WC Asten. Accessed Feb 23, 2020. http://www.campaners.com/pdf/pdf596.pdf.

Nelder, John A. and R. Mead. "A Simplex Method for Function Minimization." Computer Journal 7, no. 4 (January 1965): 308–313.

Ligeti, György. *Ligeti in Conversation*, edited by Péter Várnai et al. London: Eulenburg Books, 1983.

"List of intervals." Huygen-Fokker Foundation Center for Microtonal Music. Accessed January 21, 2020. http://www.huygens-fokker.org/docs/intervals.html.

Lutosławski, Witold. *Lutosławski on Music*. Edited by Zbigniew Skowron. Lanham, Maryland: Scarecrow Press, Inc., 2007.

McKinnon, K.I.M. “Convergence of the Nelder-Mead Simplex method to a non-stationary point.” *Society for Industrial and Applied Mathematics* 9, no. 1 (May 1996): 148-158.

Moscovich, Viviana. “French Spectral Music: an Introduction.” *Tempo* 200, no. 3 (April 1997): 21-28.

Murail, Tristan. “After-thoughts,” *Contemporary Music Review* 24/2-3 (2005): 5-9. quoted in Christopher Gainey, “Hearing Timbre-Harmony in Spectral Music.” PhD diss., The University of British Columbia, 2019.

Murail, Tristan. “Cloches d'adieu, et un sourire... in memoriam Olivier Messiaen.” Works. Tristan Murail Official Website. Accessed February 5, 2020. https://www.tristanmurail.com/en/oeuvre-fiche.php?cotage=27527.

Murail, Tristan. “Les sept Paroles.” Works. Tristan Murail Official Website. Accessed February 5, 2020. https://www.tristanmurail.com/en/oeuvre-fiche.php?cotage=28868.

Murail, Tristan. “Target Practice.” translated by Joshua Cody, *Contemporary Music Review* 24/2-3 (2005): 149-171.

Murail, Tristan. “Villeneuve-les-Avignon Conferences, Centre Acanthes, 9-11 and 13 July 1992” Translated by Aaron Berkowitz & Joshua Fineberg. *Contemporary Music Review* 24, no.2/3 (2005): 187-267.

Oñate, Eugenio. *Finite Element Method. Linear Statics. Volume 1. Basis and Solids*. Barcelona: International Center for Numerical Methods in Engineering, 2009.

“Optimize Engineering Designs with the Optimization Module.” Product: Optimization Module, COMSOL. Accessed February 3, 2020. https://www.comsol.com/optimization-module.

Perrin, Robert, T. Charnley, H. Banut, and T. D. Rossing. “Chladni’s Law and the Modern English Church Bell.” *Journal of Sound and Vibration* vol. 102, no. 1 (1985): 11–19.

Perrin, Robert and Charnley, T. “Normal Modes of the Modern English Church Bell.” Journal of Soundand Vibration (1983) 90(l): 29-49.

Rameau, Jean-Philippe. *Treatise on Harmony*. Translated by Philip Gossett. New York: Dover Publications, Inc., 1971.

Roozen-Kroon, P. J. M. “Structural optimization of bells.” PhD thesis., Eindhoven University of Technology, 1992.

Rossing, Thomas D. “The Acoustics of Bells: Studying the vibrations of large and small bells helps us understand the sounds of one of the world's oldest musical instruments.” In *American Scientist*, vol. 72, no. 5 (September-October 1984): 440-447.

Rossing, Thomas D., F. Richard Moore, Paul A. Wheeler. *The Science of Sound*, 3rd ed. San Francisco: Addison Wesley, 2002.

Rossing, Thomas D. *Science of Percussion Instrument*. River Edge: World Scientific Publishing Co. Pte. Ltd., 2000.

Rossing, Thomas D. "The Acoustics of Bell: Studying the vibrations of large and small bells helps us understand the sounds of one of the world's oldest musical instruments." *American Scientist*, 72, no. 5 (September-October 1984): 440-447.

Rossing, Thomas D and R. Perrin. "Vibration of Bells," *Applied Acoustics*, no. 20 (1987): 41-70.

Sabat, Marc. "An informal introduction to the Helmholtz-Ellis Accidentals." *Marc Sabat: music & writings*. Accessed January 22, 2020. http://www.marcsabat.com/pdfs/legend.pdf.

Schneider, Albrecht, ed. *Studies in Musical Acoustics and Psychoacoustics*. Hamburg: Springer, 2017.

Schneider, Albrecht, B. A. Lau, Peter Wriggers, Rolf Bader. "Finite-element transient calculation of a bell struck by a clapper." *The Journal of the Acoustical Society of America*, no. 119 (May 2006): 137-156. https://doi.org/10.1121/1.4808852.

Schneider, Albrecht, Marc Leman. "Sound, Pitches and Tuning of a Historic Carillon." in *Studies in Musical Acoustics and Psychoacoustics*, edited by Albrecht Schneider, 247-293, Hamburg: Springer, 2017.

Schoenberg, Arnold. *Theory of Harmony*, 3rd ed. Translated by Roy E. Carter. Berkeley: University of California Press, 1922.

Schoofs, A. J. G. "Experimental design and structural optimization," PhD diss., Department of Mechanical Engineering, Eindhoven, 1987.

Schoofs, A. J. G., F. van Asperen, P. Maas, A. Lehr. "Computation of Bell Profiles Using Structural Optimization." *Music Perception* Vol. 4, No. 3 (Spring 1987): 245-254.

Shimizu, Yoshihiko. "The Creative Quest into Temple Bell Sonorities: Works of *Musique Concrète* by Toshiro Mayuzumi." *Contemporary Music Review*, 27/1-2 (2018): 36-48.

Siebert, Alexander, Gunther Blankenhorn, and Karl Schweizerhof. "Investigating the vibration behavior and sound of church bells considering ornaments and reliefs using LS-DYNA." In *Proceedings of the 9th International LS-DYNA Conference*, Detroit, USA, Pub. LSTC, Livermore, California, 2006.

Stucky, Steven. *Lutoslawski and His Music*. Cambridge, MA: Cambridge University Press, 2009.

Stucky, Steven. “Tanglewood Celebrates Composer Steven Stucky In Its Festival of Contemporary Music.” Accessed May 1, 2017. https://www.bostonglobe.com/arts/music/2016/07/13/steven-stucky-celebrated-peers-and-students-tanglewood/6WKAJG78z3FVB6rK0SigFJ/story.html.

Stravinsky, Igor. *Poetics of Music*. Cambridge, MA: Harvard University Press, 1970.

Takakura, Yuriko (高倉優理子). “A Comparison of the Compositional Process between the Nirvana Symphony and the Mandala Symphony: An Analysis of the “Campanology Documents”.” accessed March 5, 2020, https://www.musicology-japan.org/publish/v63/Takakura_en.pdf. translated by unknown author, “黛敏郎《涅槃交響曲》と《曼荼羅交響曲》の成立過程比較ー「Campanology 資料」の分析を中心にー.” *ONGAKUGAKU: Journal of the Musicological Society of Japan*, 63, no. 2 (2018), 61-77. https://doi.org/10.20591/ongakugaku.63.2_61.

Takemitsu, Toru. *Confronting Silence: Selected Writings*. Translated and Edited by Yoshiko Kakudo and Glenn Glasow. Berkeley, California: Fallen Leaf Press, 1995.

Tenney, James. *A History of ‘Consonance’ and ‘Dissonance’* New York: Excelsior Music Publishing, 1988.

Webern, Anton. *The Path to the New Music*. Edited by Willi Reich and translated by Leo Black. Bryn Mawr, Pennsylvania: Theodore Presser Co. / Universal Edition, 1963. Originally published as *Wege zur neuen Musik* (Vienna: Universal Edition, 1960).

Martin, Edward Paul. “Harmonic Progression in the Music of Magnus Lindberg.” DMA diss., University of Illinois at Urbana-Champaign, 2005. https://search.proquest.com/docview/305001160?accountid=14553.

Nigjeh, Behzad Keramati, Pavel Trivailo, Neil McLachlan. 2002. “Application of Modal Analysis to Musical Bell Design.” In *Acoustics 2002 - Innovation in Acoustics and Vibration - Annual Conference of the Australian Acoustical Society*, Adelaide, Australia, November 2002, 127-135.

Xenakis, Iannis. *Formalized Music: Thought and Mathematics in Music*. Hillsdale, NY: Pendragon, 1992.

Yih, Chen Cheng. *Two-Tone Set-Bells of Marquis Yi*. Farrer Road, Singapore: World Scientific Publishing Co. Pte. Ltd., 1994.

APPENDIX A: SIMPLE HARMONIC MOTION

If we consider a simple mass-spring system with simple damping force (a damped harmonic oscillator):

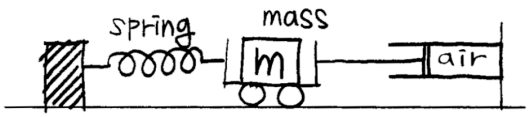

The equilibrium position can be represented by the following equation.

$$mx" = -kx - cx'$$

where m is the mass of the moving object, k is the spring constant, and c is the constant of proportionality and is called the damping factor. This equation can be rewritten as following:

$$x" + \frac{c}{m}x' + \frac{k}{m}x = 0$$

We can change the form of constants of this equation as following:

$$y" + 2py' + {\omega_0}^2 y = 0$$

By substituting $y = e^{rt}$

$$r^2 + 2pr + {\omega_0}^2 = 0$$

From here we get $r = -p \pm \sqrt{p^2 - {\omega_0}^2}$.

1. Undamped case (the damping coefficient c = 0)

$y" + {\omega_0}^2 y = 0$

The general solution $r = -0 \pm \sqrt{0^2 - {\omega_0}^2} = \pm i\omega_0$

Since $y = e^{rt} = e^{\pm i\omega_0 t}$

$$y = c_1 \cos(\omega_0 t - \phi)$$

This can be interpreted as this harmonic system is oscillating in the frequency of ω_0 with out of phase ϕ.

2. Damped case

From $r = -p \pm \sqrt{p^2 - {\omega_1}^2}$, we get

$$r = -p \pm \sqrt{-{\omega_1}^2} = -p \pm \omega_1 i,$$

Since $y = e^{rt} = e^{(-p \pm \omega_1 i)t} = e^{-pt}(c_1 \cos \omega_1 t + c_2 \sin \omega_1 t)$, we get

$$y = e^{-pt} A \cos(\omega_1 t - \phi)$$

This system can be represented by a graph with displacement y over time t.

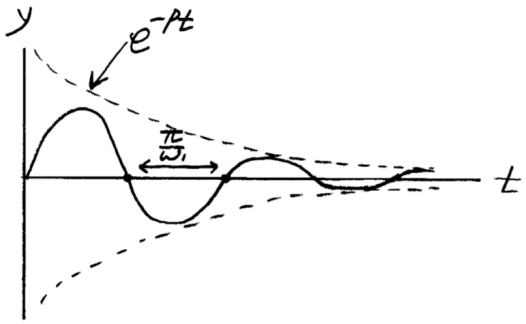

APPENDIX B: SOLVING PROCESS OF A GENERAL FIRST ORDER LINEAR SYSTEM'S ORDINARY DIFFERENTIAL EQUATION

As mentioned in Preface, the general first order differential equation with two degrees of freedom can be expressed as the following.

$$\begin{bmatrix} x \\ y \end{bmatrix}' = \begin{bmatrix} a & b \\ c & d \end{bmatrix}\begin{bmatrix} x \\ y \end{bmatrix}$$

This matrix equation A has a trial solution as:

$$\begin{bmatrix} a_1 \\ a_2 \end{bmatrix} e^{\lambda t} = \begin{bmatrix} x \\ y \end{bmatrix}$$

By substituting x and y,

$$\lambda\begin{bmatrix} a_1 \\ a_2 \end{bmatrix} = \begin{bmatrix} a & b \\ c & d \end{bmatrix}\begin{bmatrix} x \\ y \end{bmatrix}$$

The homogeneous solution would be

$$\begin{bmatrix} a-\lambda & b \\ c & d-\lambda \end{bmatrix}\begin{bmatrix} a_1 \\ a_2 \end{bmatrix} = 0$$

Since this equation is solvable, it has a non-trivial solution, which satisfies the determinant of matrix as zero. (Det $= 0$)

$$\begin{vmatrix} a-\lambda & b \\ c & d-\lambda \end{vmatrix} = 0$$

$$(a-\lambda)(d-\lambda) - bc = 0$$

$$\lambda^2 - (a+d)\lambda + ad - bc = 0$$

The roots λ_1, λ_2 are the eigenvalues of A, which is also called as characteristic values or proper values.

For each λ_i, we can find associated $\overrightarrow{\alpha_i} = \begin{bmatrix} a_{1i} \\ a_{2i} \end{bmatrix}$ by solving system $A - \lambda I = \begin{bmatrix} a-\lambda & b \\ c & d-\lambda \end{bmatrix}\begin{bmatrix} a_1 \\ a_2 \end{bmatrix} = 0$. The general solution would be

$$\begin{bmatrix} x \\ y \end{bmatrix} = c_1\begin{bmatrix} a_{11} \\ a_{21} \end{bmatrix} e^{\lambda_1 t} + c_2\begin{bmatrix} a_{12} \\ a_{22} \end{bmatrix} e^{\lambda_2 t}$$

In matrix–vector notation, $\begin{bmatrix} x \\ y \end{bmatrix} = \vec{X}$, $\begin{bmatrix} a & b \\ c & d \end{bmatrix} = A$, and $\vec{X}' = \mathrm{A}\vec{X}$. The trial solution would be

$\vec{X} = \vec{\alpha}\, e^{\lambda t}$, and this satisfies $\lambda\vec{\alpha}e^{\lambda t} = A\vec{\alpha}e^{\lambda t}$. From here, we get $\mathrm{A}\vec{\alpha} = \lambda\vec{\alpha}$,

and $(A - \lambda I)\vec{\alpha} = 0$. This can be solved by using det$|A - \lambda I| = 0$.

The general solution would be

$$\vec{X} = c_1\overrightarrow{\alpha_1}e^{\lambda_1 t} + c_2\overrightarrow{\alpha_2}e^{\lambda_2 t}$$

APPENDIX C: DISTRIBUTION OF VARIOUS TUNINGS AMONG 363 WESTERN EUROPEAN CHURCH BELLS. (LEHR, 1987)[156]

Bell Type	Tonal Structure			
	Hum	Fundamental	Nominal	%
Octave bell with perfect fundamental	C_4	C_5	C_6	17.4
Octave bell with diminished fundamental	C_4	B_4	C_6	14.3
Minor-ninth bell with perfect fundamental	B_3	C_5	C_6	7.4
Minor-ninth bell with augmented fundamental	B_3	$C\#_5$	C_6	7.2
Octave bell with augmented fundamental	C_4	$C\#_5$	C_6	6.9
Major-seventh bell with perfect fundamental	$C\#_4$	C_5	C_6	5.8
Major-seventh bell with diminished fundamental	C_4	B_5	C_6	5.5
Minor-ninth bell with diminished fundamental	B_3	B_4	C_6	4.7
Major-seventh with double diminished fundamental	$C\#_4$	B_{b4}	C_6	4.1
Octave bell with double diminished fundamental	C_4	B_{b4}	C_6	3.6
Minor-seventh bell with diminished fundamental	D_4	B_4	C_6	2.7
Minor-seventh bell with double diminished fundamental	D_4	B_{b4}	C_6	2.5
Minor-seventh bell with triple diminished fundamental	D_4	A_4	C_6	2.5

[156] Andre Lehr, *The Designing of Swinging Bells and Carillon Bells in the Past and Present* (Asten: Athanasius Kircher Foundation, 1987), quoted in Neville H. Fletcher and T. D. Rossing, *The Physics of Musical Instruments*, 2nd ed. (New York: Springer, 2010), 687

APPENDIX D: GENERALIZED EIGENVALUE PROBLEM AND STEADY STATE ANALYSIS EQUILIBRIUM EQUATION

For steady-state analysis problem:
$U = \frac{1}{2}\,\mathrm{U^T K\,U}$, where U is the strain energy of the system, $\mathrm{U^T}$ is a transposition matrix of $\begin{bmatrix} \mathrm{u1} \\ \mathrm{u2} \\ \mathrm{u3} \end{bmatrix}$, K is a stiffness matrix, and U is a displacement matrix [u_1, u_2, u_3].

Total potential of the loads $W = \mathrm{U^T R}$ where R denotes the total applied load matrix.

If we simplify this into one dimension with a simple spring of stiffness k and applied load P with the displacement of the spring u, we have

$$U = \frac{1}{2}\,\mathrm{ku^2} \text{ and } W = \mathrm{Pu}$$

The total potential energy

$$\Pi = U - W; \quad \Pi = \frac{1}{2}\,\mathrm{ku^2} - \mathrm{Pu} \quad (1.1)$$

The condition for obtaining the equations for the state variables is

$$\delta\Pi = 0$$

From (1.1), we obtain

$$\delta\Pi = (\mathrm{ku} - \mathrm{P})\delta\mathrm{u}$$

$$\frac{\partial\Pi}{\partial\mathrm{u}} = (\mathrm{ku} - \mathrm{P}) \quad (1.2)$$

The equilibrium condition is $\delta\Pi = 0$, thus $\frac{\partial\Pi}{\partial\mathrm{ui}} = 0$.

Applying this to (1.2) gives

$$\mathrm{KU} = \mathrm{R}$$

(steady – state analysis equilibrium equation)

Where R is a matrix form of loads.
For the analysis of a system with temporal factor with an implied unique solution, we need to include the d'Alembert forces:

$$\mathrm{F} = \mathrm{ma} = \mathrm{M\ddot{U}(t)}$$

Now the characteristic equation would be:

$$KU(t) = R(t) - M\ddot{U}(t)$$

This would be a typical linear second order ordinary differential equation and can be solved by substituting the function of time with e^{rt} with a given initial condition. When no loads is applied, we obtain the equation in free vibration condition

$$M\ddot{U}(t) + KU(t) = 0$$

let $U = \Phi \sin\ \omega(t - \tau)$ then

$$-\omega^2 M\Phi \sin\ \omega(t - \tau) + K\Phi \sin\ \omega(t - \tau) = 0$$

$$K\Phi = \omega^2 M\Phi$$

(generalized eigenvalue problem)

Assume there exists the applied load vector R(t) with damping forces CU, then the equilibrium equation in dynamic analysis would be

$$M\ddot{U}(t) + C\dot{U}(t) + KU(t) = R(t) \quad (1.3)$$

in other words,

Inertia forces + Damping/frictional forces + Elastic forces = External loads

total sum of internal forces = externally applied nodal point loads

where M is mass matrix, U is damping coefficient matrix, and K is stiff matrix. U is a displacement vector, $\dot{U}$ is velocity vector, and $\ddot{U}$ is acceleration vector at a nodal point.

APPENDIX E: 2D GEOMETRY OF 31 VIRTUAL BELLS

Bell 001

r_d	0.38197
w_ht	0.9
w_h_rto	0.32527
h_ht	w_ht*w_h_rto
waist_inc	0.02
hip_inc	0.0325
t_d	0.069999
t_d_head_rto	1.176
t_d_shldr_rto	0.37
t_d_belly_rto	0.53
t_d_hip_rto	0.65
bow_thick	0.040541
head_r_d_rto	0.5
Objective	0.0030848
ratios	2, (9/7), (3/2), (12/7)

* unit: meter
* ratios: prime/hum, tierce/hum, quint/hum, nominal/hum

Bell 002

r_d	0.36398
w_ht	0.9
w_h_rto	0.30918
h_ht	w_ht*w_h_rto
waist_inc	0.02
hip_inc	0.0325
t_d	0.067446
t_d_head_rto	1.176
t_d_shldr_rto	0.37
t_d_belly_rto	0.53
t_d_hip_rto	0.65
bow_thick	0.03719
head_r_d_rto	0.5
Objective	0.0000017053
ratios	(15/8), (9/7), (3/2), (7/4)

Bell 003

r_d	0.3145
w_ht	0.9
w_h_rto	1/(3.25)
h_ht	w_ht*w_h_rto
waist_inc	0.021
hip_inc	0.0325
t_d	0.056
t_d_head_rto	1.0779
t_d_shldr_rto	0.37915
t_d_belly_rto	0.41494
t_d_hip_rto	0.58569
bow_thick	0.025
head_r_d_rto	0.5
Objective	0.0000017053
ratios	(9/5), (6/5), (3/2), (4)

Bell 004

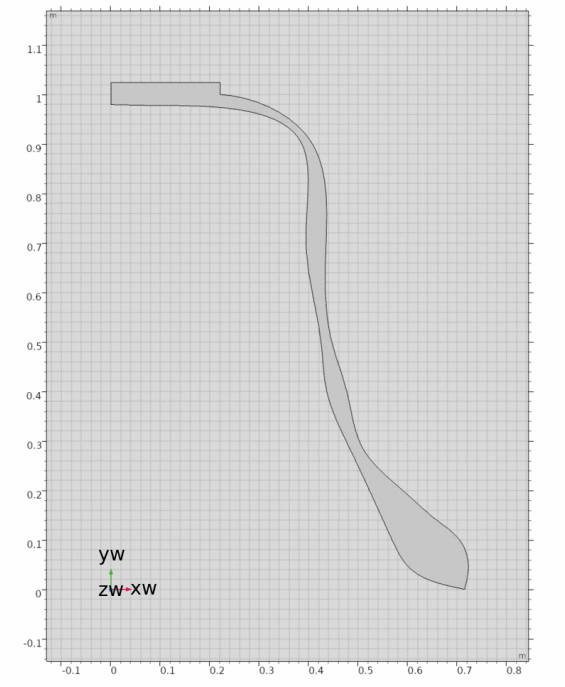

r_d	0.39344
w_ht	0.9
w_h_rto	0.31947
h_ht	w_ht*w_h_rto
waist_inc	0.021
hip_inc	0.038
t_d	0.040837
t_d_head_rto	1.176
t_d_shldr_rto	0.37
t_d_belly_rto	0.53
t_d_hip_rto	0.65
bow_thick	0.032245
head_r_d_rto	0.5
Objective	0.00068303
ratios	(11/6), (22/9), (3), (64/15=16/15)

Bell 005

r_d	0.39704
w_ht	0.9
w_h_rto	0.2837
h_ht	w_ht*w_h_rto
waist_inc	0.027336
hip_inc	0.034649
t_d	0.062172
t_d_head_rto	1.176
t_d_shldr_rto	0.37
t_d_belly_rto	0.53
t_d_hip_rto	0.65
bow_thick	0.047024
head_r_d_rto	0.5
Objective	0.0040696
ratios	2, (18/7=9/7), (11/4), (15/4)

Bell 006

r_d	0.36398
w_ht	0.9
w_h_rto	0.30918
h_ht	w_ht*w_h_rto
waist_inc	0.02
hip_inc	0.0325
t_d	0.067446
t_d_head_rto	1.176
t_d_shldr_rto	0.37
t_d_belly_rto	0.53
t_d_hip_rto	0.65
bow_thick	0.03719
head_r_d_rto	0.5
Objective	0.0000017053
ratios	(15/8), (9/7), (3/2), (7/4)

Bell 007

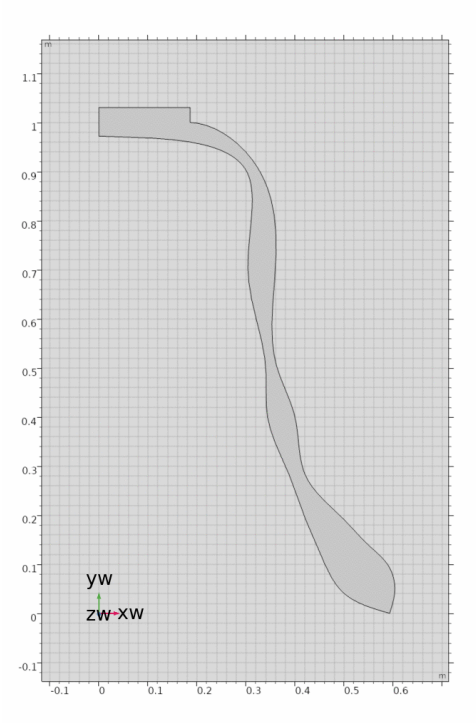

r_d	0.31162
w_ht	0.9
w_h_rto	0.3133
h_ht	w_ht*w_h_rto
waist_inc	0.02
hip_inc	0.0325
t_d	0.056107
t_d_head_rto	1.0779
t_d_shldr_rto	0.37915
t_d_belly_rto	0.41494
t_d_hip_rto	0.58569
bow_thick	0.024219
head_r_d_rto	0.5
Objective	0.0000013185
ratios	(7/4), (12/5), (28/9=14/9), (4)

Bell 008

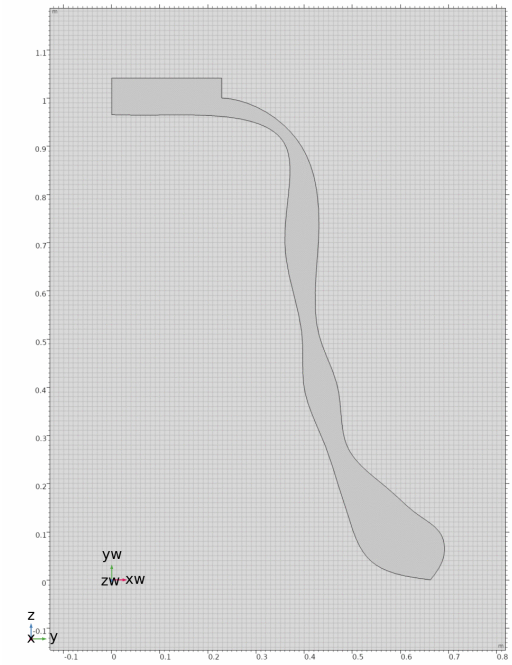

r_d	0.37428
w_ht	0.9
w_h_rto	0.30462
h_ht	w_ht*w_h_rto
waist_inc	0.02
hip_inc	0.0335
t_d	0.069908
t_d_head_rto	1.176
t_d_shldr_rto	0.37
t_d_belly_rto	0.53
t_d_hip_rto	0.65
bow_thick	0.036852
head_r_d_rto	0.5
Objective	0.0067752
ratios	(2), (6/5), (3/2), (12/7)

Bell 009

r_d	0.39704
w_ht	0.9
w_h_rto	0.20395
h_ht	w_ht*w_h_rto
waist_inc	0.02
hip_inc	0.0325
t_d	0.038388
t_d_head_rto	1.176
t_d_shldr_rto	0.37
t_d_belly_rto	0.53
t_d_hip_rto	0.65
bow_thick	0.024997
head_r_d_rto	0.5
Objective	0.00093134
ratios	(12/11), (6/5), (3/2), (15/4)

Bell 010

r_d	0.37939
w_ht	0.9
w_h_rto	0.3191
h_ht	w_ht*w_h_rto
waist_inc	0.02
hip_inc	0.038281
t_d	0.036931
t_d_head_rto	1.176
t_d_shldr_rto	0.37
t_d_belly_rto	0.53
t_d_hip_rto	0.65
bow_thick	0.037114
head_r_d_rto	0.5
Objective	0.010364
ratios	(12/7), (18/7=9/7), (11/4), (44/10=11/5)

Bell 011

r_d	0.37798
w_ht	0.9
w_h_rto	0.27988
h_ht	w_ht*w_h_rto
waist_inc	0.02
hip_inc	0.0325
t_d	0.062044
t_d_head_rto	1.176
t_d_shldr_rto	0.37
t_d_belly_rto	0.53
t_d_hip_rto	0.65
bow_thick	0.041543
head_r_d_rto	0.5
Objective	0.00043747
ratios	(15/8), (9/7), (11/4), (12/7)

Bell 012

r_d	0.34194
w_ht	0.9
w_h_rto	0.32256
h_ht	w_ht*w_h_rto
waist_inc	0.02
hip_inc	0.0325
t_d	0.069417
t_d_head_rto	1.0779
t_d_shldr_rto	0.37915
t_d_belly_rto	0.41494
t_d_hip_rto	0.58569
bow_thick	0.031771
head_r_d_rto	0.5
Objective	0.0063908
ratios	(15/8), (14/6), (28/9=14/9), (14/4)

Bell 013

r_d	0.35241
w_ht	0.9
w_h_rto	0.32527
h_ht	w_ht*w_h_rto
waist_inc	0.02
hip_inc	0.0325
t_d	0.065929
t_d_head_rto	1.176
t_d_shldr_rto	0.37
t_d_belly_rto	0.53
t_d_hip_rto	0.65
bow_thick	0.032155
head_r_d_rto	0.5
Objective	0.000033162
ratios	(15/8), (10/4), (3/2), (7/4)

Bell 014

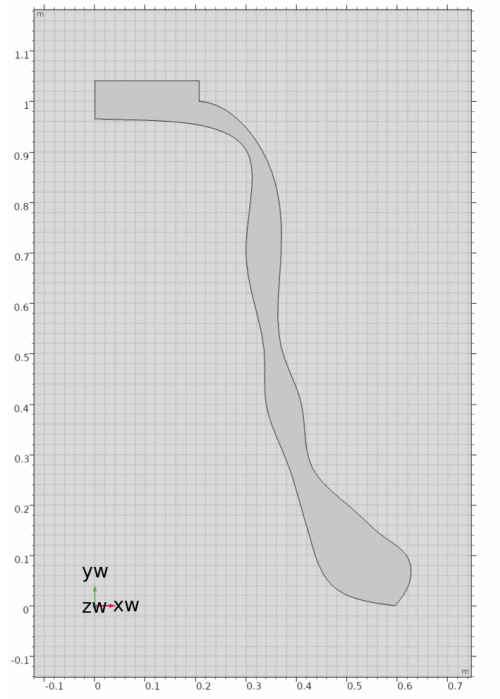

r_d	0.3145
w_ht	0.9
w_h_rto	0.30769
h_ht	w_ht*w_h_rto
waist_inc	0.02
hip_inc	0.0325
t_d	0.07
t_d_head_rto	1.176
t_d_shldr_rto	0.37
t_d_belly_rto	0.53
t_d_hip_rto	0.65
bow_thick	0.0375
head_r_d_rto	0.52686
Objective	0.0000017053
ratios	(15/8), (9/7), (3/2), (7/4)

Bell 015

r_d	0.3409
w_ht	0.9
w_h_rto	0.34515
h_ht	w_ht*w_h_rto
waist_inc	0.033
hip_inc	0.03
t_d	0.07
t_d_head_rto	1.176
t_d_shldr_rto	0.37
t_d_belly_rto	0.53
t_d_hip_rto	0.65
bow_thick	0.045153
head_r_d_rto	0.5
Objective	0.010276
ratios	(2), (10/4), (16/5), (24/7=12/7)

Bell 016

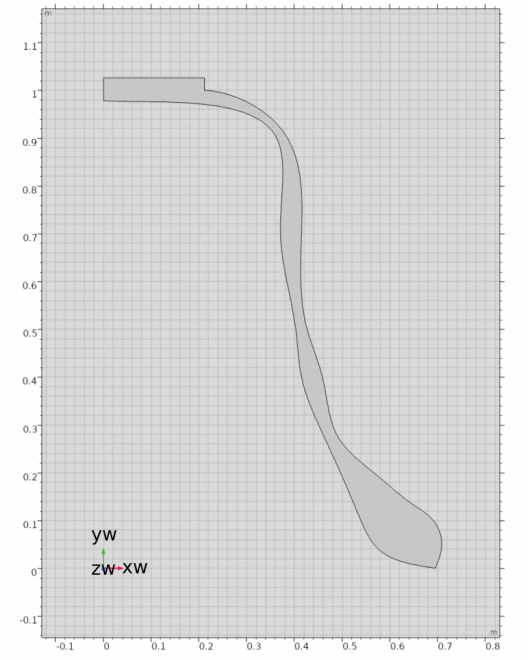

r_d	0.37069
w_ht	0.9
w_h_rto	0.30976
h_ht	w_ht*w_h_rto
waist_inc	0.021914
hip_inc	0.038014
t_d	0.044392
t_d_head_rto	1.176
t_d_shldr_rto	0.37
t_d_belly_rto	0.53
t_d_hip_rto	0.65
bow_thick	0.036523
head_r_d_rto	0.5
Objective	0.015466
ratios	(13/8),(26/10=13/5), (26/9=13/9), (4)

Bell 017

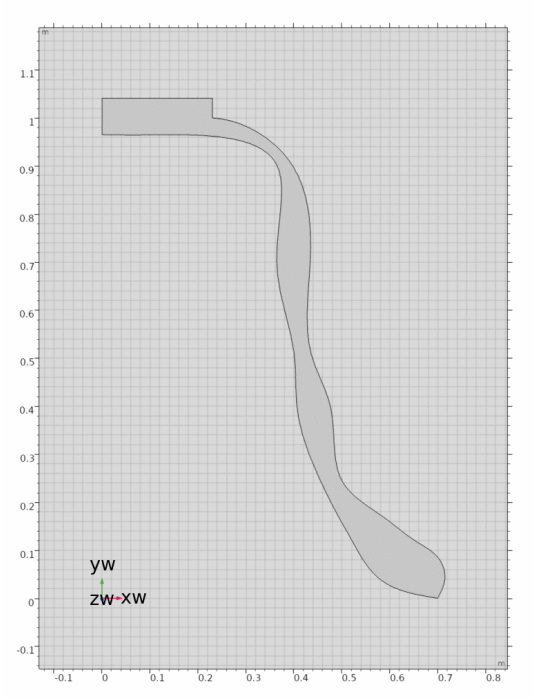

r_d	0.37791
w_ht	0.9
w_h_rto	0.26884
h_ht	w_ht*w_h_rto
waist_inc	0.021
hip_inc	0.038
t_d	0.07
t_d_head_rto	1.176
t_d_shldr_rto	0.37
t_d_belly_rto	0.53
t_d_hip_rto	0.65
bow_thick	0.03
head_r_d_rto	0.5
Objective	0.0026779
ratios	(15/8), (14/6), (6/2), (48/15=12/15)

Bell 018

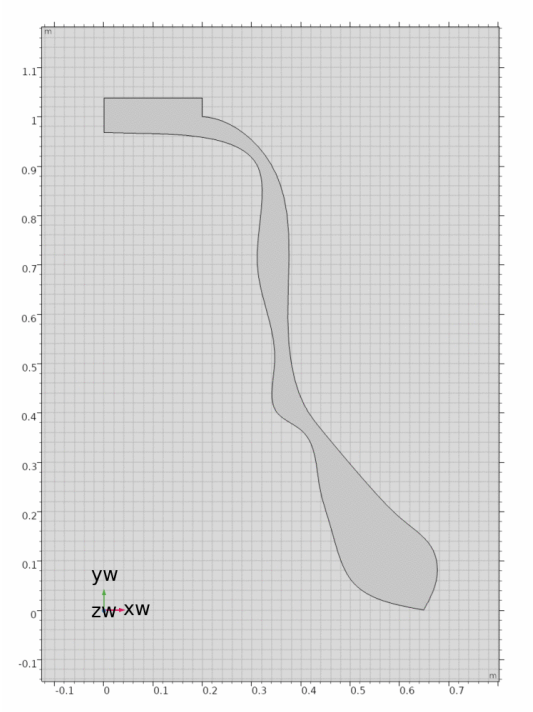

r_d	0.32308
w_ht	0.9
w_h_rto	0.40364
h_ht	w_ht*w_h_rto
waist_inc	0.02
hip_inc	0.039051
t_d	0.064237
t_d_head_rto	1.176
t_d_shldr_rto	0.37
t_d_belly_rto	0.53
t_d_hip_rto	0.65
bow_thick	0.04344
head_r_d_rto	0.5
Objective	0.0031483
ratios	(3/2), (12/5), (6/2), (48/15=12/15)

Bell 019

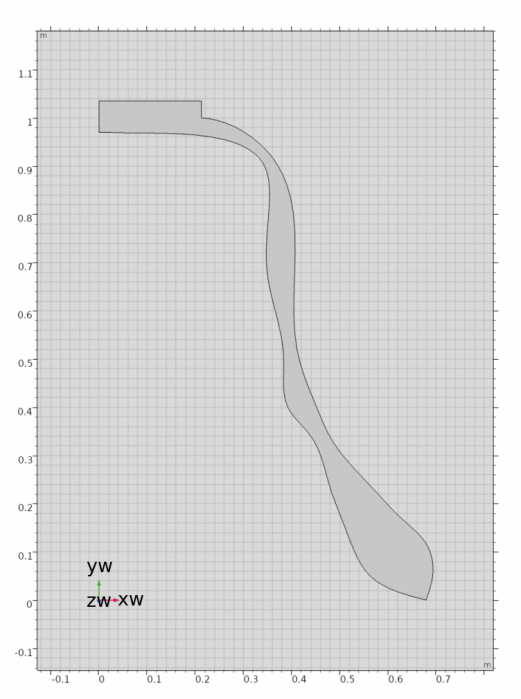

r_d	0.3546
w_ht	0.9
w_h_rto	0.37684
h_ht	w_ht*w_h_rto
waist_inc	0.022449
hip_inc	0.037805
t_d	0.059948
t_d_head_rto	1.176
t_d_shldr_rto	0.37
t_d_belly_rto	0.53
t_d_hip_rto	0.65
bow_thick	0.032249
head_r_d_rto	0.5
Objective	0.00051315
ratios	(11/6), (22/9=11/9), (10/3), (4)

Bell 020

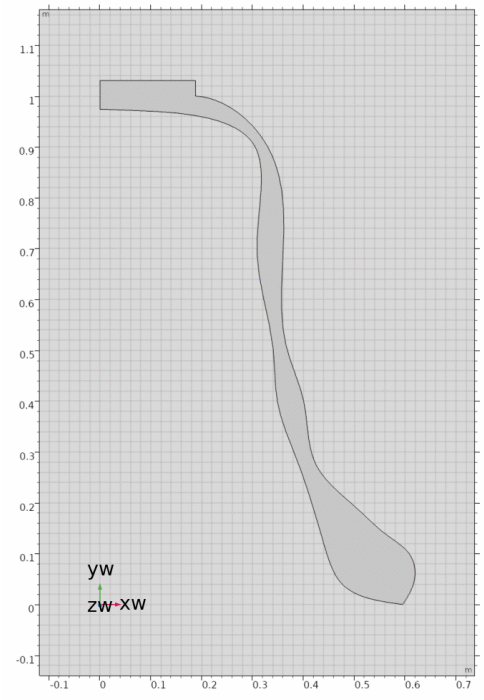

r_d	0.3145
w_ht	0.9
w_h_rto	0.30769
h_ht	w_ht*w_h_rto
waist_inc	0.02
hip_inc	0.0325
t_d	0.052
t_d_head_rto	1.176
t_d_shldr_rto	0.37
t_d_belly_rto	0.53
t_d_hip_rto	0.65
bow_thick	0.0375
head_r_d_rto	0.5
Objective	0.0087595
ratios	(8/5), (12/5), (3/2), (18/5)

Bell 021

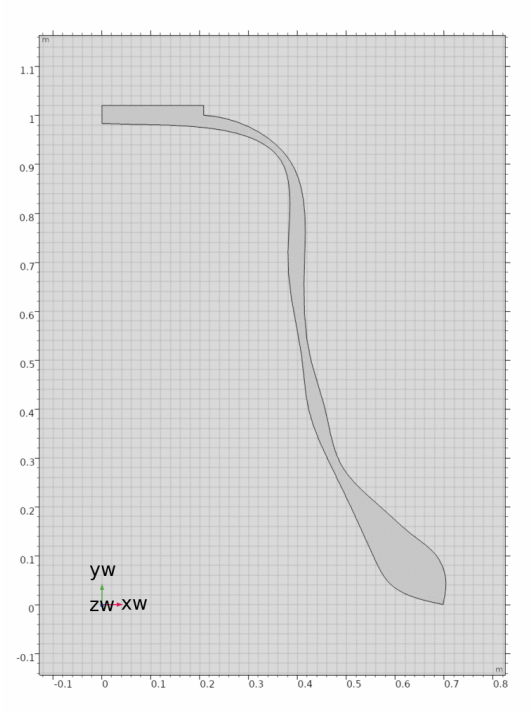

r_d	0.37615
w_ht	0.9
w_h_rto	0.31947
h_ht	w_ht*w_h_rto
waist_inc	0.021
hip_inc	0.038
t_d	0.034
t_d_head_rto	1.176
t_d_shldr_rto	0.37
t_d_belly_rto	0.53
t_d_hip_rto	0.65
bow_thick	0.032245
head_r_d_rto	0.5
Objective	0.0016744
ratios	(11/6), (22/9=11/9), (3), (64/15=16/15)

Bell 022

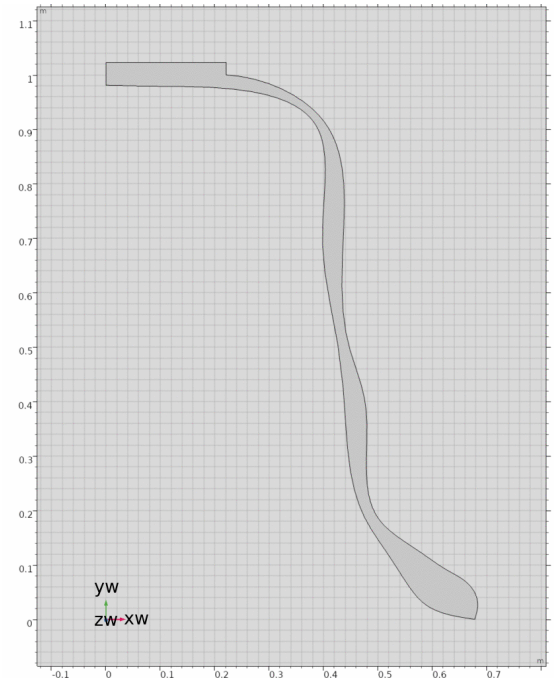

r_d	0.39704
w_ht	0.9
w_h_rto	0.20395
h_ht	w_ht*w_h_rto
waist_inc	0.02
hip_inc	0.0325
t_d	0.038388
t_d_head_rto	1.176
t_d_shldr_rto	0.37
t_d_belly_rto	0.53
t_d_hip_rto	0.65
bow_thick	0.024997
head_r_d_rto	0.5
Objective	0.00093134
ratios	(24/11=12/11), (12/5), (6/2), (30/8=15/8)

Bell 023

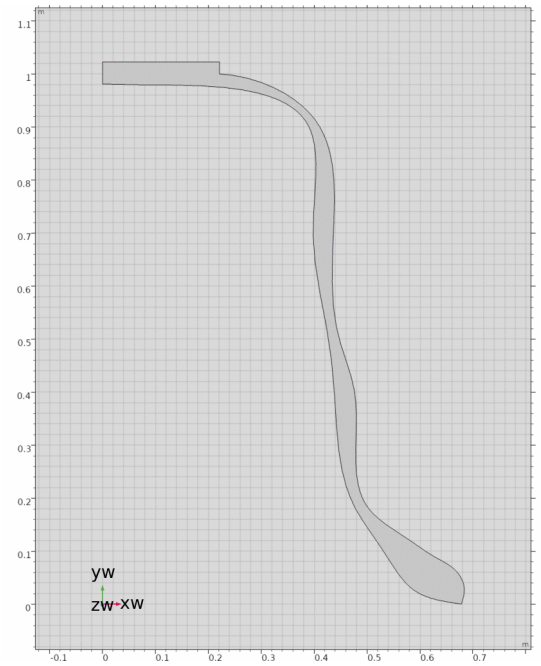

r_d	0.39704
w_ht	0.9
w_h_rto	0.20142
h_ht	w_ht*w_h_rto
waist_inc	0.02
hip_inc	0.0325
t_d	0.038388
t_d_head_rto	1.176
t_d_shldr_rto	0.37
t_d_belly_rto	0.53
t_d_hip_rto	0.65
bow_thick	0.024997
head_r_d_rto	0.5
Objective	0.0013977
ratios	(16/15), (14/6), (16/11), (15/4)

Bell 024

r_d	0.379
w_ht	0.9
w_h_rto	0.30769
h_ht	w_ht*w_h_rto
waist_inc	0.02125
hip_inc	0.038
t_d	0.034
t_d_head_rto	1.176
t_d_shldr_rto	0.395
t_d_belly_rto	0.53
t_d_hip_rto	0.95
bow_thick	0.02375
head_r_d_rto	0.5
Objective	0.0041536
ratios	(24/11=12/11), (12/5), (6/2), (30/8=15/8)

Lehr 001

r_d	0.379
w_ht	0.9
w_h_rto	0.30769
h_ht	w_ht*w_h_rto
waist_inc	0.021
hip_inc	0.038
t_d	0.0445
t_d_head_rto	1.0779
t_d_shldr_rto	0.37915
t_d_belly_rto	0.41494
t_d_hip_rto	0.58569
bow_thick	0.025
head_r_d_rto	0.5
Objective	0.0000017053
ratios	(9/5), (6/5), (3/2), (4)

Lehr 002

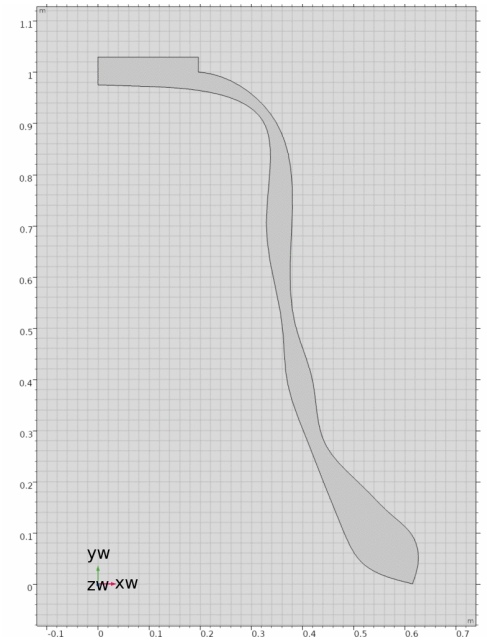

r_d	0.33412
w_ht	0.9
w_h_rto	0.3076
h_ht	w_ht*w_h_rto
waist_inc	0.02
hip_inc	0.0325
t_d	0.049991
t_d_head_rto	1.176
t_d_shldr_rto	0.37
t_d_belly_rto	0.53
t_d_hip_rto	0.65
bow_thick	0.027196
head_r_d_rto	0.5
Objective	0.000062097
ratios	(15/8), (10/4), (6/2), (4)

Lehr 003

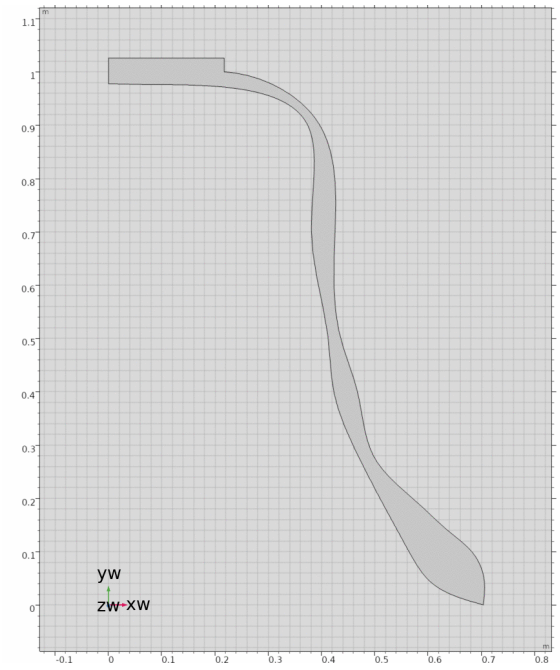

r_d	0.38194
w_ht	0.9
w_h_rto	0.31053
h_ht	w_ht*w_h_rto
waist_inc	0.021
hip_inc	0.038
t_d	0.0445
t_d_head_rto	1.176
t_d_shldr_rto	0.37
t_d_belly_rto	0.5405
t_d_hip_rto	0.65
bow_thick	0.025
head_r_d_rto	0.5
Objective	0.002423
ratios	(9/5), (6/5), (3/2), (4)

Lehr 004

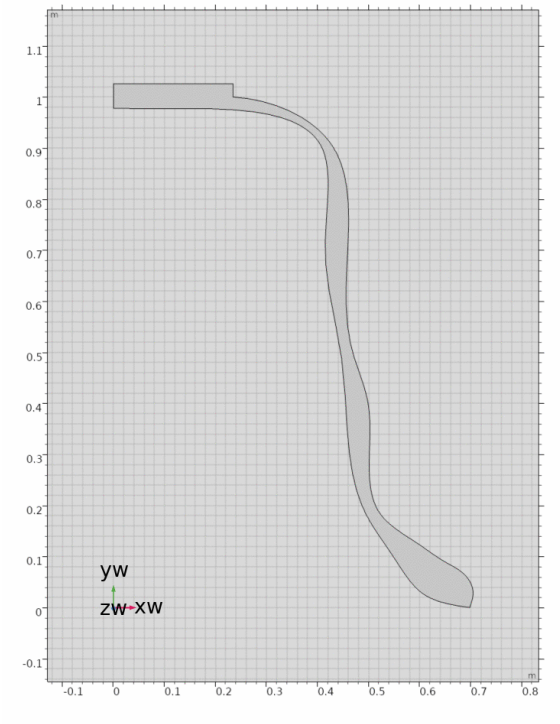

r_d	0.41675
w_ht	0.9
w_h_rto	0.2024
h_ht	w_ht*w_h_rto
waist_inc	0.02
hip_inc	0.0325
t_d	0.044348
t_d_head_rto	1.176
t_d_shldr_rto	0.37
t_d_belly_rto	0.53
t_d_hip_rto	0.65
bow_thick	0.024373
head_r_d_rto	0.5
Objective	0.018675
ratios	(16/7), (10/4), (16/5), (64/15=16/15)

Lehr 005

r_d	0.39219
w_ht	0.9
w_h_rto	0.31947
h_ht	w_ht*w_h_rto
waist_inc	0.02125
hip_inc	0.038
t_d	0.040837
t_d_head_rto	1.176
t_d_shldr_rto	0.37
t_d_belly_rto	0.53
t_d_hip_rto	0.65
bow_thick	0.032245
head_r_d_rto	0.5
Objective	0.000067665
ratios	(11/6), (22/9=11/9), (3), (64/15=16/15)

Lehr 006

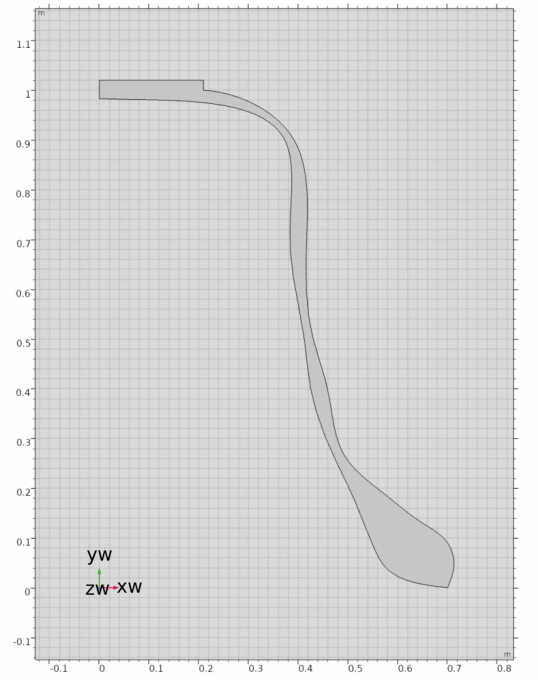

r_d	0.379
w_ht	0.9
w_h_rto	0.29892
h_ht	w_ht*w_h_rto
waist_inc	0.021
hip_inc	0.038
t_d	0.034
t_d_head_rto	1.176
t_d_shldr_rto	0.37
t_d_belly_rto	0.53
t_d_hip_rto	0.65
bow_thick	0.0395
head_r_d_rto	0.5
Objective	0.003335
ratios	(15/8), (9/7), (3/2), (7/4)

Lehr 007

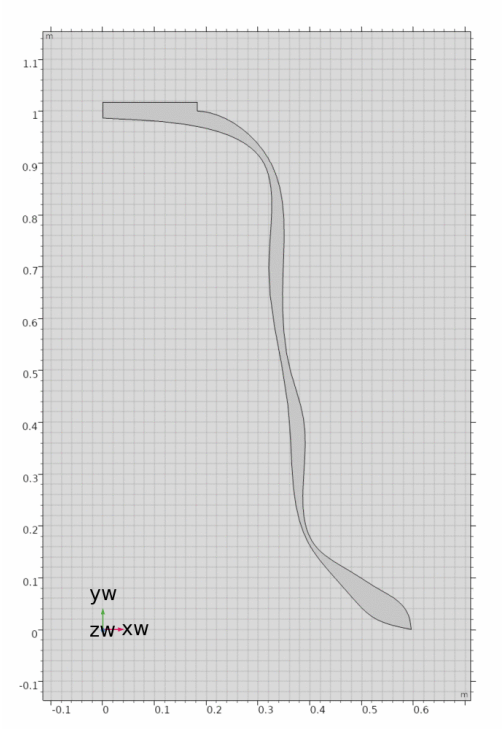

r_d	0.3145
w_ht	0.9
w_h_rto	0.17617
h_ht	w_ht*w_h_rto
waist_inc	0.02
hip_inc	0.0325
t_d	0.028
t_d_head_rto	1.1896
t_d_shldr_rto	0.3
t_d_belly_rto	0.53
t_d_hip_rto	0.4
bow_thick	0.0183
head_r_d_rto	0.52686
Objective	0.043105
ratios	(15/8), (9/7), (3/2), (7/4)